NASA Contractor Report 159186

HUMAN COMFORT RESPONSE TO DOMINANT RANDOM MOTIONS IN LONGITUDINAL MODES OF AIRCRAFT MOTION

Ralph W. Stone, Jr.

RESEARCH LABORATORIES FOR THE
ENGINEERING SCIENCES
University of Virginia, Charlottesville, VA 22901

Contract No. NAS1-14908
January 1980

NASA
National Aeronautics and
Space Administration

Langley Research Center
Hampton, Virginia 23665
AC 804 827-3966

A Report

HUMAN COMFORT RESPONSE TO DOMINANT RANDOM MOTIONS IN LONGITUDINAL MODES OF AIRCRAFT MOTION

Submitted to:

National Aeronautics and Space Administration
Langley Research Center
Hampton, Virginia 23665

Submitted by:

Ralph W. Stone, Jr.
Associate Professor

Department of Civil Engineering
RESEARCH LABORATORIES FOR THE ENGINEERING SCIENCES
SCHOOL OF ENGINEERING AND APPLIED SCIENCE
UNIVERSITY OF VIRGINIA
CHARLOTTESVILLE, VIRGINIA

Report No. UVA/528156/MAE-CE79/130

November 1979

Copy No._____

SECTION I

SUMMARY

The effects of random vertical and longitudinal accelerations and pitching velocity in various pairs on passenger ride comfort responses were examined on the NASA Langley Visual Motion Simulator. Limited effects of power spectral density shape were studied for motions where the peak power was between 0 and 2 Hz.

This paper presents the subjective rating data and the physical motion data obtained in this study. No attempt at interpretation or detailed analysis of the data is made. There existed during this study motions in all other degrees of freedom as well as the particular pair of longitudinal airplane motions being studied. These unwanted motions, being caused by the characteristics of the simulator may have introduced some interactive effects on passenger responses.

SECTION II
INTRODUCTION

Consideration of the quality of airplane rides is becoming increasingly important, especially in terminal area operations and in short travel operations using relatively small, light wing-loaded aircraft (ref. 1). Recent deregulation has stimulated commuter airline growth and further emphasized the differences in the ride quality of short takeoff and landing aircraft in contrast to that of current jet aircraft. Operations at low altitudes and/or with relatively light wing loaded aircraft leads to conditions of flight where the motions of the aircraft may be less comfortable and less acceptable to passengers than is experienced in current jet aircraft operations. Understanding and defining the problems of passenger acceptance and developing methods and systems for aircraft design that will allow for acceptable ride comfort have been encompassed in programs described in references 2 and 3. These programs have included the simultaneous measurement of subjective ride comfort responses and vehicle motions made on both aircraft and simulators.

Much physical and subjective passenger acceptance data has been collected during exposure of people to the full six degrees of freedom motion of a aircraft (refs. 4 - 8). The interactions of the various degrees of freedom of motion as they affect human comfort responses has been under study since 1975 but is not yet fully understood, especially for the frequencies of motion for aircraft. The nature of these interactions is important to the understanding of the total human comfort response to combined motions of two or more degrees of freedom in aircraft. An extensive amount of data exists which documents subjective comfort response to single degree of freedom motion for sinusoidal and random oscillations (refs. 9 - 13). However, these data apply to vibrations with spectral content greater than 2 Hz. Consequently, there is a need for detailed information about this type of response for vibrations with energy below 2 Hz.

The influence of single degree of freedom motions having random oscillations typical of those aircraft in turbulence therefore is not

fully understood. Typical airplane responses to turbulence have power spectra shapes with peak power below 2 Hertz and often below 1 Hertz with rapid decreases in power beyond these frequencies. However, some response motions of airplanes (particularly the angular motions) have somewhat flatter power spectra shapes. Whether these different spectral shapes will have a significant influence on ride comfort is not clear. A program to measure human comfort responses in single degree of freedom random motions and the interactions of these motions, in two, three, and six degrees of freedom using two types of power spectra shapes and three frequency ranges was performed on the Visual-Motion Simulator at the NASA Langley Research Center (Figure 1).

References 14, 15, 16, 17, 18, and 19 present data obtained for the study of subjective ride comfort responses to random vertical, transverse, and longitudinal accelerations and to random rolling and pitching velocities and to combined yawing and rolling velocities, respectively. The present study was made to measure the subjective ride comfort response ratings obtained when using paired combinations of random vertical and longitudinal accelerations and pitching velocity.

SYMBOLS

R_s	ride comfort response
σ_{R_s}	standard deviation of ride comfort response
g	acceleration due to gravity
Hz	frequency, cps.

TESTS AND TEST CONDITIONS

Motion Stimuli

The investigation was initiated to measure human comfort response ratings to single degree of freedom motions and to multiple degree of freedom motions using random motions like those experienced in airplane flight. A program was developed using 14 separate simulator "flights," each flight consisting of 24 segments. Each of the segments consisted of either a single degree of freedom motions, a two-, three-, or six-

degree of freedom motion. The segments for the six single degrees of freedom (vertical, transverse and longitudinal accelerations; and pitch, roll and yaw rates) were scattered throughout six flights. Any one single degree of freedom was contained within only two of the six flights. The various two degrees of freedom segments were similarly scattered throughout four flights. The various three degrees of freedom segments were scattered throughout two flights, and six degrees of freedom similarly in two flights.

As mentioned previously, typical airplane responses to turbulence have power spectra that decrease rapidly beyond 1 to 2 Hertz. However, some responses, particularly angular motions, have flatter power spectra. In order to investigate the effect of spectral shape and the frequency distribution of the response power on ride comfort, six power spectral density distributions were developed to drive the simulator. There were two general groups, the first termed "typical," having variations with frequency like those experienced on typical aircraft and the second termed "flat" with shallower decreases at the high frequencies. In each group, three distinct frequency distributions were used; the first with peak power centered between 0 and 1 Hz, the second between 0 and 2 Hz, and the third between 1 and 2 Hz. For the study of this paper both typical and flat spectra were used having peak power centered between 0 and 2 Hz.

Each "flight" of twenty-four segments was flown five times so that ten subjects experienced each motion. As these flights were not precisely duplicated, as just noted, the data presented in the "Data" section of this paper are average values of the five flights used. The average deviation of the RMS vertical acceleration, longitudinal acceleration and the pitching velocity from the average values for the various segments in terms of percent of the average values is 1.67, 1.81, and 8.54 percent respectively. The maximum deviation was 5.98, 10.73, and 28.17 percent, respectively. The actual output of the simulator for a test segment respresenting most nearly the average output for a given segment, and therefore the motions

essentially experienced by the subjects are presented in Figures 2 to 7, for representative segments. These figures include time histories for all six degrees of freedom, histograms of the paired imput motions, and power spectra of the paired input motions. The conditions for Figures 2 to 7 are as follows:

FIGURE	PAIRED MOTION INPUTS
2 and 3	Longitudinal and Vertical Acceleration
4 and 5	Vertical Acceleration and Pitching Velocity
6 and 7	Longitudinal Acceleration and Pitching Velocity

Both typical and flat spectra shapes were used for each component input. All peak frequency ranges were 0 - 2 Hz. The three related segments in the figures are for progressively increasing values of the particular variable input component.

The reference axis used was relative to the seated passengers and is shown in Figure 8. The longitudinal modes of aircraft motion used as inputs for this study were linear accelerations along the longitudinal and vertical axis and angular velocity (pitch) about the transverse axis of Figure 8. The actual motions of the simulator as experienced by the passengers, and shown in Figures 2 to 7, were measured by an inertial instrument package containing three linear accelerometers, one alined with each axis, and three rate gyros also alined with each axis.

The six power spectra shapes were tailored by filtering the output of a random number generator. The nominal shapes of these spectra are shown in Figure 9. In designing the spectra shapes to suit the simulator characteristics the "flat" spectra were not as flat as was intended and in Figure 9 appear to have more power in the 1 to 3 Hz range than the typical spectra for conditons with the same peak power. This increase in power, over the typical spectra, ranges from 35 percent for the 1 to 2 Hz spectra to 170 percent for the 0 to 1 Hz spectra.

The nominal spectra shown in Figure 9 are normalized to have a peak of 1. For the actual motions on the simulator the magnitude was raised for each spectra shape by adjusting the gain of the input signal. For the study reported herein, using paired input motions, one motion was input with a fixed magnitude and three magnitudes were input for the other motion.

For the two degrees of freedom studies four flights of twenty-four segments each (96 total flight segments) were used. For the study of paired longitudinal motions forty of these segments were used, being randomly distributed among the four flights.

Simulator

The Langley Visual-Motion Simulator (VMS) is primarily used for piloted flight, stability, control, and display studies, and does not contain a passenger compartment. The passengers used in this study sat in the pilot's compartment and rode passively, the controls and instruments being inoperative for these experiments. Figure 10 is an interior view of the cockpit. Two passengers rode each experimental "flight."

The normal operational envelope of motion frequencies and magnitudes of the VMS are presented in reference (2). The largest practicable input frequency is about 3 Hz. As noted in references 7 and 8, the major energy in aircraft motions is in the region of 2 Hertz and less.

The VMS is a large mechanical device with six hydraulically operated telescoping legs and associated switching values. In order to obtain the desired motions without exceeding the mechanical limitations of the simulator, various controls and limiting systems are incorporated. The simulator, as a dynamic device, has its own natural frequencies and damping, and thus exerts an effect on the resulting motions. For the precise development of a pair of motions the six legs would have to move synchronously in accordance with computer command. Because of friction in the hydraulic systems and valves, and variations in the hydraulic pressure, it was not possible to produce the precise conditions necessary for a pair of degrees of freedom. Therefore, the motions developed by the simulator, when obtaining the data for this paper, had paired combinations of the longitudinal motions as the dominant motion with various lesser amounts of the other four degrees of freedom. For these same reasons, the motions were not precisely duplicated even for identical computer inputs. Also, as a result of the dynamic characteristics of the simulator, the actual motion power spectra experienced by the subjects was somewhat different than the nominal spectra used as input to the simulator from the computer.

The different magnitudes of motion previously mentioned were adjusted through the computer input and should have been the same for the two spectra shapes studied. However, because of the dynamic response characteristics of the simulator, different RMS values of the various longitudinal modes of motion were obtained for the different spectra shapes.

Experimental Procedure

As noted previously, the segments of simulated flight used in examining paired combinations of the longitudinal modes of motion were randomly scattered in four "flights." Each flight was 36 minutes long, and consisted of twenty-four, one and one-half minute segments. The subjects rated a 20 second portion in the center of each segment. A computer driven buzzer system was used to identify this center portion of the segment. The subjects were instructed to consider only this 20 second portion of the segment when making their comfort response ratings. The subjects rated the segments on a seven-statement scale, as follows:

Very comfortable
Comfortable
Somewhat comfortable
Acceptable
Somewhat uncomfortable
Uncomfortable
Very uncomfortable

Many subjective ride comfort indices have been based on a five-point numerical scale (see refs. 5 and 8 for example). Accordingly, for analysis purposes the seven-statement rating scale was converted to numerical values for a five-point scale as follows:

1 = Very comfortable
2 = Comfortable
2½ = Somewhat comfortable
3 = Acceptable
3½ = Somewhat uncomfortable
4 = Uncomfortable
5 = Very uncomfortable

For the data presented herein, average numerical ratings for the subjects based on this scale and standard deviations from these averages are used.

The subjects, in general, were supplied by the Hampton Institute and consisted of a relatively broad spectra of people. For the total program,

138 passenger "flights" were made using a total of 98 persons. No person rode the same flight twice. A general profile of the persons used on these "flights" is shown in Table 1.

DATA

The mean RMS values for all six degrees of freedom of the five segments performed for each input segment along with the mean subjective ride comfort response ratings (R_s) and standard deviation are then shown in Tables II to IV as follows:

TABLE	PAIRED MOTION INPUTS
II	Longitudinal and Vertical Acceleration
III	Vertical Acceleration and Pitching Velocity
IV	Longitudinal Acceleration and Pitching Velocity

Cross correlation coefficients for the various motions components are shown in Tables V, VI, and VII, corresponding to Tables II, III, and IV respectively. The three segments of motion on the tables for each specific paired combination are for progressively increasing RMS values of the particular variable involved.

In addition to the paired modes of longitudinal motion input to the simulator, there existed, as noted previously, components of the other four degrees of freedom, the RMS magnitudes of which are shown on Tables II, III, and IV. It is not yet clear how significant these unwanted motions are in the subjective ride comfort responses presented in this paper. The average RMS values of these unwanted motions were as follows:

Longitudinal Acceleration	- 0.0260 g's
Transverse Acceleration	- 0.0201 g's
Vertical Acceleration	- 0.0478 g's
Pitching Velocity	- 1.2864 deg/sec.
Rolling Velocity	- 2.4214 deg/sec.
Yawing Velocity	- 1.0900 deg/sec.

All these average values appear to be above the apparent thresholds of sensitivity indicated in references 3, and 14 through 19. The subjective response values expected for these unwanted motions would range between comfortable to acceptable ratings. This implies little discomfort from

these unwanted motions when experienced separately. It would seem that the existence of these unwanted motion components possibly was sensed by the passengers during these tests although the motions in themselves may not have illicited uncomfortable responses. Whether any of these motions were sufficient to have altered the subjective ride comfort response ratings from those that might have been obtained from the intended paired inputs alone is not clear. The interactive effects of multiple degrees of freedom must be more clearly understood before this assessment can be made.

The subjective ride comfort responses on Tables II, III, and IV have an average standard deviation for all segments of 0.596, with a maximum of 0.890. These compare favorably with other experience, references 14 through 19, for example.

The purpose of this study was to determine to what extent the presence of a second motion altered the subjective ride comfort responses to a specific motion. Figures 11 to 16 are presented to show, at least, a qualitative influence of a second motion. On these figures the subjective ride comfort responses ratings (R_s) are plotted against the $\log_{10}$ of the RMS values of the motions involved. It should not be construed by these figures that a Weber-Fechner psychophysical model is proposed as representing these data, however, as in reference 14 to 19, there is a reasonable linearity shown in such semi-log plots which allows some observations relative to the data. On figures 11 to 16 are shown in solid lines the best fit regression line for the current data. There appears to be rather meager data to perform such regressions. Remembering, however, that each data point represents 10 subjective responses and that at this point only trends will be noted this approach seems reasonable. Also shown in Figures 11 to 16, as dashed lines are regression lines taken from references 14, 16, and 18. Figures 11 and 12 present the effects for paired longitudinal and vertical accelerations. From Figure 11 it appears that a constant vertical acceleration with a variable longitudinal acceleration may have

Page Intentionally Left Blank

CONCLUDING REMARKS

A study has been made on the Langley Visual Motion Simulator to examine the influence of paired combinations of the three longitudinal modes of aircraft motions (longitudinal, vertical, and pitching motions) on human subjective ride comfort responses. The effects of two general shapes of power spectral density of the modes of motion were examined. A peak power frequency of 0 - 2 Hz was used for all data. The data indicates a rather complex relationship between the comfort response ratings and the magnitudes of the specific paired modes of motion. Although this study was made basically to examine the influence of pairs of motion, because of the characteristics of the simulator there occurred in the study some amounts of motion in all other degrees of freedom. Analysis of these data must maintain cognizance of this fact.

REFERENCES

1. DOT TST-10-4, NASA SP-265. Joint DOT-NASA Civil Aviation Research and Development Policy Study, March 1971.

2. NASA TM X-2620. Symposium on Vehicle Ride Quality Held at Langley Research Center, Hampton, Virginia, July 6-7, 1972, October 1972.

3. NASA TM X-3295. DOT-TSC-OST-75-40 1975 Ride Quality Symposium, held at Williamsburg, Virginia, August 11-12, 1975, November 1975.

4. Jacobson, Ira D.: Environmental Criteria for Human Comfort - A Study of the Related Literature. NASA CR-132424, University of Virginia, Charlottesville, Virginia, February 1974.

5. Jacobson, Ira D.; and Richards, Larry G.: Ride Quality Evaluation II: Modelling of Airline Passenger Comfort. Memorandum Report 403217, University of Virginia, Charlottesville, Virginia, December 1974.

6. Gruesbeck, Marta G.; and Sullivan, Daniel F.: Aircraft Motion and Passenger Comfort Data From Scheduled Commercial Airline Flights. University of Virginia, Charlottesville, Virginia, May 1974.

7. Stephens, David G.: Development and Application of Ride-Quality Criteria. NASA TM X-72008, September 1974.

8. Stone, Ralph W., Jr.: Ride Quality - An Exploratory Study and Criteria Development. NASA TM X-71922, February 1974.

9. International Organization for Standardization, International Standard ISO/DIS 2631. Guide for the Evaluation of Human Exposure to Whole-Body Vibration. 1972.

10. Dempsey, Thomas K.; and Leatherwood, Jack D.: Experimental Studies for Determining Human Discomfort Response to Vertical Sinusoidal Vibration. NASA TN D-8041, November 1975.

11. Leatherwood, Jack D.; and Dempsey, Thomas K.: Psychophysical Relationships Characterizing Human Response to Whole-Body Sinusoidal Vertical Vibration. NASA TN D-8188, June 1976.

12. Leatherwood, Jack D.; Dempsey, Thomas K,; and Clevenson, Sherman A.: An Experimental Study for Determining Human Discomfort Response to Roll Vibration. NASA TN D-8266, November 1976.

13. Dempsey, Thomas K,; and Leatherwood, Jack D.: Discomfort Criteria for Single-Axis Vibrations. NASA Technical Paper 1422, May 1979.

14. Stone, Ralph W., Jr.: Human Comfort Response to Random Motions With a Dominant Vertical Motion. NASA TM X-72691, May 1975.

REFERENCES (cont.)

15. Stone, Ralph W., Jr.: Human Comfort Response to Random Motions With a Dominant Transverse Motion. NASA TM X-72694, May 1975.

16. Stone, Ralph W., Jr.: Human Comfort Response to Random Motions With a Dominant Longitudinal Motion. NASA TM X-72746, July 1975.

17. Stone, Ralph W., Jr.: Human Comfort Response to Random Motions With a Dominant Rolling Motion. NASA TM X-72747, July 1975.

18. Stone, Ralph W., Jr.: Human Comfort Response to Random Motions With a Dominant Pitching Motion. UVA/528156/MAE-CE79/117, Research Laboratories for the Engineering Sciences, University of Virginia, Charlottesville, Virginia, July 1979.

19. Stone, Ralph W., Jr.: Human Comfort Response to Random Motion With Dominant Combined Yawing & Rolling Motions. UVA/528156/MAE-CE79/128, Research Laboratories for the Engineering Sciences, University of Virginia, Charlottesville, Virginia, August 1979.

20. Dempsey, Thomas K.; Leatherwood, Jack D.; and Clevenson, Sherman A.: Development of Noise and Vibration Ride Comfort Criteria. The Journal of the Accoustical Society of America, Volume 65, No. 1, January 1979.

TABLE I - PASSENGER PROFILE FOR
VMS RIDE QUALITY PROGRAM

Total Passengers - 98 Persons

Sex Distribution

	Number	%
Males	47	48
Females	51	52

Age Distribution

	Number	%	Sex	
			Male	Female
18-25 yrs	55	56	44%	56%
26-45 yrs	30	31	47%	53%
46 → yrs	13	13	69%	31%

TABLE II. MEAN RMS VALUES OF MEASURED MOTION COMPONENTS WITH COMBINED VERTICAL AND LONGITUDINAL ACCELERATION INPUTS AND MEAN RIDE COMFORT RESPONSES

Longitudinal Acceleration g	Transverse Acc. g	Vertical Acc. g	Pitching Velocity deg/sec.	Rolling Velocity deg/sec.	Yawing Velocity deg/sec.	R_s	σ_{R_s}
a) Variable longitudinal input, typical 0 - 2 Hz; Fixed Vertical input, typical 0 - 2 Hz							
0.0354	0.0215	0.0644	1.6252	2.6616	1.4065	2.600	.460
0.0670	0.0190	0.0583	1.1611	2.1114	0.9647	4.250	.677
0.1008	0.0212	0.0609	1.3286	2.1829	1.0926	4.650	.580
b) Variable longitudinal input, flat 0 - 2 Hz; Fixed vertical input, typical 0 - 2 Hz							
0.0327	0.0156	0.0546	1.1446	1.8556	0.9962	3.000	.333
0.0655	0.0215	0.0686	1.3696	2.2852	1.1516	3.500	.667
0.0840	0.0200	0.0627	1.1793	2.1231	1.0002	4.250	.540
c) Fixed longitudinal input, typical 0 - 2 Hz; Variable vertical input, typical 0 - 2 Hz							
0.0548	0.0164	0.0331	1.3206	1.9333	1.1377	3.250	.540
0.0670	0.0190	0.0583	1.1611	2.1114	0.9647	4.250	.580
0.0630	0.0219	0.0819	1.3325	2.3856	1.1388	3.750	.755

TABLE III. MEAN RMS VALUES OF MEASURED MOTION COMPONENTS WITH COMBINED *VERTICAL ACCELERATION AND PITCHING VELOCITY* INPUTS AND MEAN RIDE COMFORT RESPONSES

Longitudinal Acc. g	Transverse Acc. g	Vertical Acc. g	Pitching Velocity deg/sec.	Rolling Velocity deg/sec.	Yawing Velocity deg/sec.	R_s	σ_{R_s}
a) Fixed vertical input, typical 0 - 2 Hz; Variable pitching input, typical 0 - 2 Hz							
0.0232	0.0193	0.0720	2.4632	2.4909	1.0306	3.750	0.791
0.0271	0.0226	0.0762	2.8574	2.7651	1.3633	3.100	0.460
0.0330	0.0248	0.0892	3.6558	3.1414	1.0485	4.000	0.745
b) Fixed vertical input, typical 0 - 2 Hz; Variable pitching input, flat 0 - 2 Hz							
0.0165	0.0169	0.0604	1.7352	1.9822	1.0692	3.100	0.460
0.0246	0.0188	0.0745	2.4854	2.2121	1.0011	3.950	0.643
0.0332	0.0226	0.0867	4.0852	2.4508	1.1072	4.000	0.624
c) Fixed vertical input, flat 0 - 2 Hz; Variable pitching input, typical 0 - 2 Hz							
0.0168	0.0167	0.0626	1.6284	2.0511	0.9853	3.350	0.338
0.0252	0.0202	0.0730	2.4864	2.3752	0.9532	2.950	0.497
0.0376	0.0273	0.0937	4.0884	3.2363	1.5165	3.600	0.595

TABLE III. Concluded.

Longitudinal Acc. g	Transverse Acc. g	Vertical Acc. g	Pitching Velocity deg/sec.	Rolling Velocity deg/sec.	Yawing Velocity deg/sec.	R_s	σ_{R_s}
d) Fixed vertical input, flat 0 - 2 Hz; Variable pitching input, flat 0 - 2 Hz							
0.0208	0.0216	0.0670	2.0652	2.7462	1.4063	2.450	0.669
0.0264	0.0190	0.0700	2.6444	2.3231	1.0564	4.100	0.843
0.0324	0.0255	0.0849	3.4164	3.1014	1.2092	3.800	0.715
e) Variable vertical input, typical 0 - 2 Hz; Fixed pitching input, typical 0 - 2 Hz							
0.0237	0.0190	0.0563	2.4538	2.5082	1.0150	3.050	0.497
0.0271	0.0226	0.0762	2.8574	2.7651	1.3633	3.100	0.460
0.0258	0.0204	0.0948	3.0594	2.4051	1.0683	3.700	0.632
f) Variable vertical input, flat 0 - 2 Hz; Fixed pitching input, flat 0 - 2 Hz							
0.0233	0.0190	0.0568	2.4391	2.4601	1.0628	3.350	0.784
0.0264	0.0190	0.0700	2.6444	2.3231	1.0564	4.100	0.843
0.0251	0.0206	0.0842	2.8272	2.2543	1.1958	3.250	0.540

TABLE IV. MEAN RMS VALUES OF MEASURED MOTION COMPONENTS WITH COMBINED LONGITUDINAL ACCELERATION AND PITCHING VELOCITY INPUTS AND MEAN RIDE COMFORT RESPONSES

Longitudinal Acc. g	Transverse Acc. g	Vertical Acc. g	Pitching Velocity deg/sec.	Rolling Velocity deg/sec.	Yawing Velocity deg/sec.	R_s	σ_{R_s}
a) Fixed longitudinal input, typical 0 - 2 Hz; Variable pitching input, typical 0 - 2 Hz							
0.0603	0.0171	0.0268	1.5954	2.1542	1.0662	3.750	0.890
0.0678	0.0216	0.0428	2.4617	2.5694	1.2806	3.700	0.298
0.0723	0.0255	0.0675	3.1371	3.0587	1.0859	4.500	0.667
b) Fixed longitudinal input, typical 0 - 2 Hz; Variable pitching input, flat 0 - 2 Hz							
0.0541	0.0152	0.0238	1.6204	1.8207	1.0300	3.600	0.568
0.0594	0.0200	0.0500	2.4527	2.1940	0.9735	4.100	0.876
0.07084	0.0228	0.0637	3.6231	2.4895	1.1470	4.500	0.527
c) Fixed longitudinal input, flat 0 - 2 Hz; Variable pitching input, typical 0 - 2 Hz							
0.0589	0.0169	0.0262	1.6311	1.9680	1.0159	3.950	0.832
0.0579	0.0195	0.0397	2.1218	2.2607	0.9878	3.650	0.580
0.0722	0.0260	0.0619	3.3006	3.2166	1.4494	3.550	0.497

TABLE IV. Concluded.

Longitudinal Acc. g	Transverse Acc. g	Vertical Acc. g	Pitching Velocity deg/sec.	Rolling Velocity deg/sec.	Yawing Velocity deg/sec.	R_s	σ_{R_s}
d) Fixed longitudinal input, flat 0 - 2 Hz; Variable pitching input, flat 0 - 2 Hz							
0.0552	0.0192	0.0276	1.7552	2.4753	1.3338	2.900	0.516
0.0612	0.0201	0.0477	2.3361	2.2406	1.0521	4.050	0.599
0.0653	0.0269	0.0711	3.5770	3.0375	1.1857	4.350	0.580
e) Variable longitudinal input, typical 0 - 2 Hz; Fixed pitching input, typical 0 - 2 Hz							
0.0382	0.0194	0.0452	2.4551	2.5483	0.9885	3.500	0.707
0.0678	0.0216	0.0428	2.4617	2.5694	1.2806	3.700	0.258
0.0846	0.0203	0.0460	2.7677	2.2704	1.0818	4.500	0.527
f) Variable longitudinal input, flat 0 - 2 Hz; Fixed pitching input, flat 0 - 2 Hz							
0.0418	0.0192	0.0458	2.4654	2.3457	0.9096	3.300	0.422
0.0612	0.0201	0.0477	2.3361	2.2406	1.0521	4.050	0.599
0.0866	0.0223	0.0478	2.8055	2.2617	1.1729	4.450	0.599

TABLE V. CROSS-CORRELATION COEFFICIENTS WITH COMBINED VERTICAL AND LONGITUDINAL ACCELERATION INPUTS.

Longitudinal -Vertical	Longitudinal -Pitch	Transverse -Roll	Transverse -Yaw	Vertical -Pitch	Roll -Yaw
a) Variable longitudinal input, typical 0 - 2 Hz; Fixed vertical input, typical 0 - 2 Hz					
-0.0046	0.2427	0.4318	0.6558	0.1344	0.7549
-0.0120	-0.0596	0.3328	0.5682	0.0517	0.6986
0.1724	-0.0740	0.2683	0.4926	0.1018	0.7235
b) Variable longitudinal input, flat 0 - 2 Hz; Fixed vertical input, typical 0 - 2 Hz					
-0.0443	0.1571	0.5396	0.7043	0.1273	0.8198
0.1530	0.1062	0.4597	0.6337	0.2964	0.7584
-0.0718	-0.0794	0.3870	0.5640	0.2349	0.7606
c) Fixed longitudinal input, typical 0 - 2 Hz; Variable vertical input, typical 0 - 2 Hz					
0.0992	-0.0805	0.5113	0.6738	0.2437	0.8342
0.1724	-0.0740	0.2683	0.4926	0.1018	0.7235
0.1048	-0.0436	0.2276	0.4628	0.0252	0.6756

TABLE VI. CROSS-CORRELATION COEFFICIENTS WITH COMBINED VERTICAL ACCELERATION AND PITCHING VELOCITY INPUTS

Longitudinal -Vertical	Longitudinal -Pitch	Transverse -Roll	Transverse -Yaw	Vertical -Pitch	Roll -Yaw
a) Fixed vertical input, typical 0 - 2 Hz; Variable pitching input, typical 0 - 2 Hz					
0.2269	0.3772	0.3204	0.6622	-0.0074	0.6759
0.2963	0.4075	0.4074	0.6667	0.0488	0.7710
0.3979	0.3464	0.4357	0.7924	-0.0719	0.7895
b) Fixed vertical input, typical 0 - 2 Hz; Variable pitching input, flat 0 - 2 Hz					
0.1663	0.6238	0.5025	0.6959	0.1374	0.8136
0.3113	0.4134	0.4049	0.6910	-0.0115	0.7355
0.4635	0.3543	0.2977	0.6493	-0.0374	0.6749
c) Fixed vertical input, flat 0 - 2 Hz; Variable pitching input, typical 0 - 2 Hz					
0.1408	0.5194	0.4346	0.6541	0.1555	0.7763
0.3455	0.4359	0.3794	0.6661	0.0268	0.7256
0.4349	0.3646	0.3284	0.6691	0.1250	0.6855

TABLE VI. Concluded.

Longitudinal -Vertical	Longitudinal -Pitch	Transverse -Roll	Transverse -Yaw	Vertical -Pitch	Roll -Yaw
d) Fixed vertical input, flat 0 - 2 Hz; Variable pitching input, flat 0 - 2 Hz					
0.1811	0.5715	0.4680	0.6591	-0.0533	0.8052
0.3587	0.4061	0.4679	0.6930	0.0186	0.7962
0.3186	0.3881	0.3801	0.6864	0.0195	0.7297
e) Variable vertical input, typical 0 - 2 Hz; Fixed pitching input, typical 0 - 2 Hz					
0.4583	0.4959	0.4738	0.7176	0.0743	0.8085
0.2963	0.4075	0.4074	0.6667	0.0488	0.7710
0.3035	0.3817	0.3504	0.6106	0.0565	0.7352
f) Variable vertical input, flat 0 - 2 Hz; Fixed pitching input, flat 0 - 2 Hz					
0.4320	0.3703	0.4956	0.7404	0.1216	0.7967
0.3587	0.4061	0.4679	0.6930	0.0186	0.7962
0.1472	0.4216	0.3679	0.6201	-0.0394	0.7395

TABLE VII. CROSS-CORRELATION COEFFICIENTS WITH COMBINED LONGITUDINAL ACCELERATION AND PITCHING VELOCITY INPUTS.

Longitudinal -Vertical	Longitudinal -Pitch	Transverse -Roll	Transverse -Yaw	Vertical -Pitch	Roll -Yaw
a) Fixed longitudinal inputs, typical 0 - 2 Hz; Variable pitching input, typical 0 - 2 Hz					
0.1418	0.0900	0.5316	0.7125	0.2291	0.8196
0.1673	0.0731	0.3953	0.6772	0.0552	0.7190
0.2859	0.1602	0.3461	0.6474	-0.0263	0.7139
b) Fixed longitudinal input, typical 0 - 2 Hz; Variable pitching input, flat 0 - 2 Hz					
0.1571	-0.0245	0.5687	0.7125	0.2336	0.8537
0.0671	0.1279	0.3349	0.6158	0.0122	0.7165
0.3136	-0.0533	0.3292	0.6392	-0.0002	0.6781
c) Fixed longitudinal input, flat 0 - 2 Hz; Variable pitching input, typical 0 - 2 Hz					
0.0480	0.0824	0.4482	0.6256	0.1859	0.8035
0.1455	0.1089	0.4337	0.6922	0.0464	0.7675
0.2472	0.1888	0.4375	0.6925	0.0062	0.7800

TABLE VII. Concluded.

Longitudinal -Vertical	Longitudinal -Pitch	Transverse -Roll	Transverse -Yaw	Vertical -Pitch	Roll -Yaw
d) Fixed longitudinal input, flat 0 - 2 Hz; Variable pitching input, flat 0 - 2 Hz					
0.2278	0.2502	0.6905	0.7749	0.4661	0.8860
0.1951	0.0104	0.3902	0.6365	0.0508	0.7619
0.2312	0.1113	0.3131	0.6455	-0.0303	0.6874
e) Variable longitudinal input, typical 0 - 2 Hz; Fixed pitching input, typical 0 - 2 Hz					
0.3203	0.3641	0.4834	0.7367	0.7728	0.7887
0.1673	0.0731	0.3953	0.6772	0.0552	0.7190
0.2815	-0.1885	0.3239	0.5777	0.0426	0.7187
f) Variable longitudinal input, flat 0 - 2 Hz; Fixed pitching input, flat 0 - 2 Hz					
0.3310	0.1768	0.3072	0.6111	0.0852	0.7280
0.1951	0.0104	0.3902	0.6365	0.0508	0.7619
0.2564	-0.0271	0.3354	0.5797	0.0710	0.7314

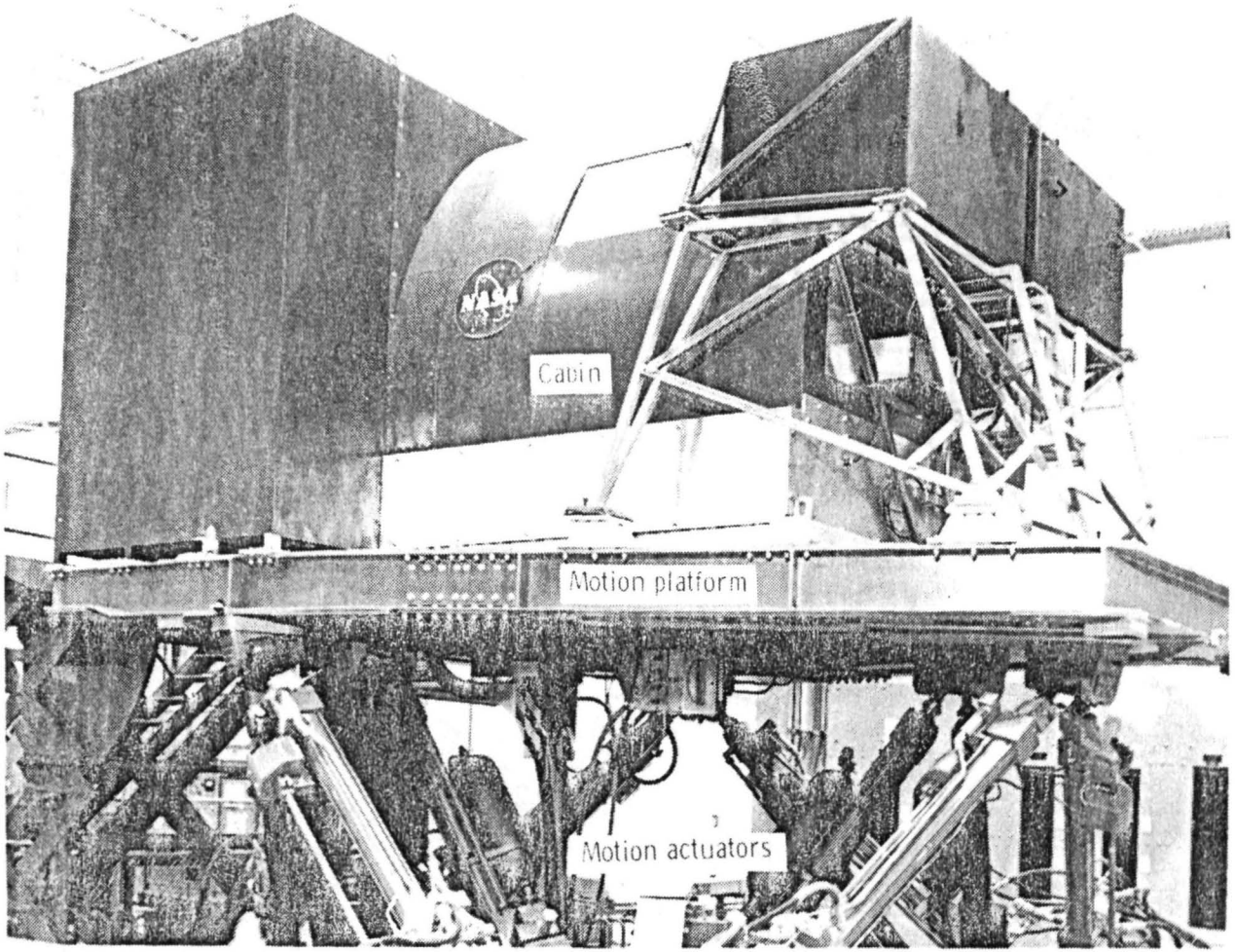

Figure 1 - Langley six-degree-of-freedom, vision motion simulator.

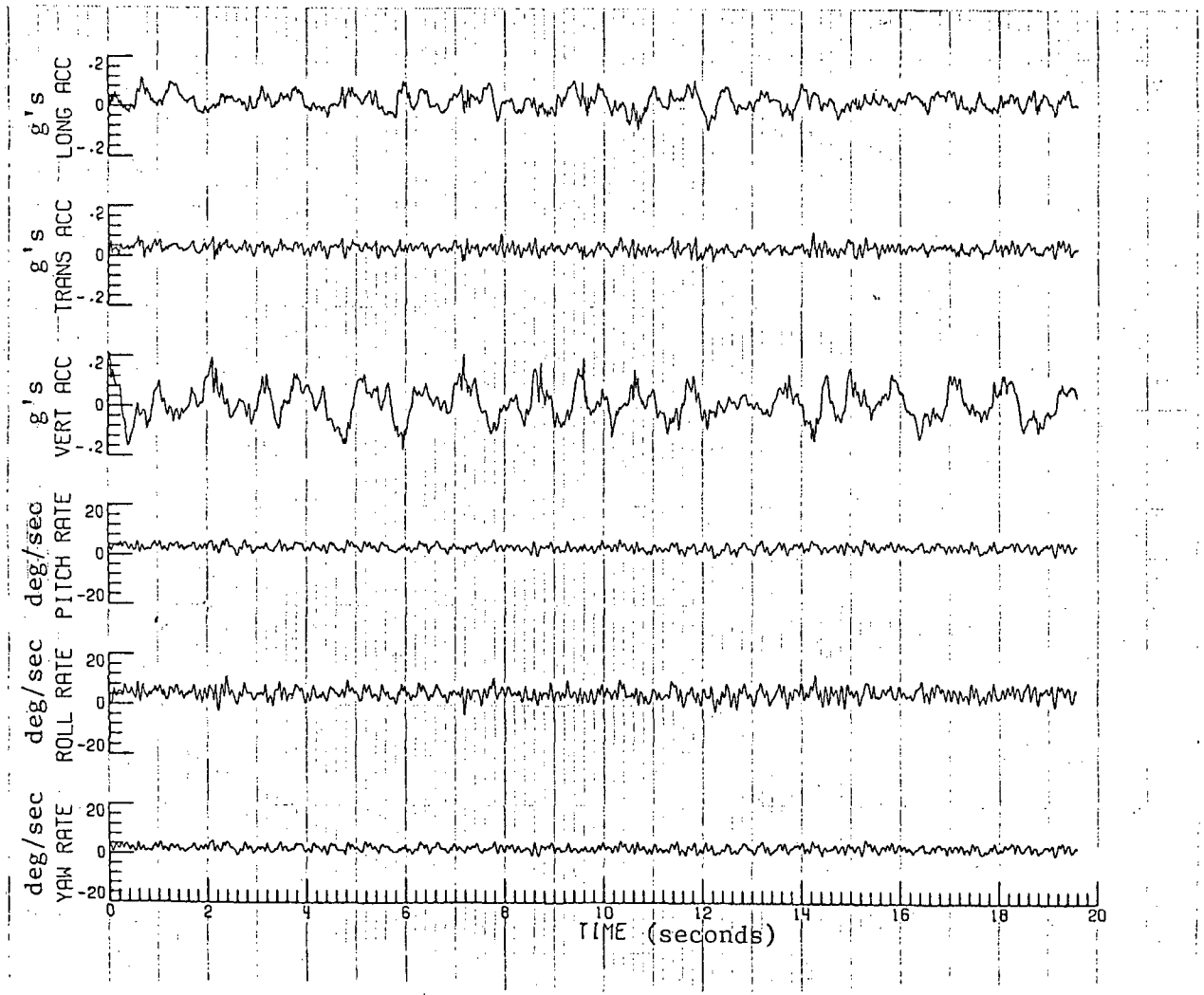

(a) Time histories (RMS-longitudinal acceleration 0.0354 g's; RMS-vertical acceleration 0.0644 g's)

FIGURE 2. MEASURED MOTION CHARACTERISTICS USING AN APPROXIMATELY CONSTANT RMS-VERTICAL ACCELERATION WITH A VARIABLE RMS-LONGITUDINAL ACCELERATION

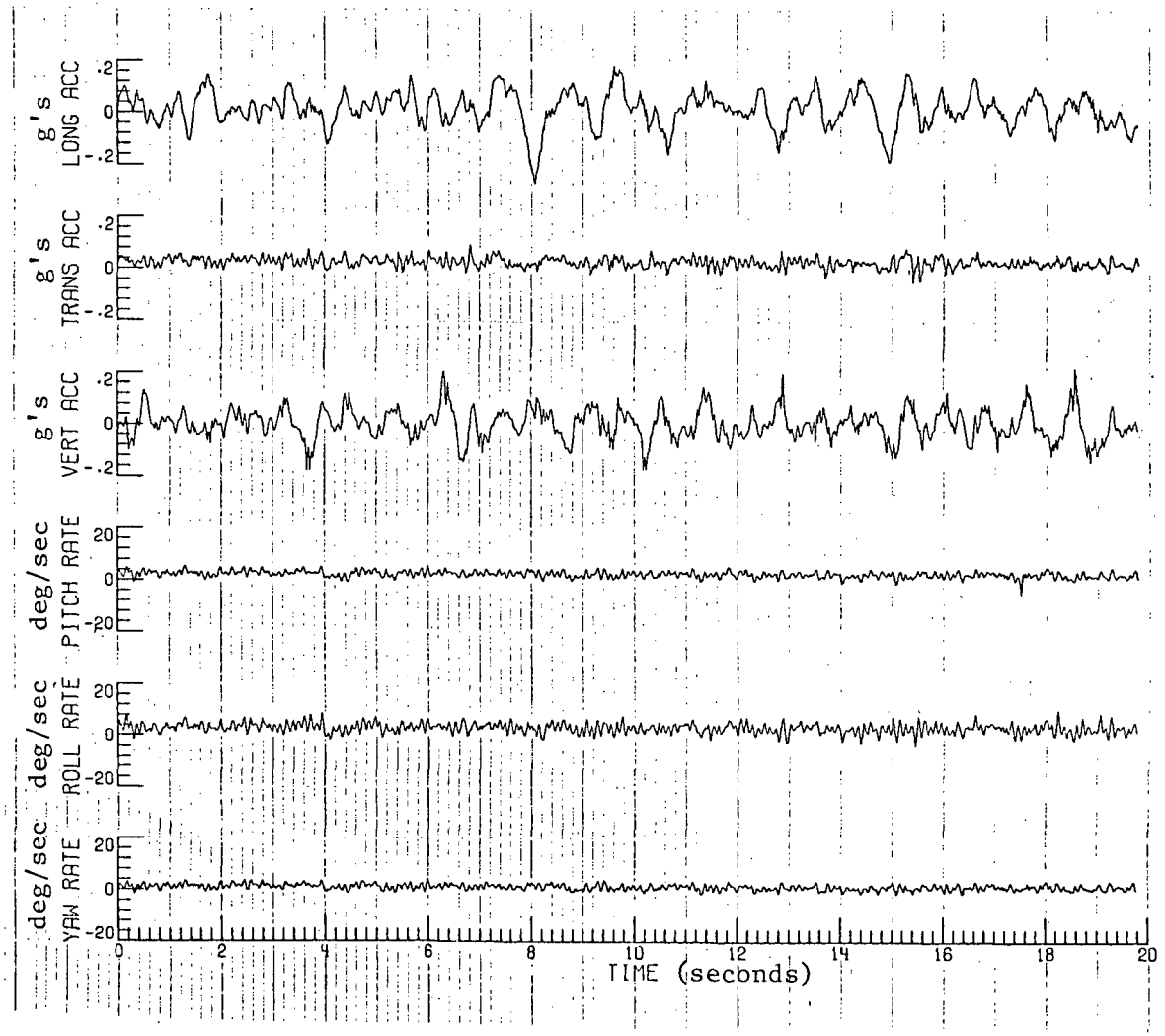

(a) Time histories (RMS-longitudinal acceleration 0.0670 g's; RMS-vertical acceleration 0.0583 g's)

FIGURE 2. Continued.

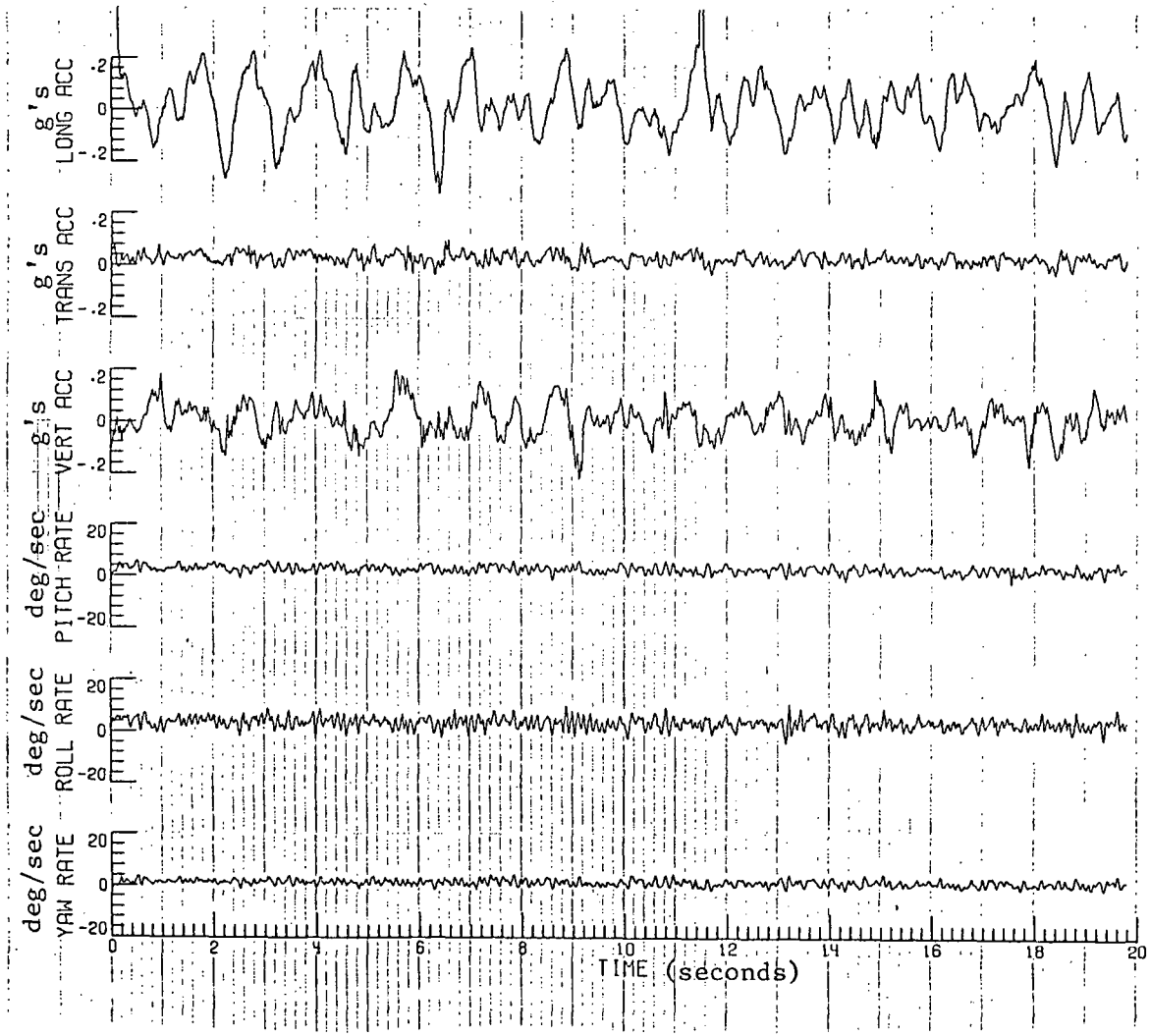

(a) Time histories (RMS-longitudinal acceleration 0.1008 g's; RMS-vertical acceleration 0.0604 g's)

FIGURE 2. Continued.

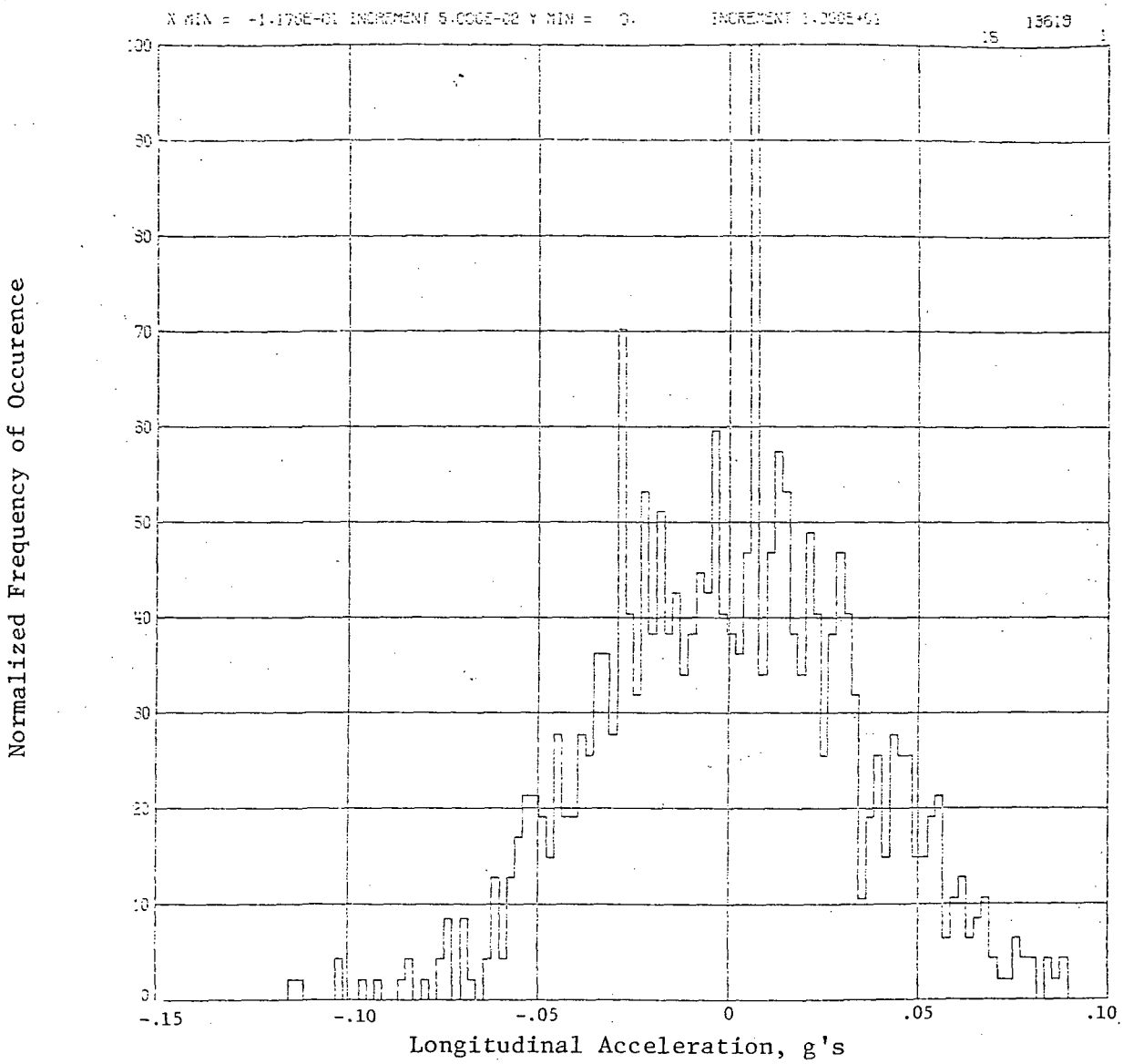

(b) Longitudinal acceleration histogram (RMS-longitudinal acceleration 0.0354 g's)

FIGURE 2. Continued.

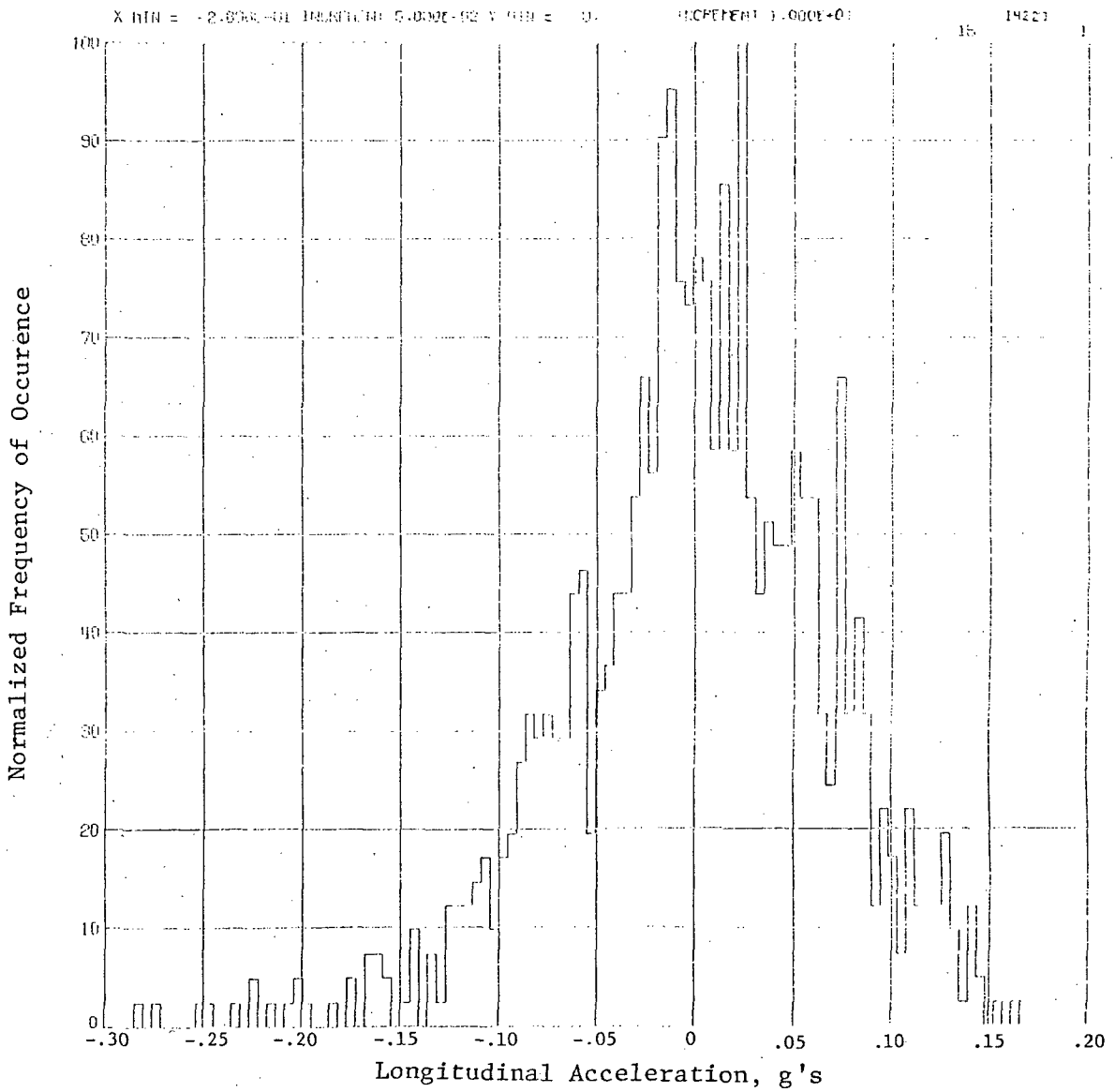

(b) Longitudinal acceleration histogram (RMS-longitudinal acceleration 0.0670 g's)

FIGURE 2. Continued.

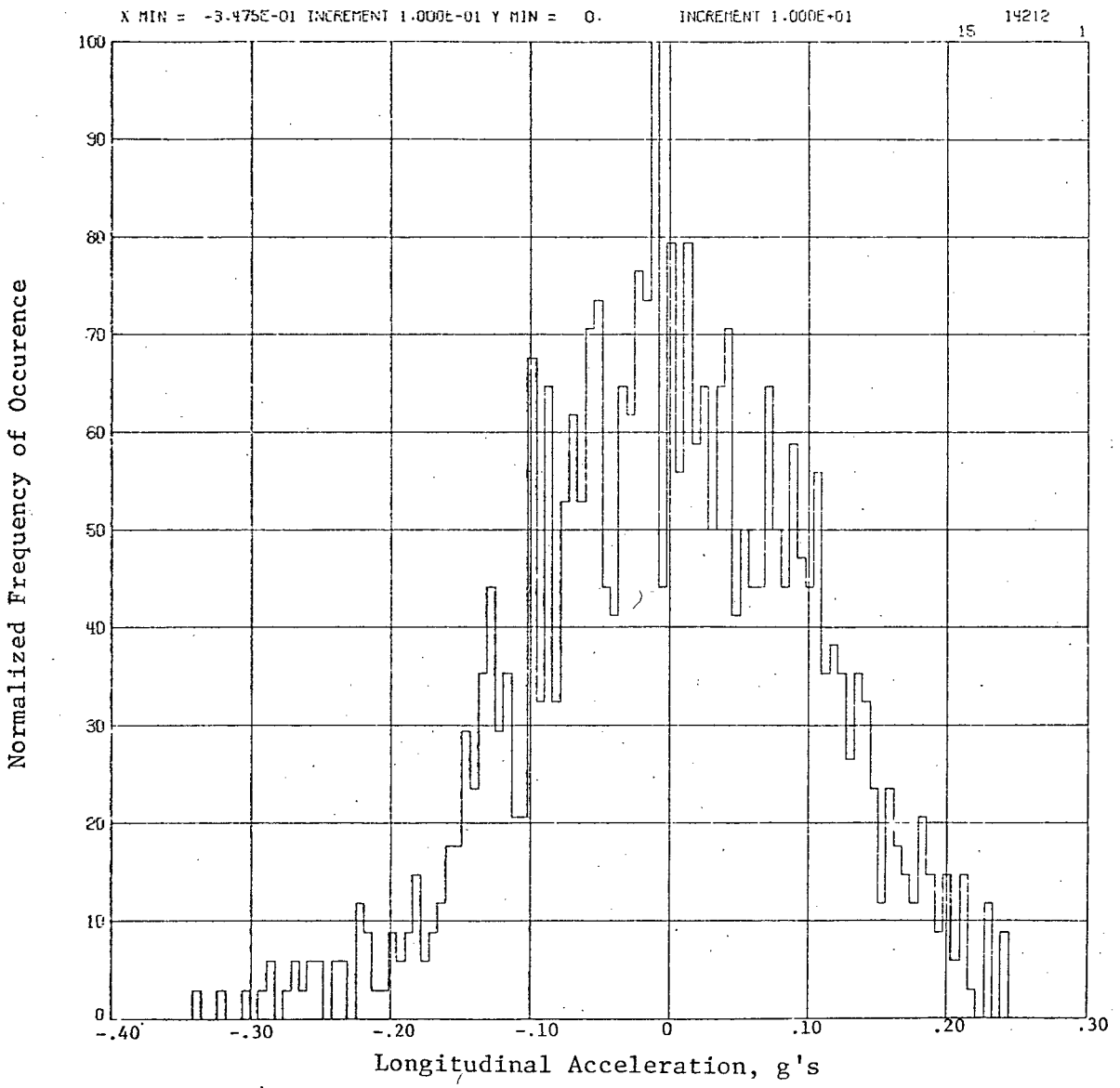

(b) Longitudinal acceleration histogram (RMS-longitudinal acceleration 0.1008 g's

FIGURE 2. Continued.

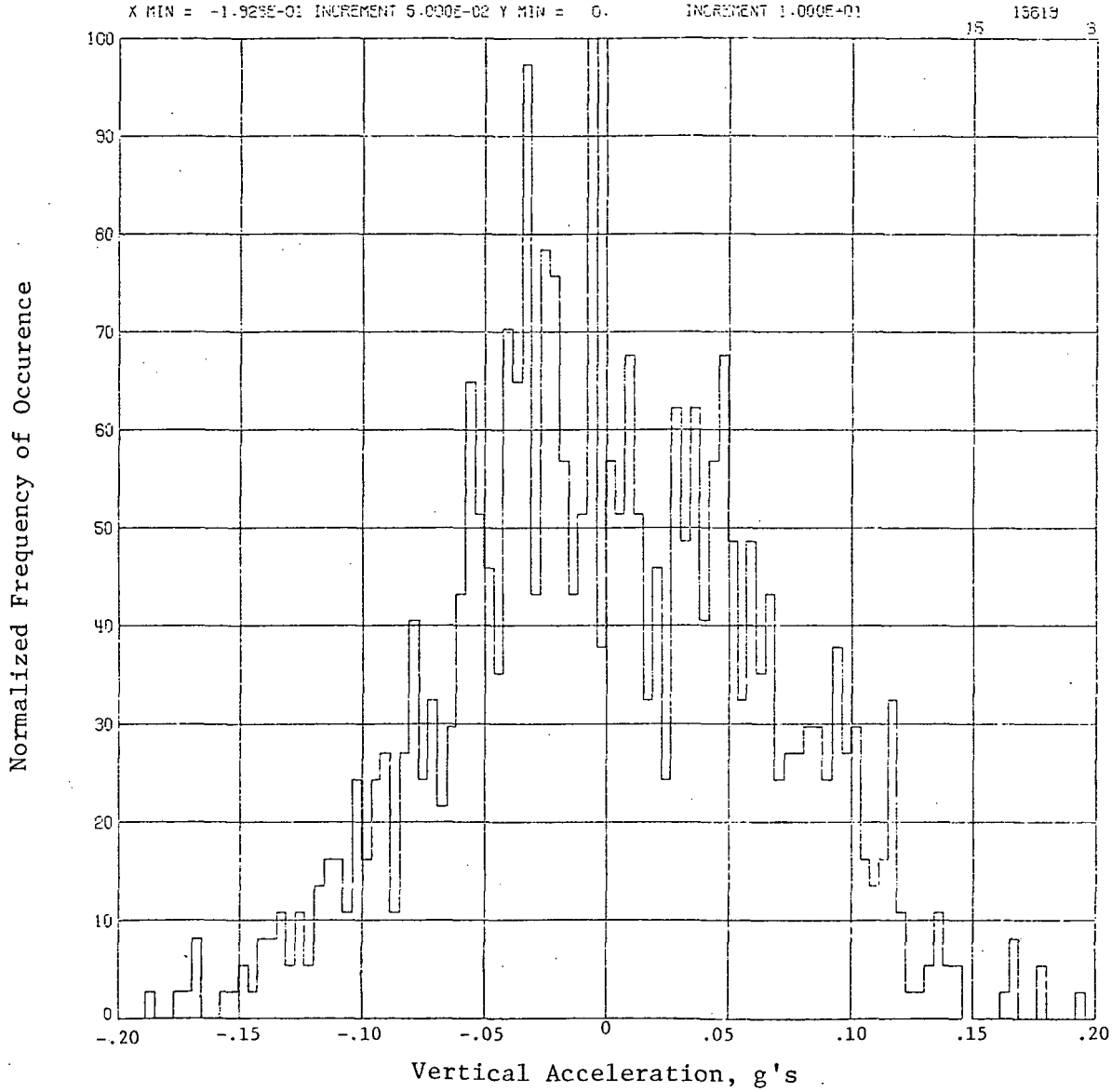

(c) Vertical acceleration histogram (RMS-vertical acceleration 0.0644 g's)

FIGURE 2. Continued.

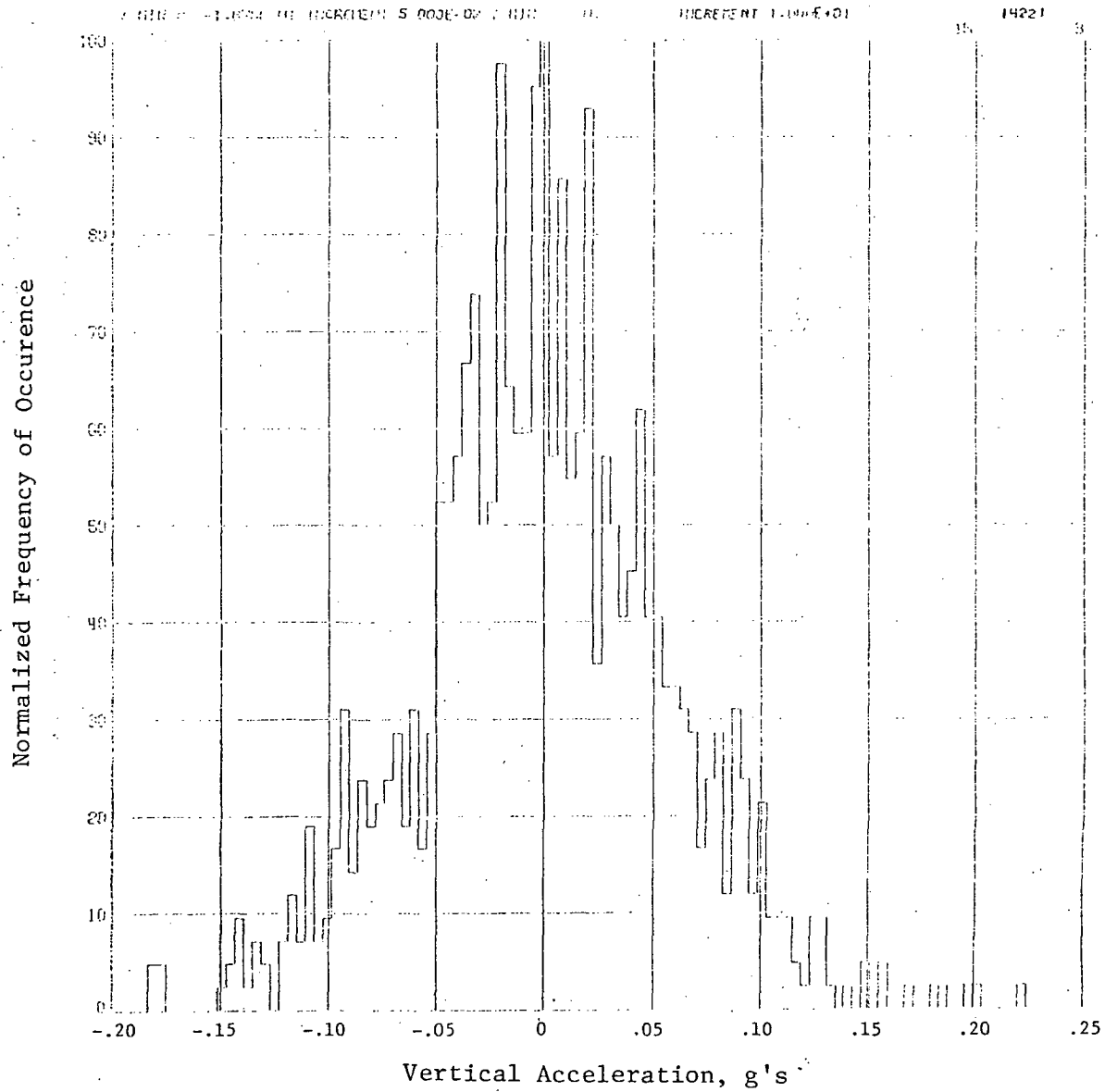

(c) Vertical acceleration histogram (RMS-vertical acceleration 0.0583 g's)

FIGURE 2. Continued.

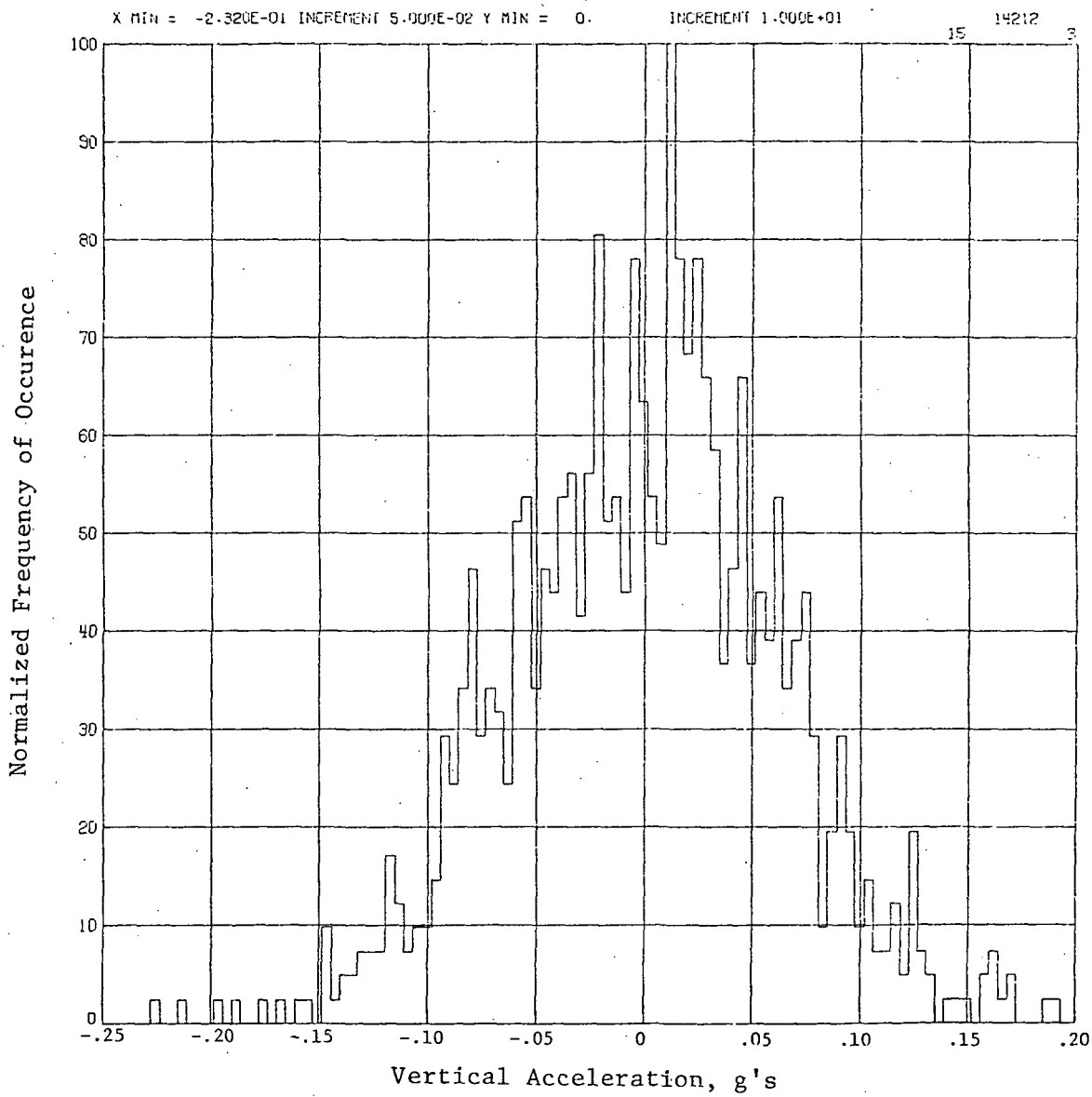

(c) Vertical acceleration histogram (RMS-vertical acceleration 0.0609 g's)

FIGURE 2. Continued.

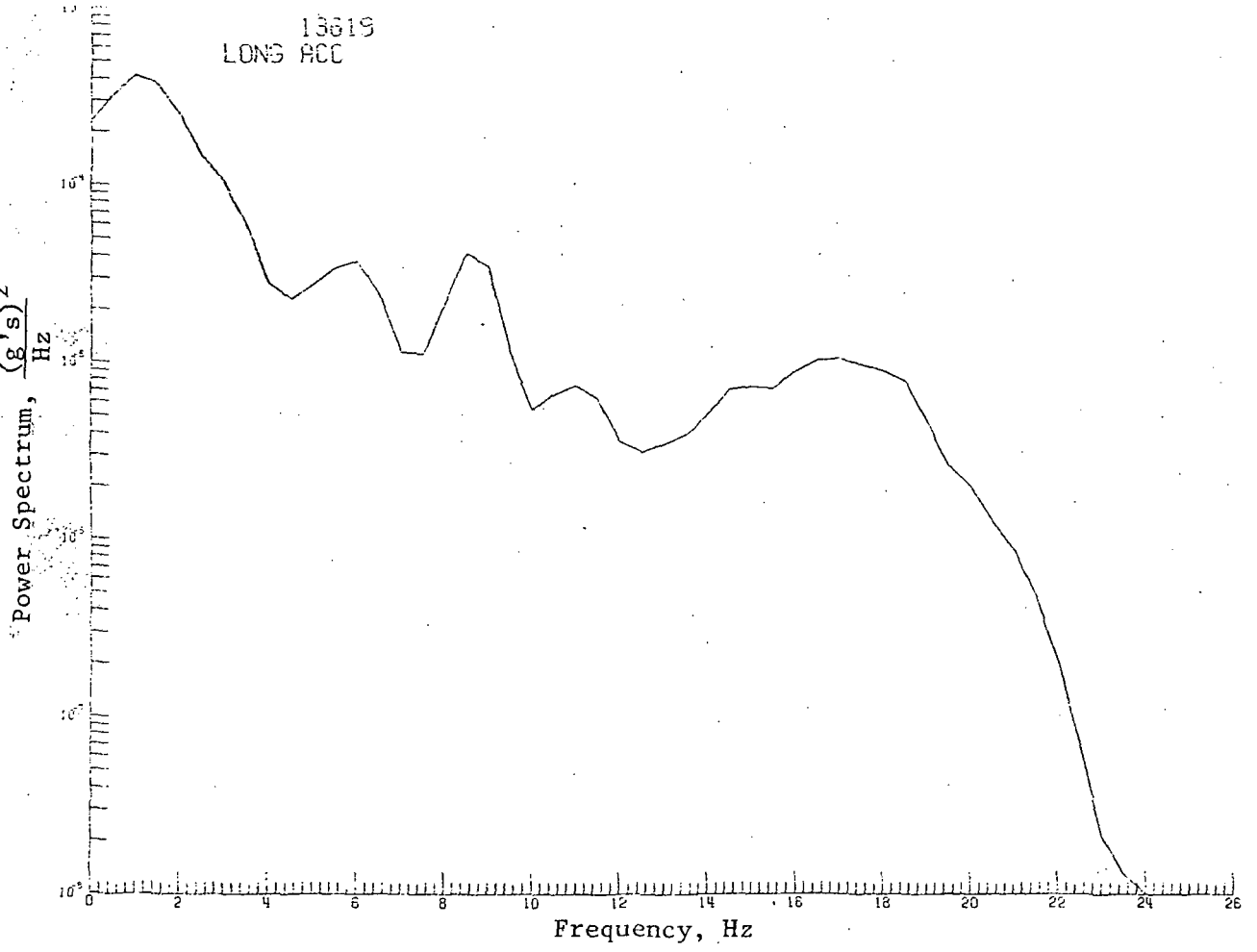

(d) Longitudinal acceleration power spectrum
(RMS-longitudinal acceleration 0.354 g's)

FIGURE 2. Continued.

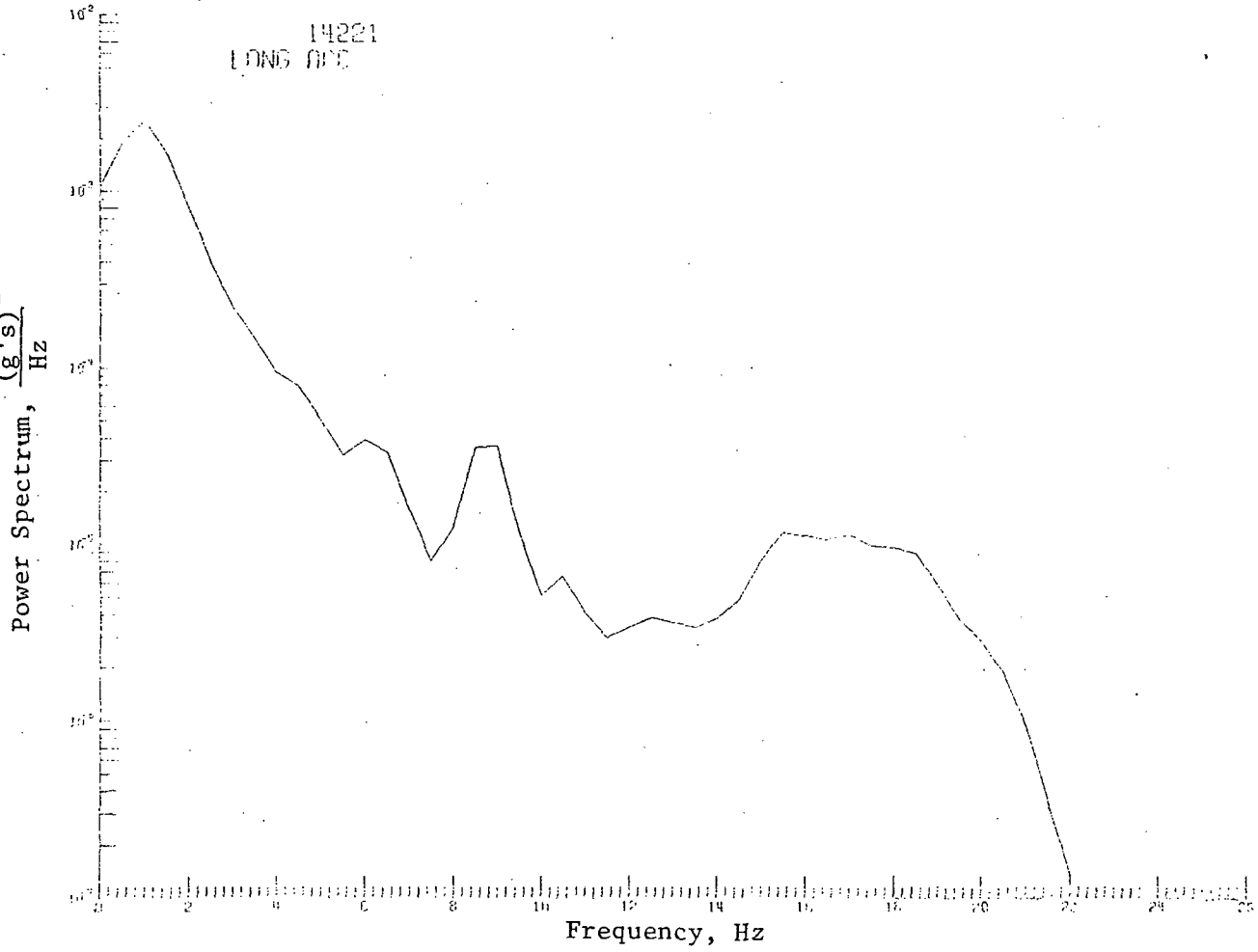

(d) Longitudinal acceleration power spectrum
(RMS-longitudinal acceleration 0.0670 g's)

FIGURE 2. Continued.

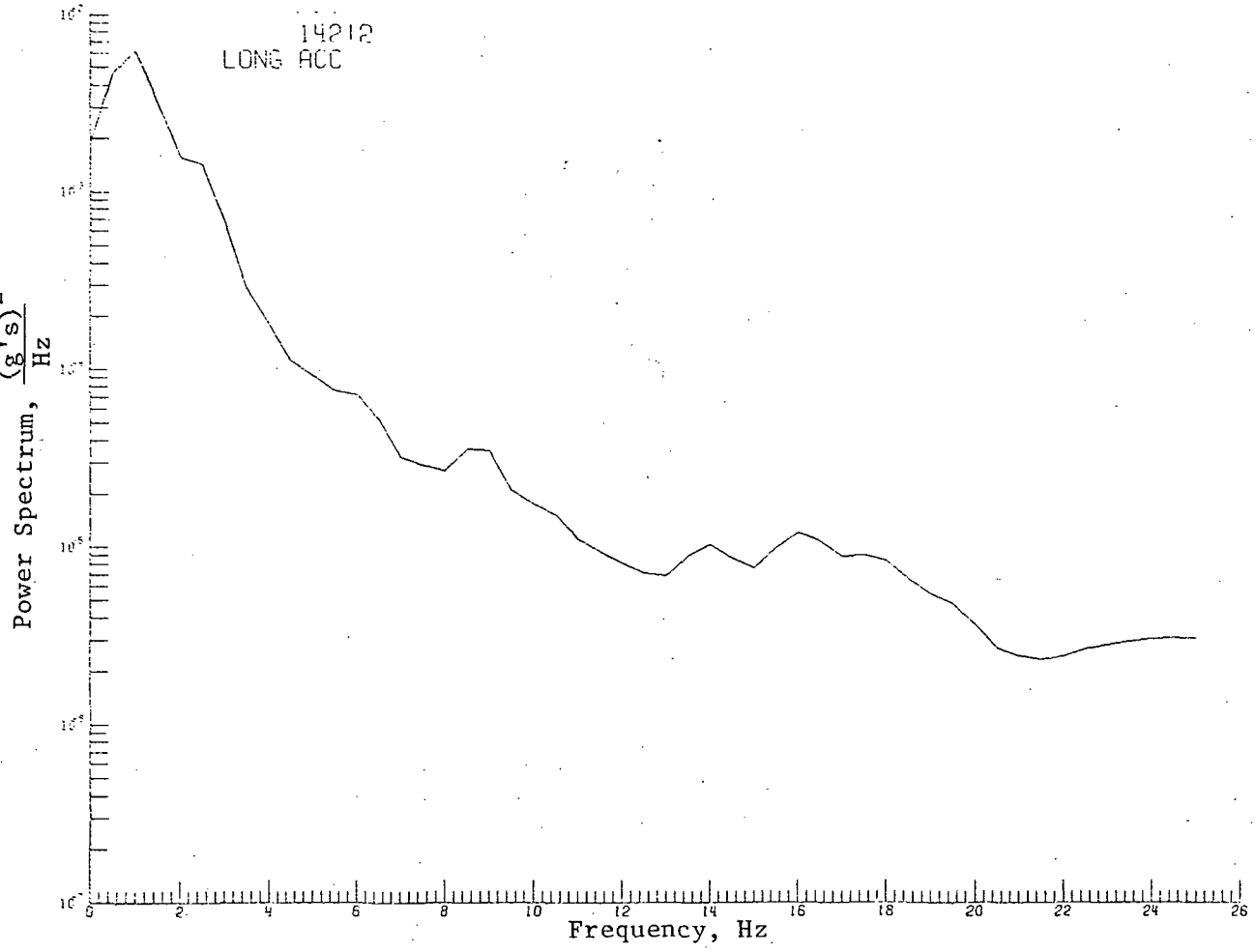

(d) Longitudinal acceleration power spectrum
(RMS-longitudinal acceleration 0.1008 g's)

FIGURE 2. Continued.

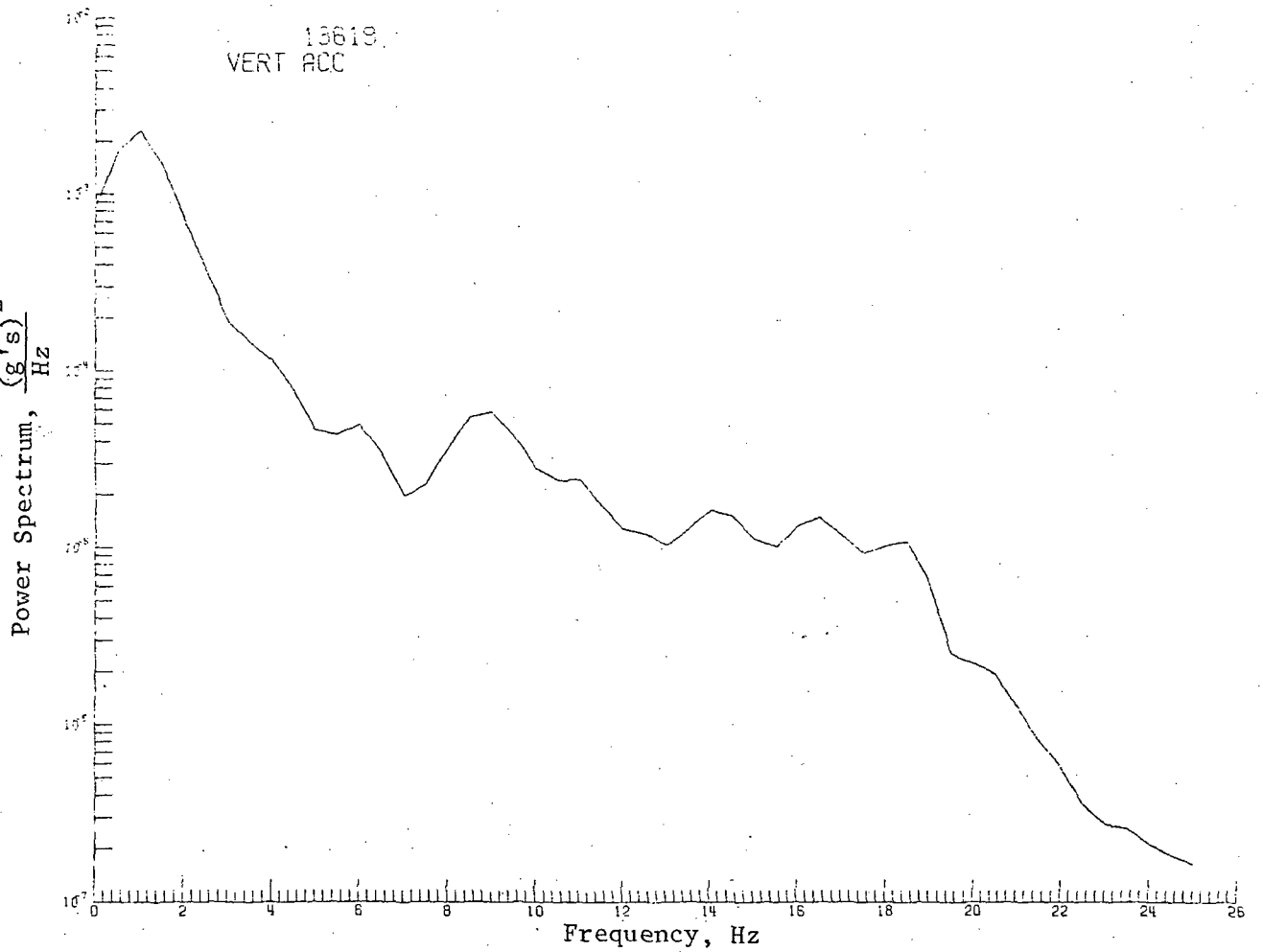

(e) Vertical acceleration power spectrum
(RMS-vertical acceleration 0.0644 g's)

FIGURE 2. Continued.

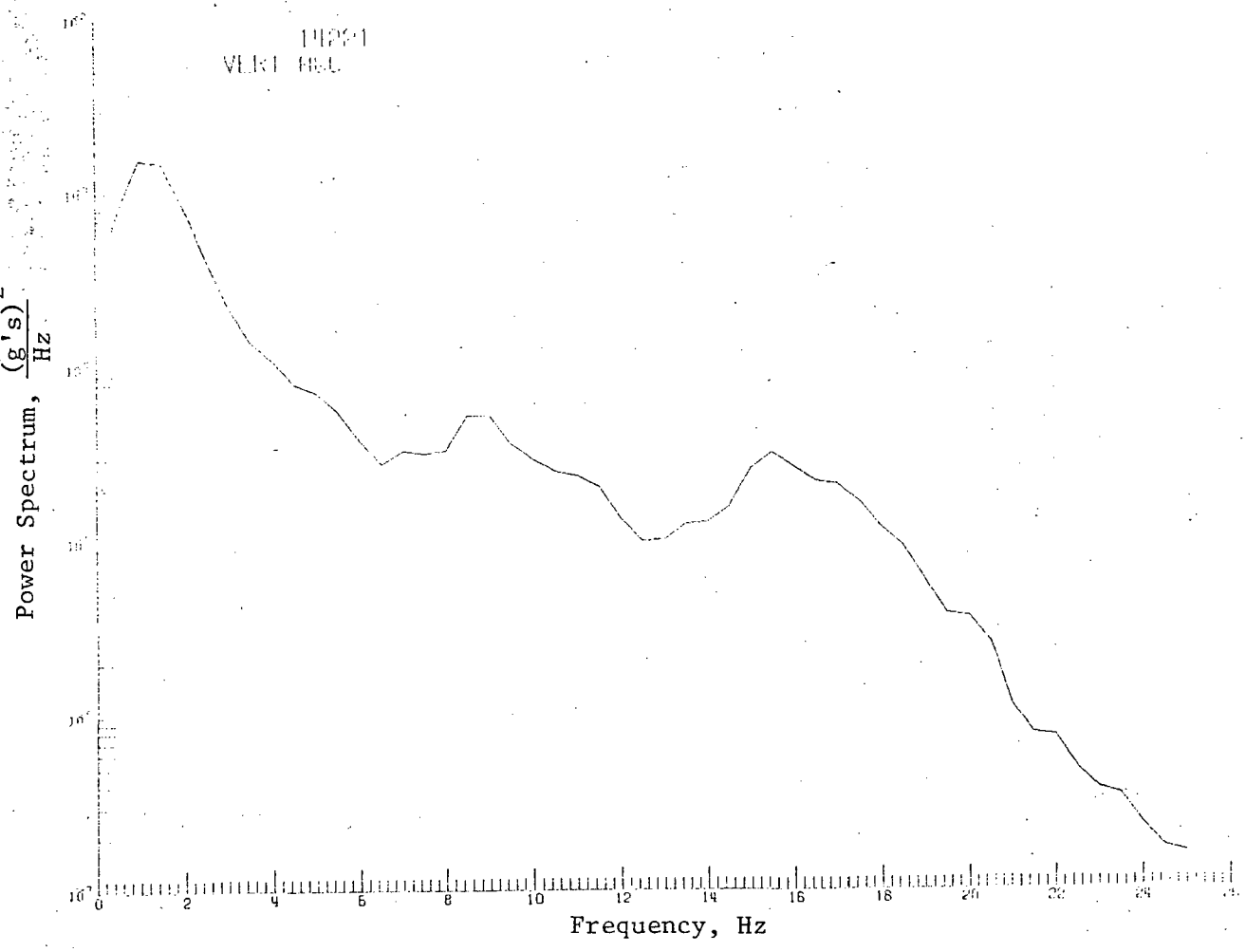

(e) Vertical acceleration power spectrum
(RMS-vertical acceleration 0.0583 g's)

FIGURE 2. Continued.

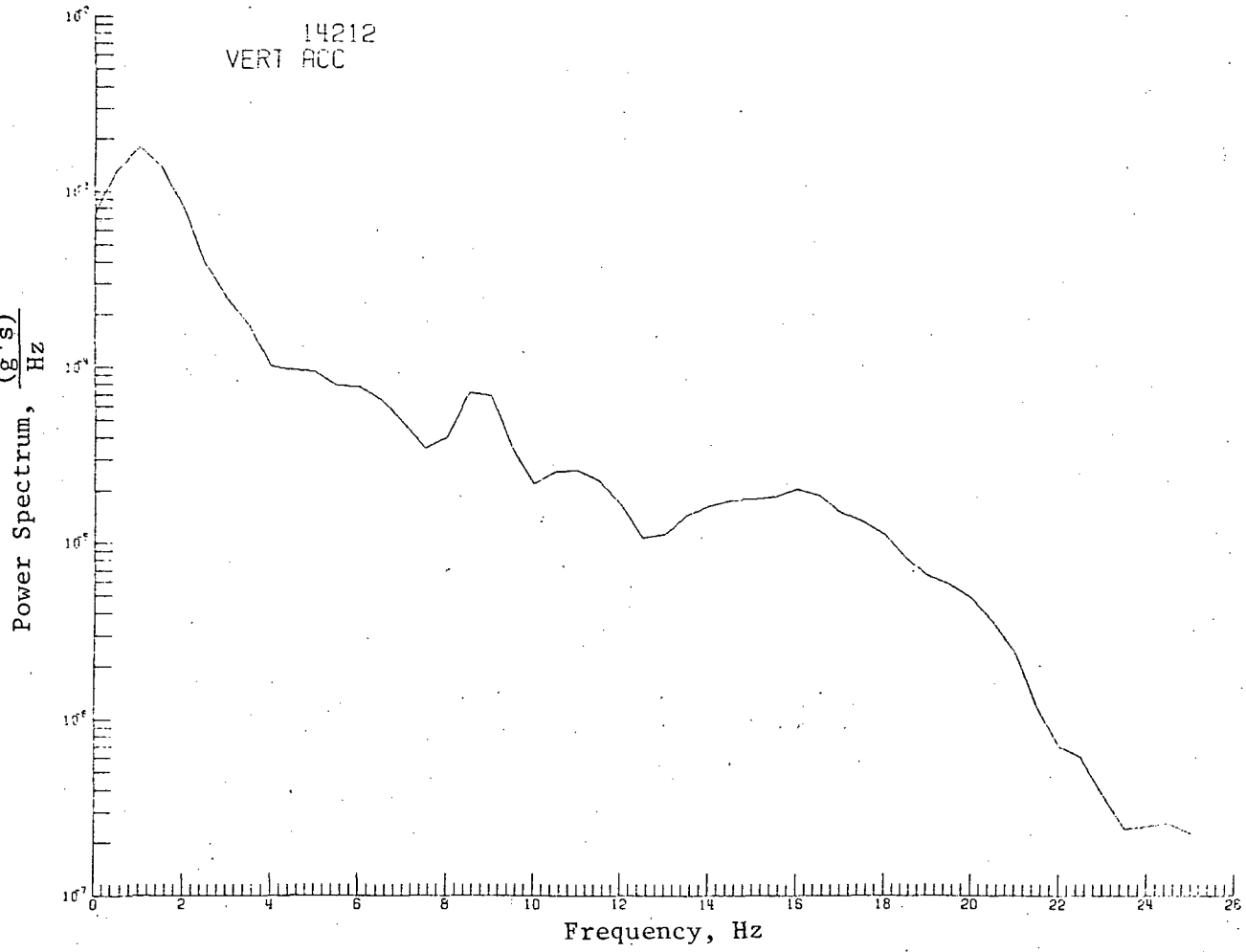

(e) Vertical acceleration power spectrum
(RMS-vertical acceleration 0.0609 g's)

FIGURE 2. Concluded.

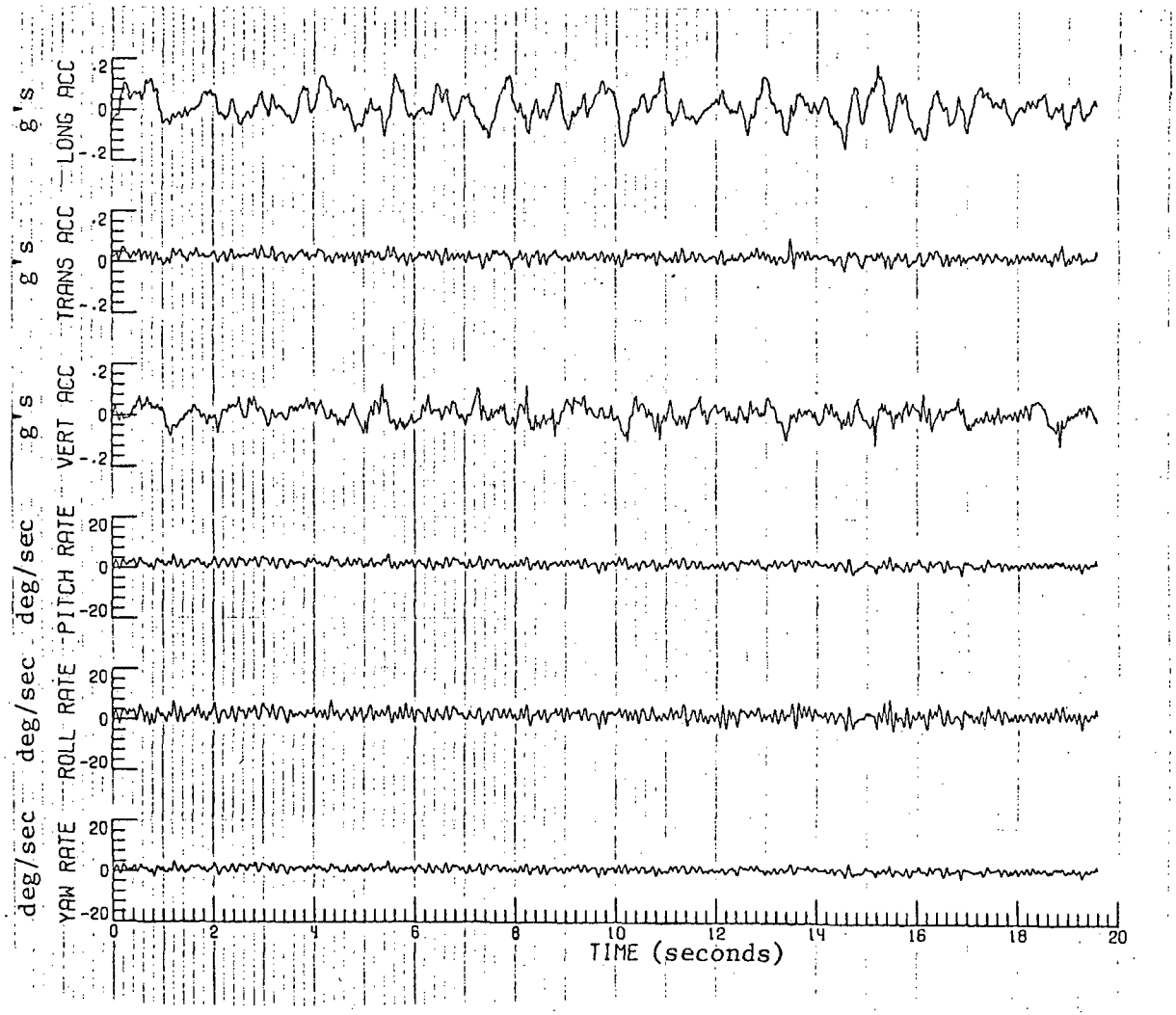

(a) Time histories (RMS-vertical acceleration 0.0331 g's; RMS-longitudinal acceleration 0.0548 g's)

FIGURE 3. MEASURED MOTION CHARACTERISTICS USING AN APPROXIMATELY CONSTANT RMS-LONGITUDINAL ACCELERATION WITH A VARIABLE RMS-VERTICAL ACCELERATION

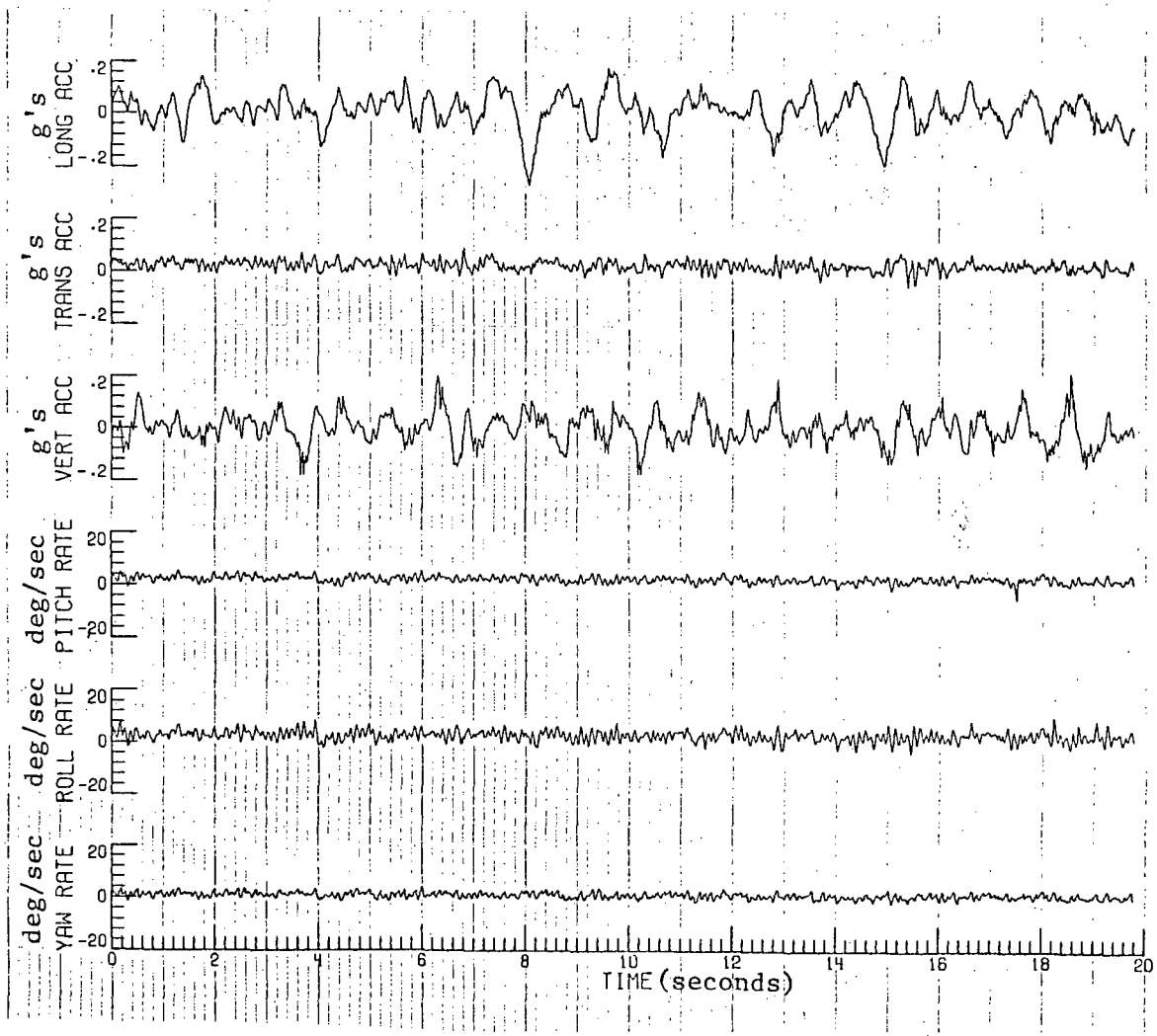

(a) Time histories (RMS-vertical acceleration 0.0583 g's; RMS-longitudinal acceleration 0.0670 g's)

FIGURE 3. Continued.

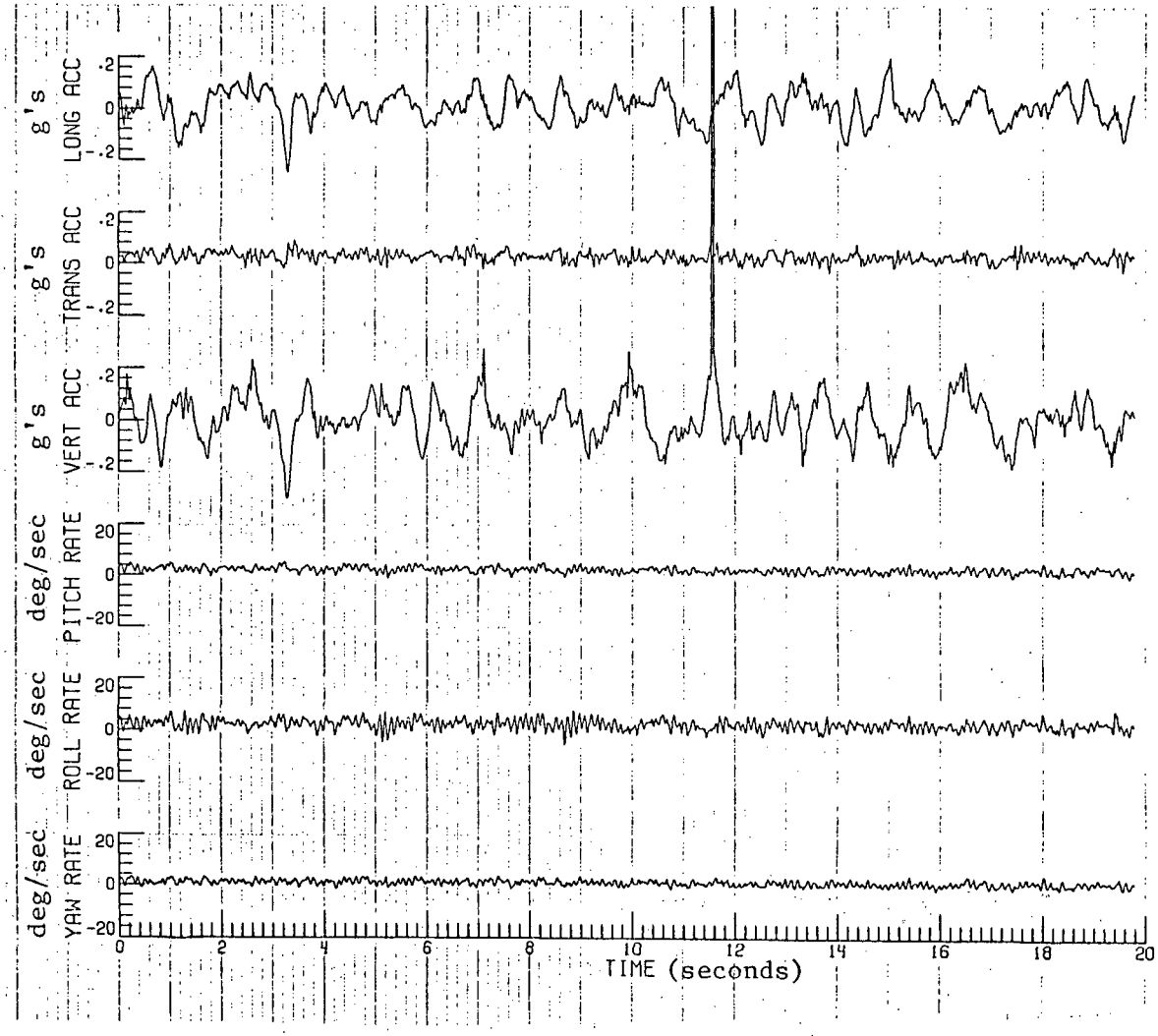

(a) Time histories (RMS-vertical acceleration 0.0819 g's; RMS-longitudinal acceleration 0.0630 g's).

FIGURE 3. Continued.

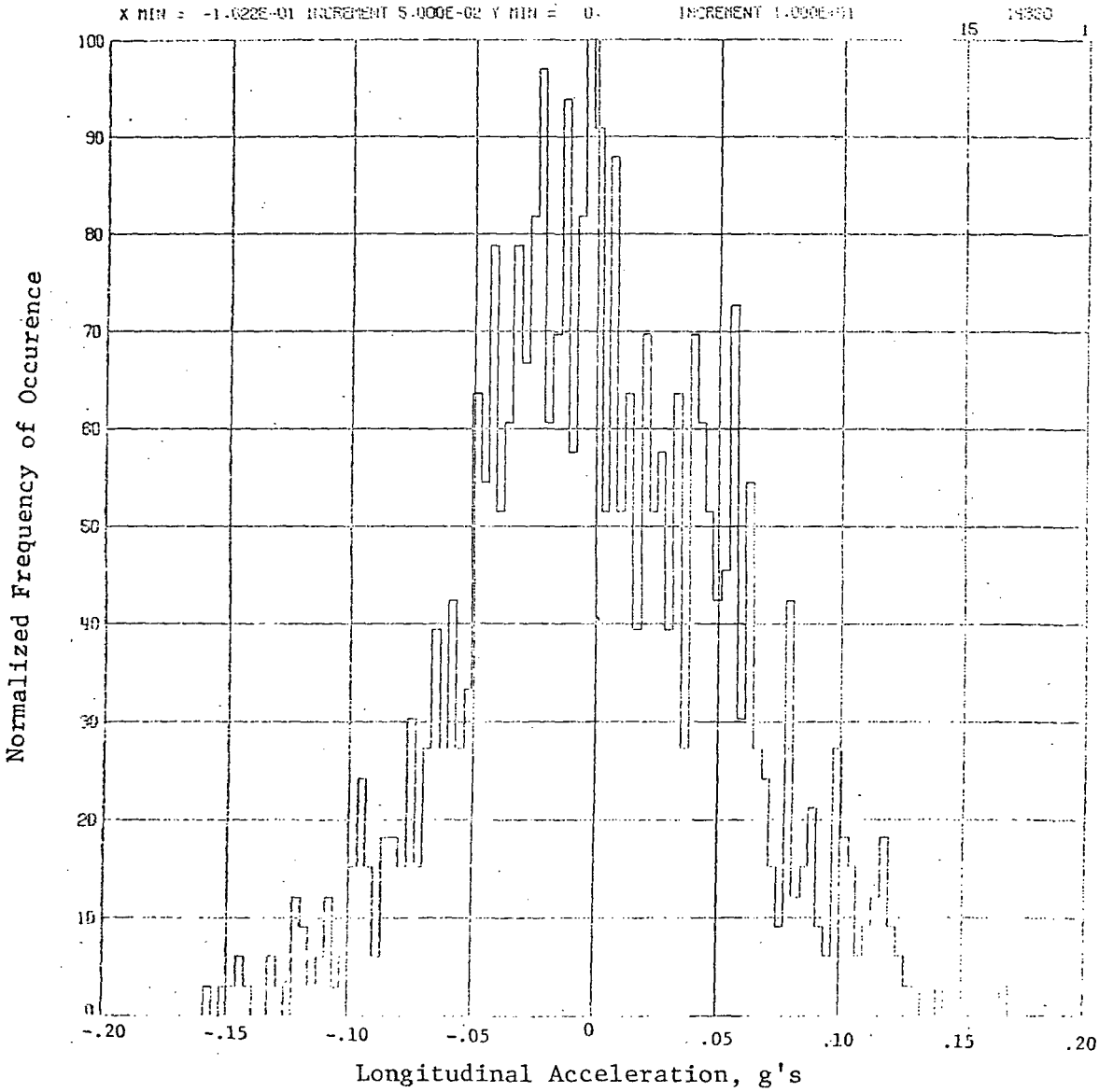

(b) Longitudinal acceleration histogram
(RMS-longitudinal acceleration 0.0548 g's)

FIGURE 3. Continued.

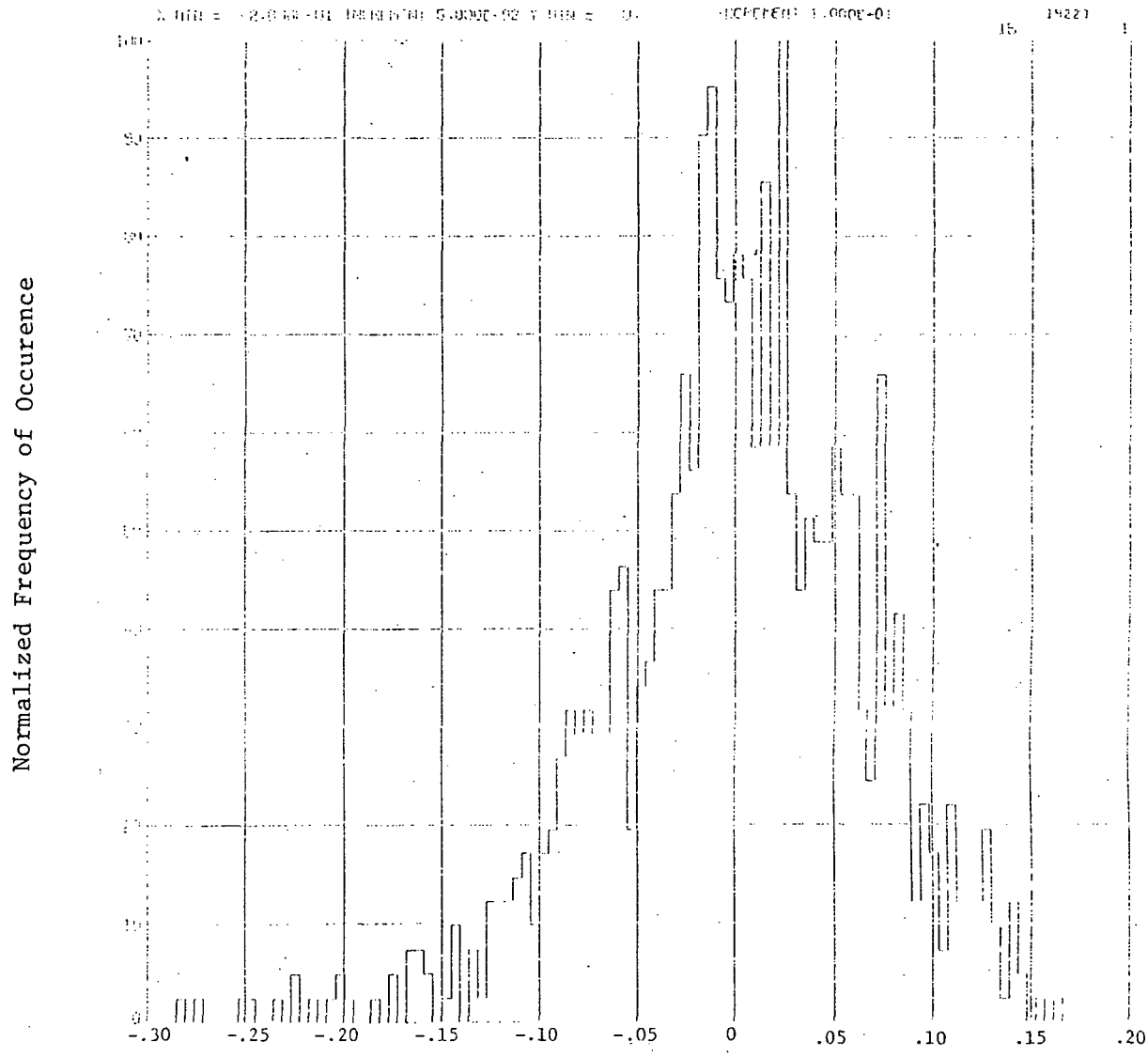

(b) Longitudinal acceleration histogram
(RMS-longitudinal acceleration 0.0670 g's)

FIGURE 3. Continued.

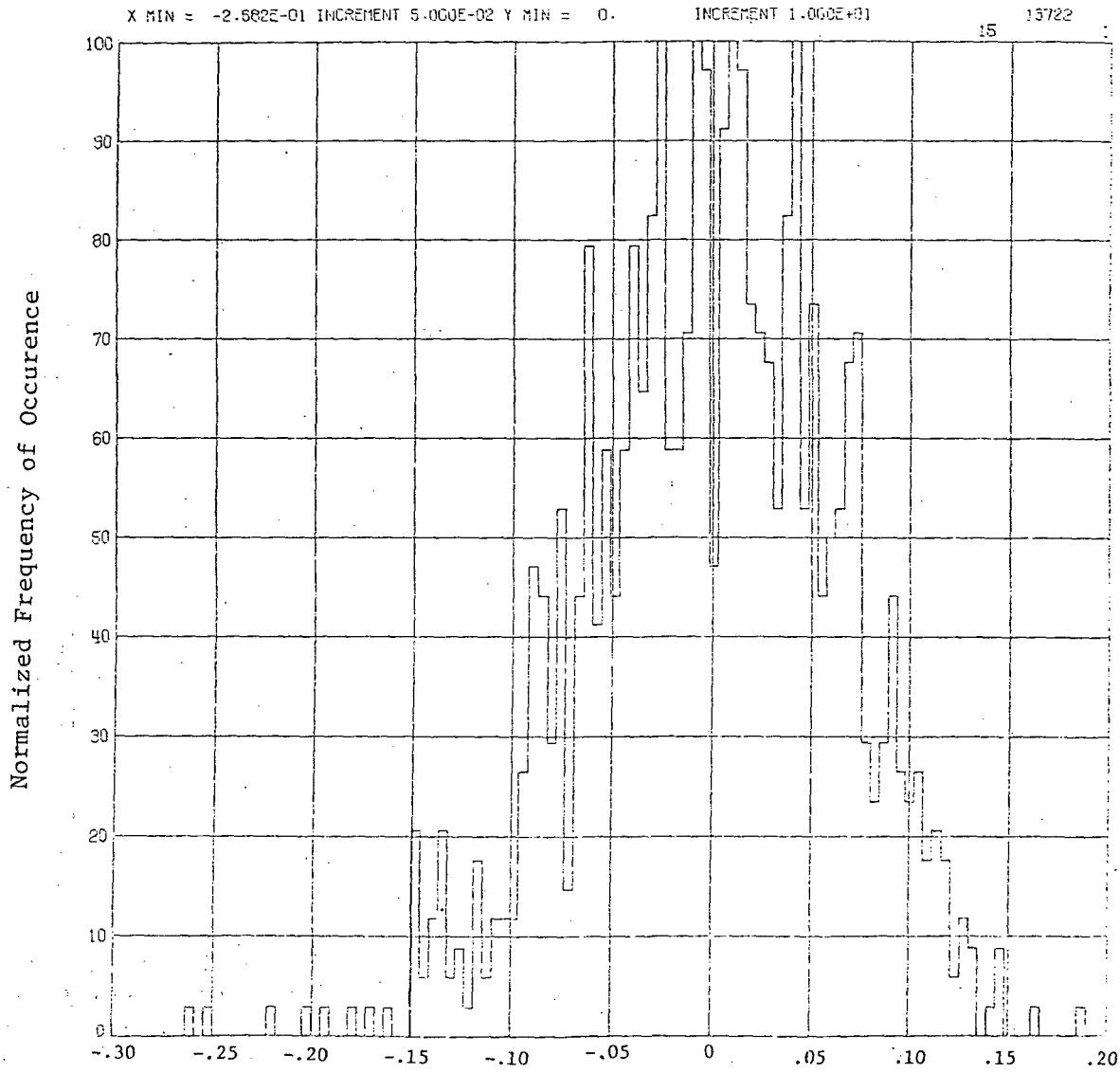

(b) Longitudinal acceleration histogram
(RMS-longitudinal acceleration 0.0630 g's)

FIGURE 3. Continued.

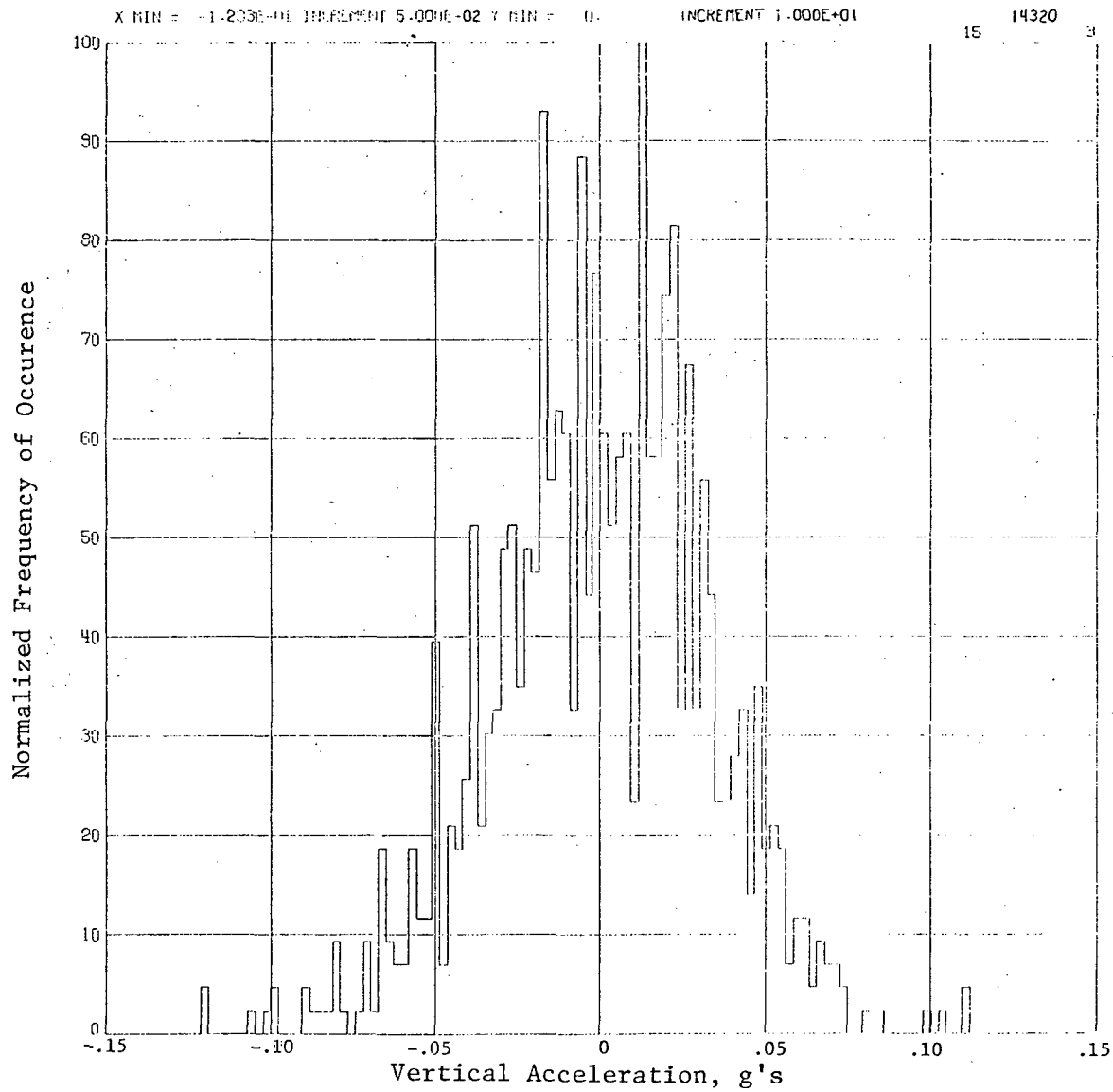

(c) Vertical acceleration histogram
(RMS-vertical acceleration 0.0331 g's)

FIGURE 3. Continued.

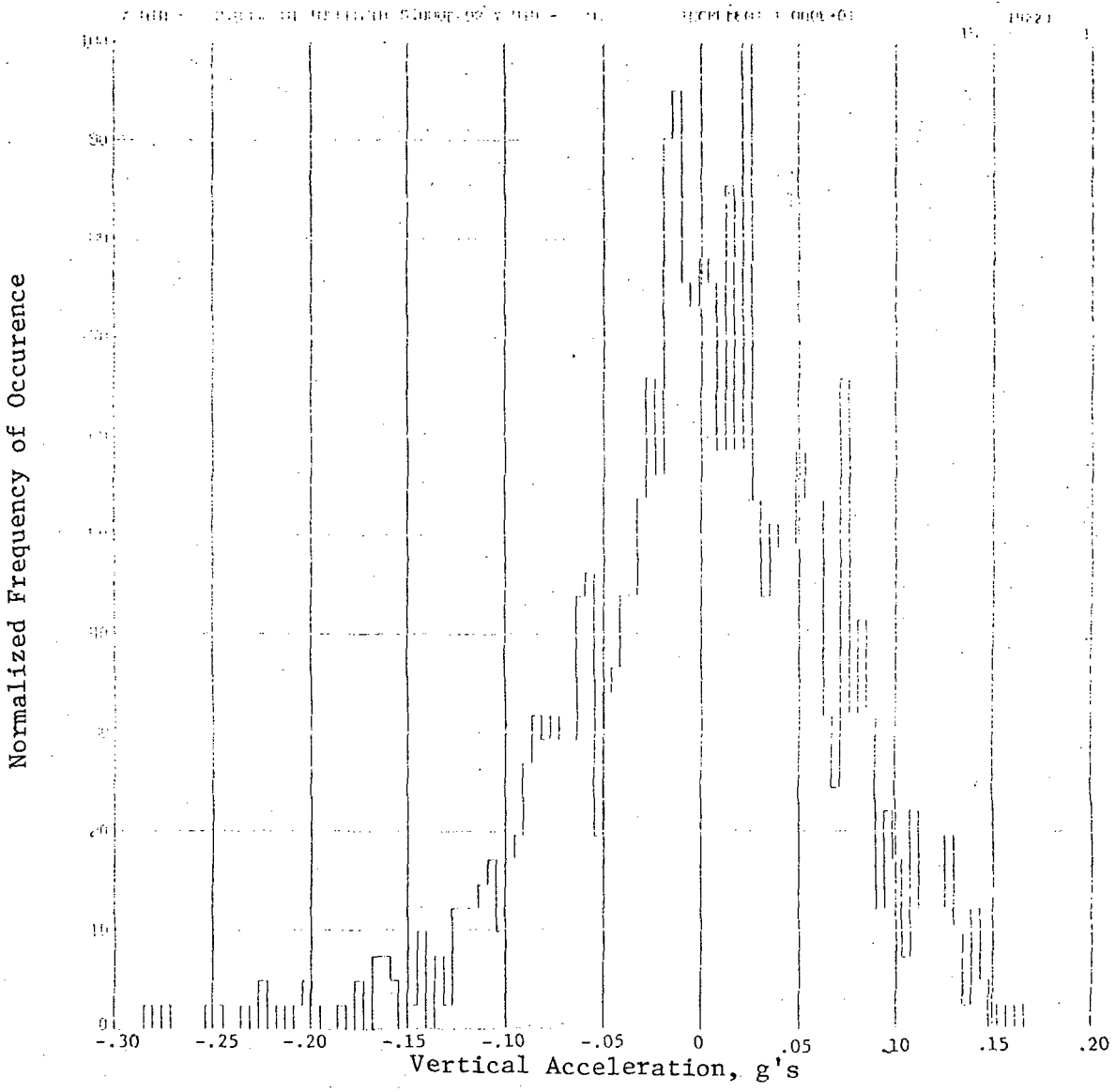

(c) Vertical acceleration histogram
(RMS-vertical acceleration 0.0583 g's)

FIGURE 3. Continued.

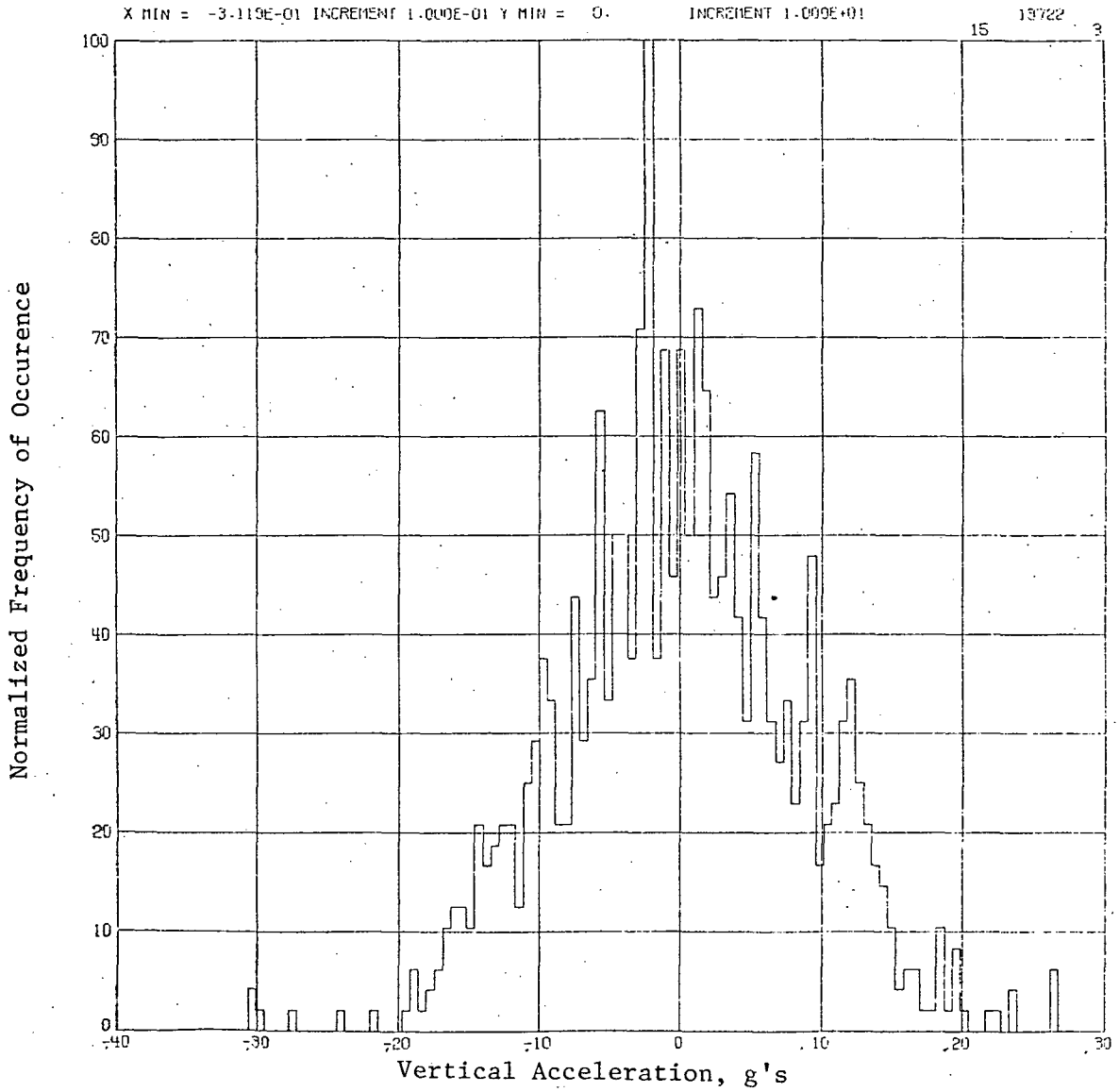

(c) Vertical acceleration histogram
(RMS-vertical acceleration 0.0819 g's)

FIGURE 3. Continued.

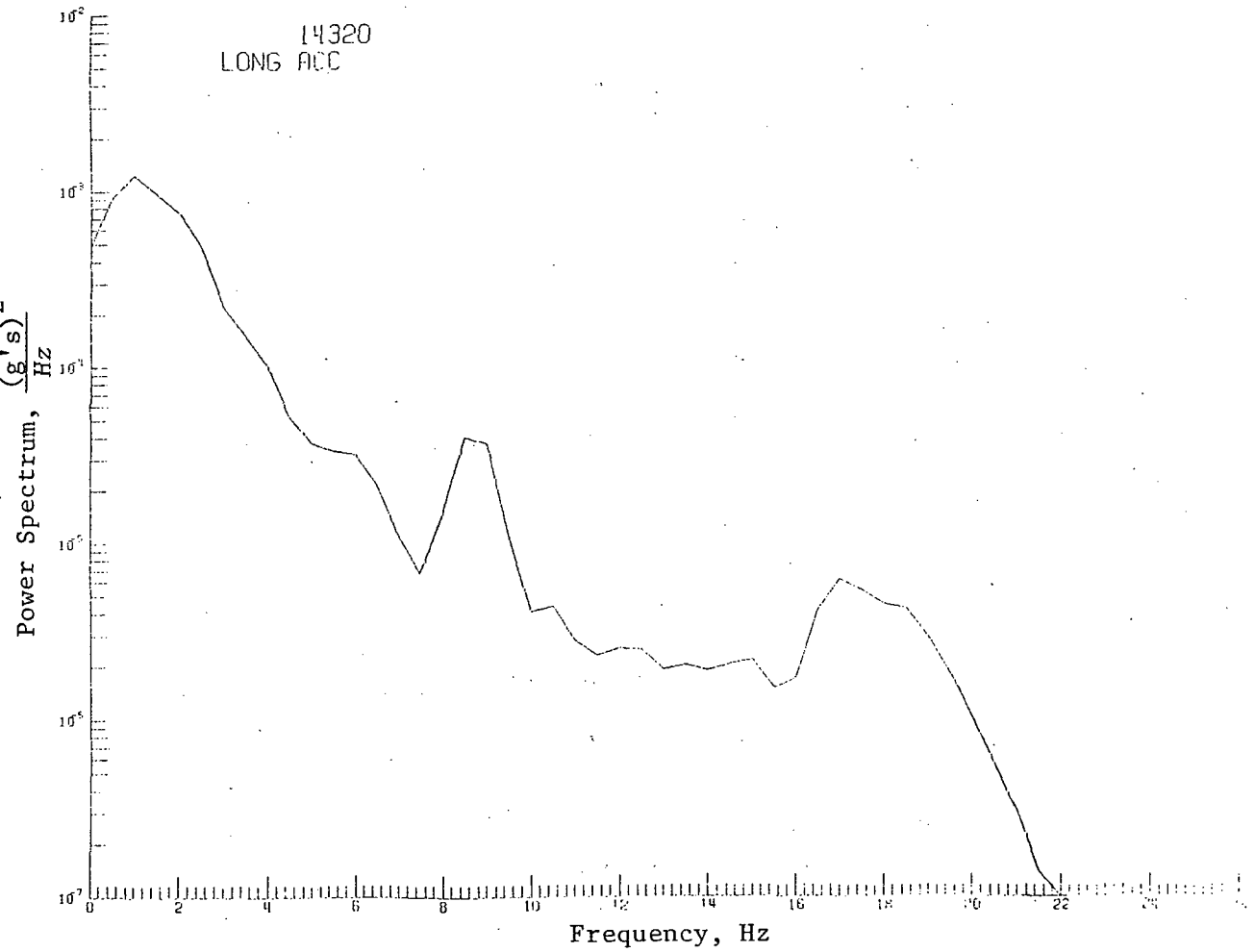

(d) Longitudinal acceleration power spectrum
(RMS-longitudinal acceleration 0.0548 g's)

FIGURE 3. Continued.

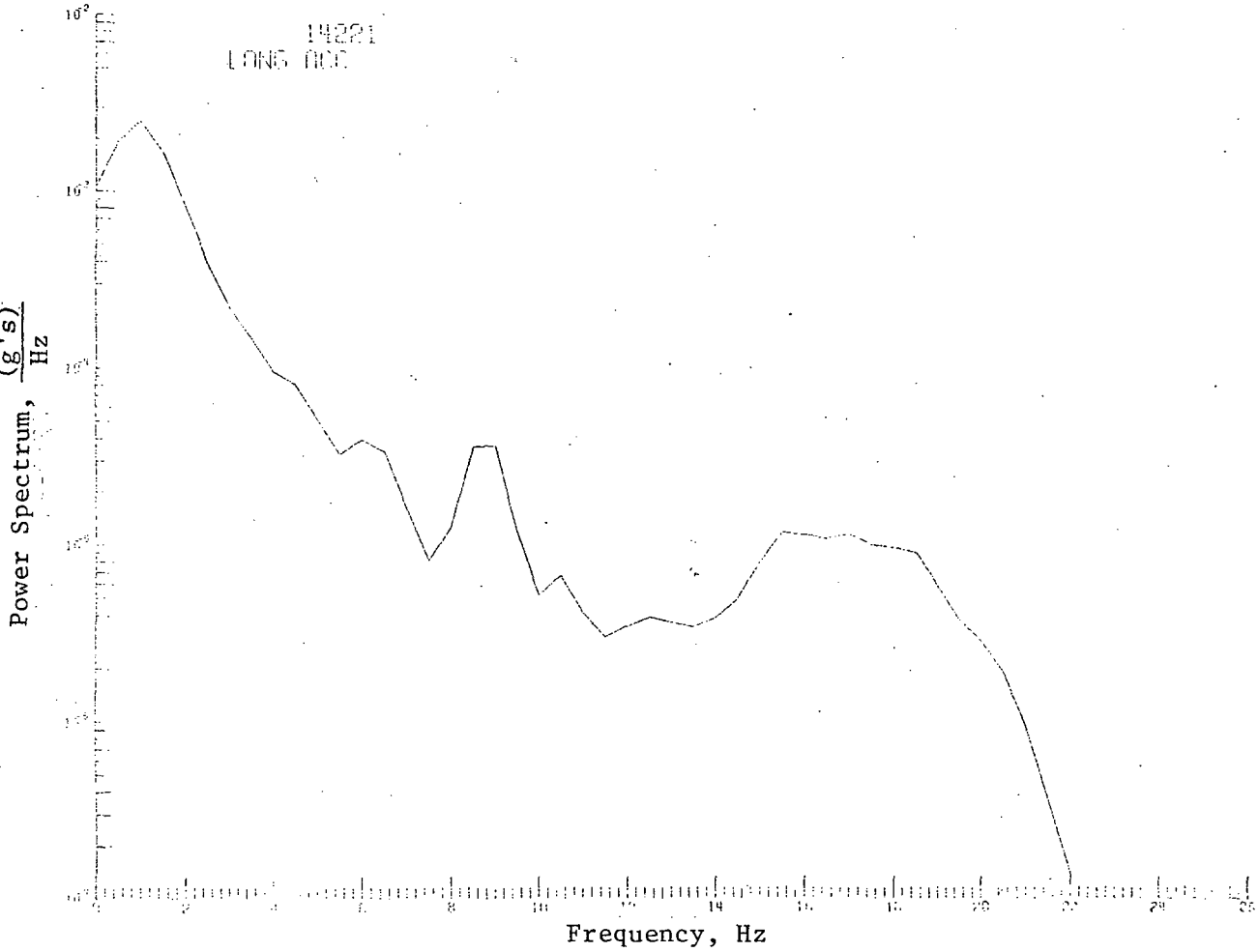

(d) Longitudinal acceleration power spectrum
(RMS-longitudinal acceleration 0.0670 g's)

FIGURE 3. Continued.

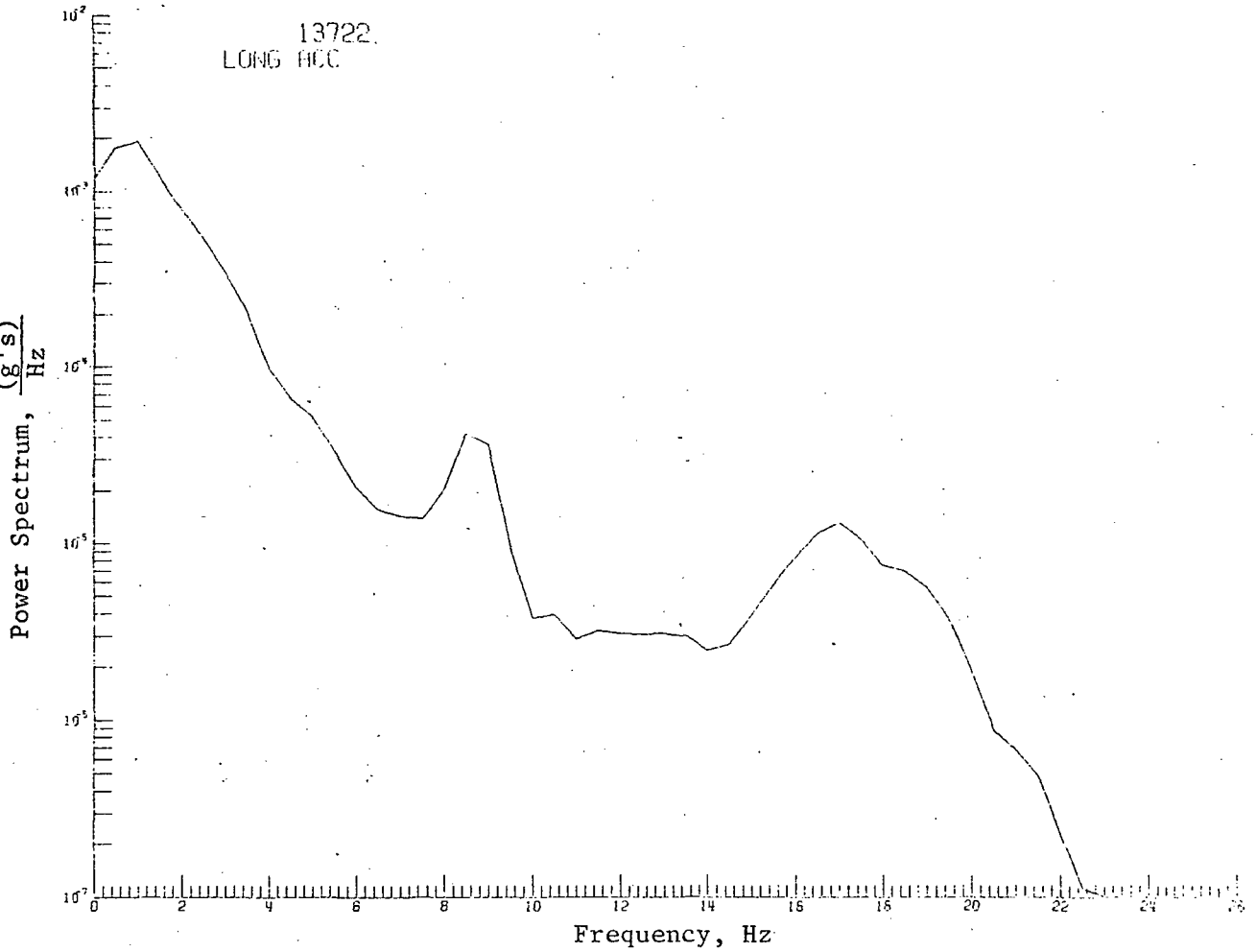

(d) Longitudinal acceleration power spectrum
(RMS-longitudinal acceleration 0.0630 g's)

FIGURE 3. Continued.

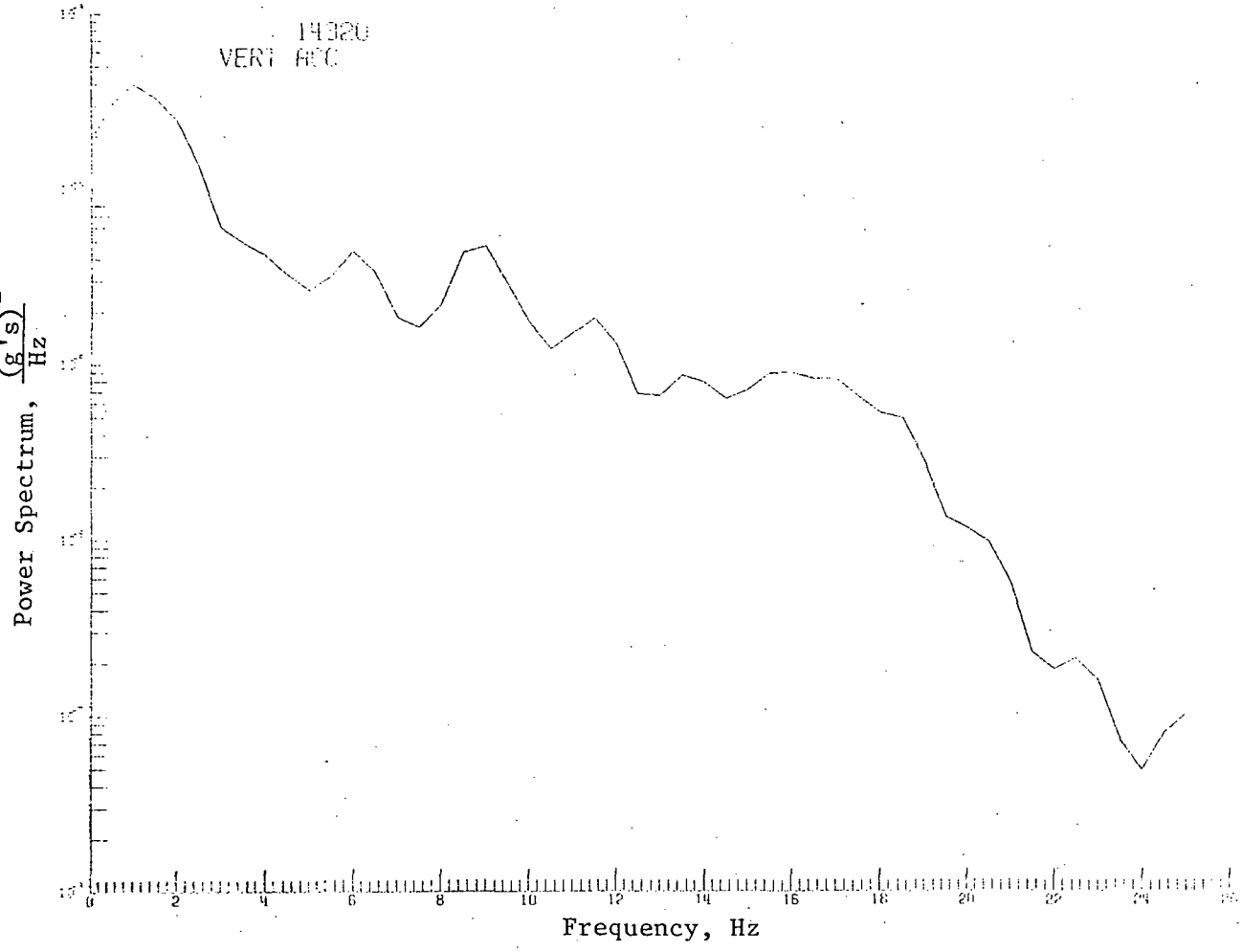

(e) Vertical acceleration power spectrum
(RMS-vertical acceleration 0.0331 g's)

FIGURE 3. Continued.

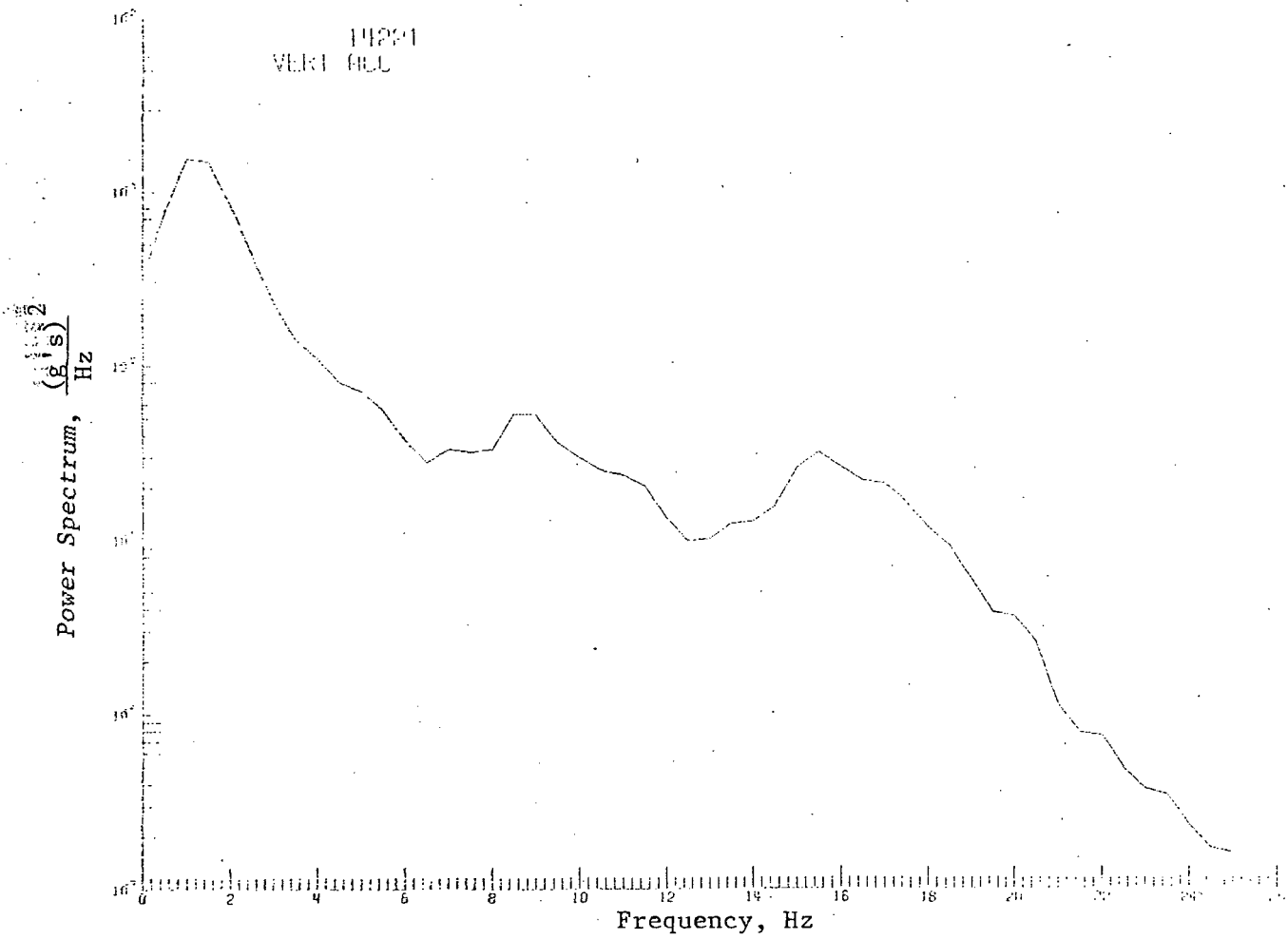

(e) Vertical acceleration power spectrum
(RMS-vertical acceleration 0.0583 g's)

FIGURE 3. Continued.

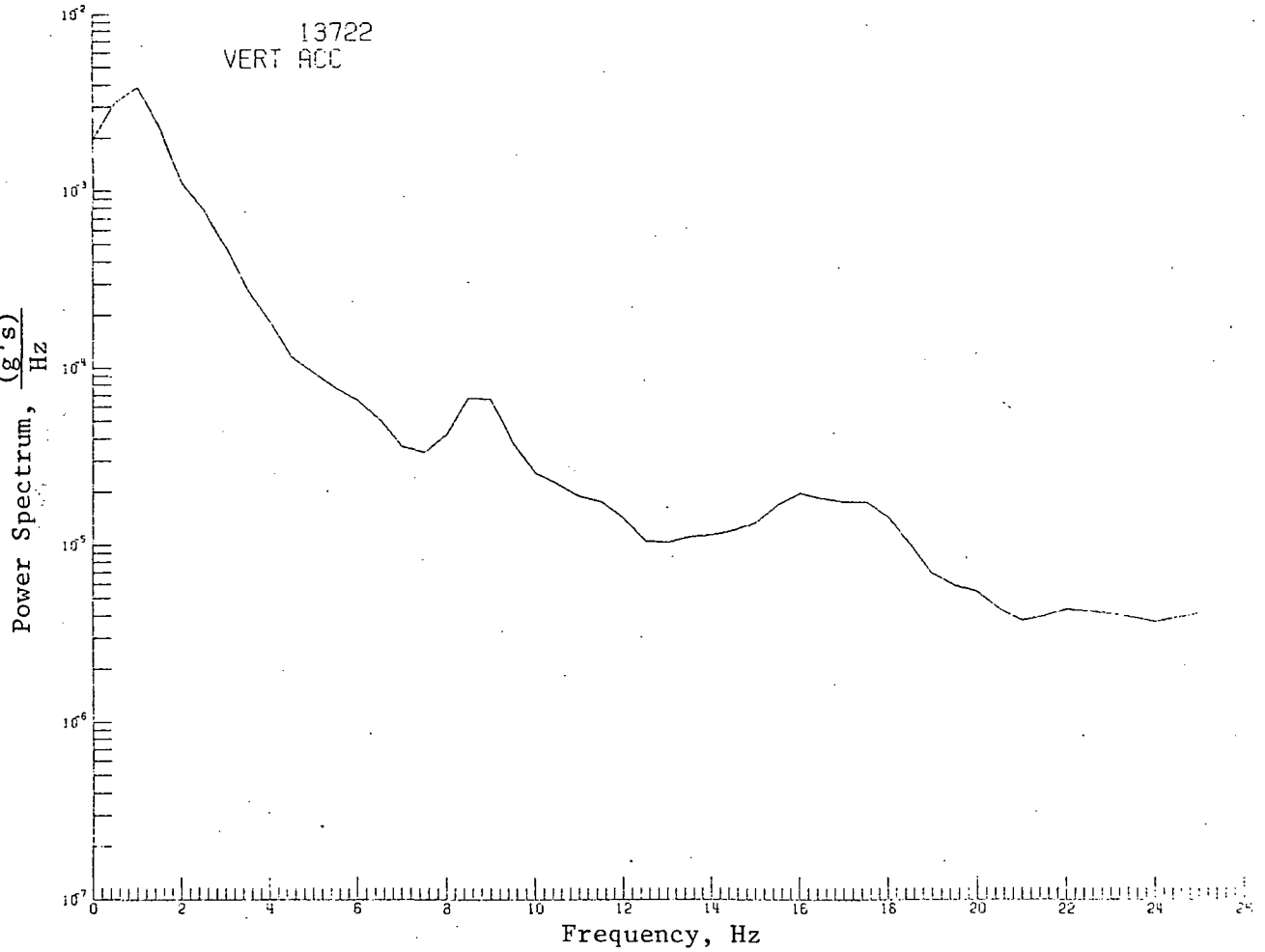

(e) Vertical acceleration power spectrum
(RMS-vertical acceleration 0.0819 g's)

FIGURE 3. Concluded.

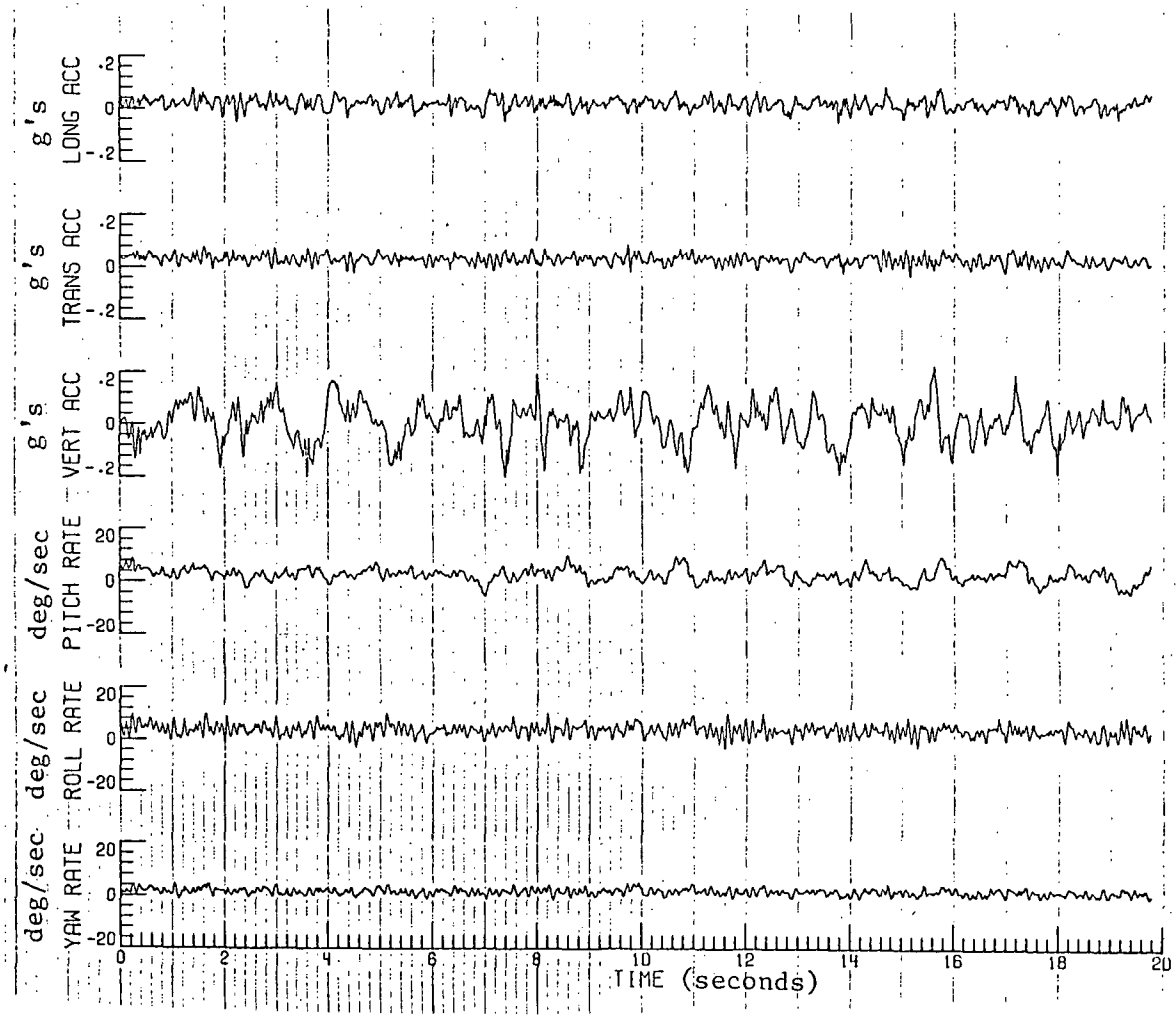

(a) Time histories (RMS-pitching velocity 2.4632 deg/sec; RMS-vertical acceleration 0.0720 g's)

FIGURE 4. MEASURED MOTION CHARACTERISTICS USING AN APPROXIMATELY CONSTANT RMS-VERTICAL ACCELERATION WITH A VARIABLE RMS-PITCHING VELOCITY

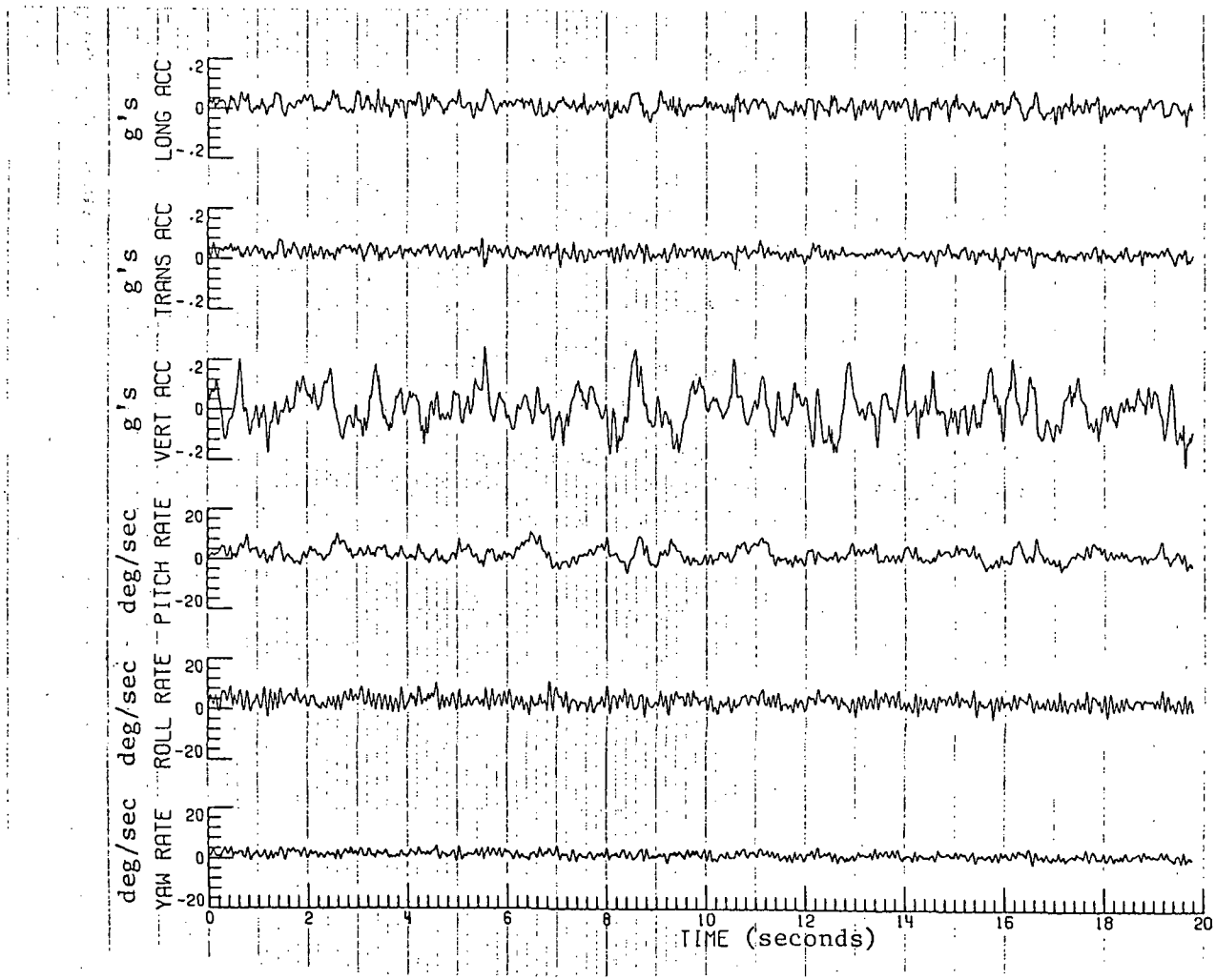

(a) Time histories (RMS-pitching velocity 2.8574 deg/sec; RMS-vertical acceleration 0.0762 g's)

FIGURE 4. Continued.

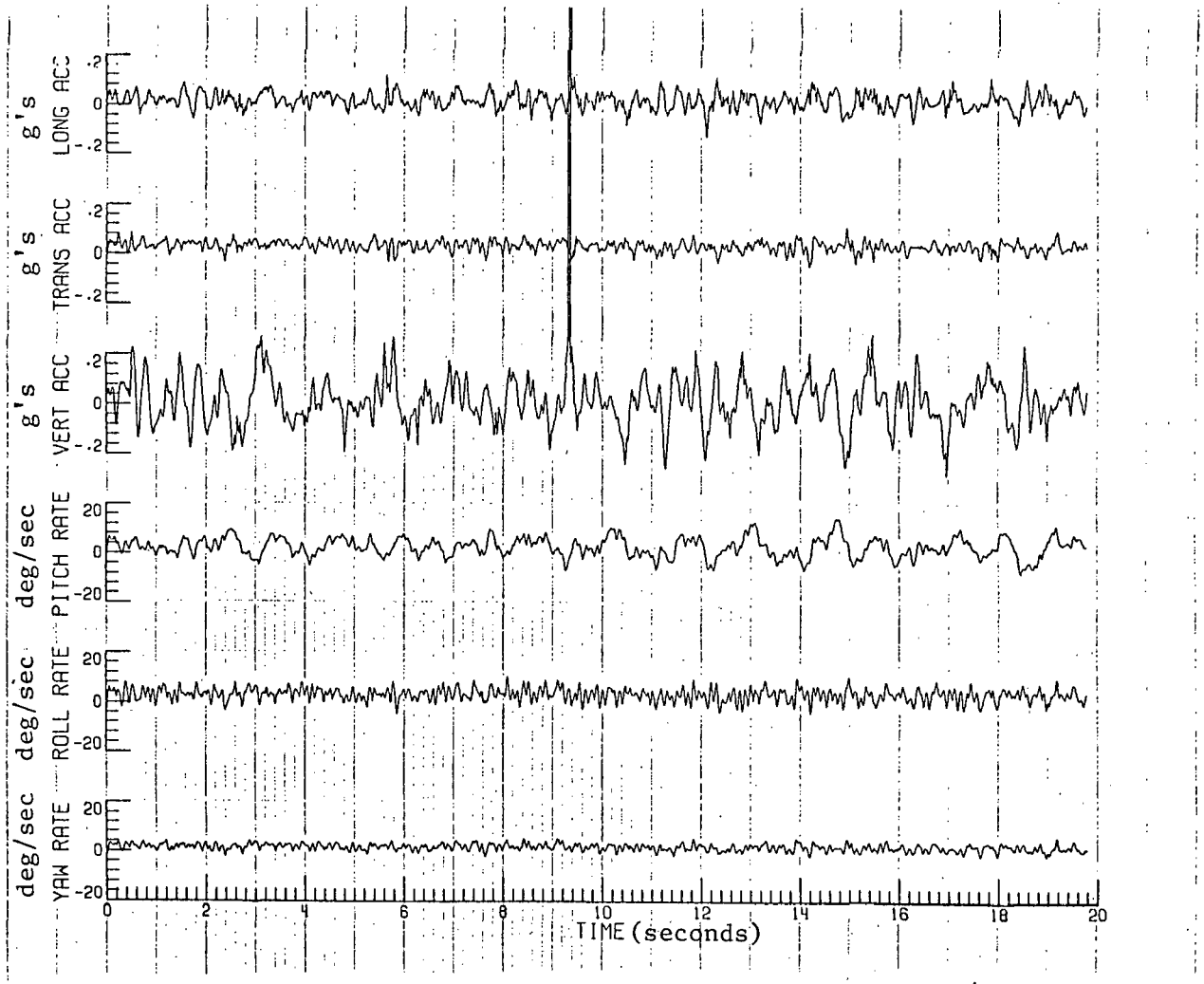

(a) Time histories (RMS-pitching velocity 3.6558 deg/sec; RMS-vertical acceleration 0.0892 g's)

FIGURE 4. Continued.

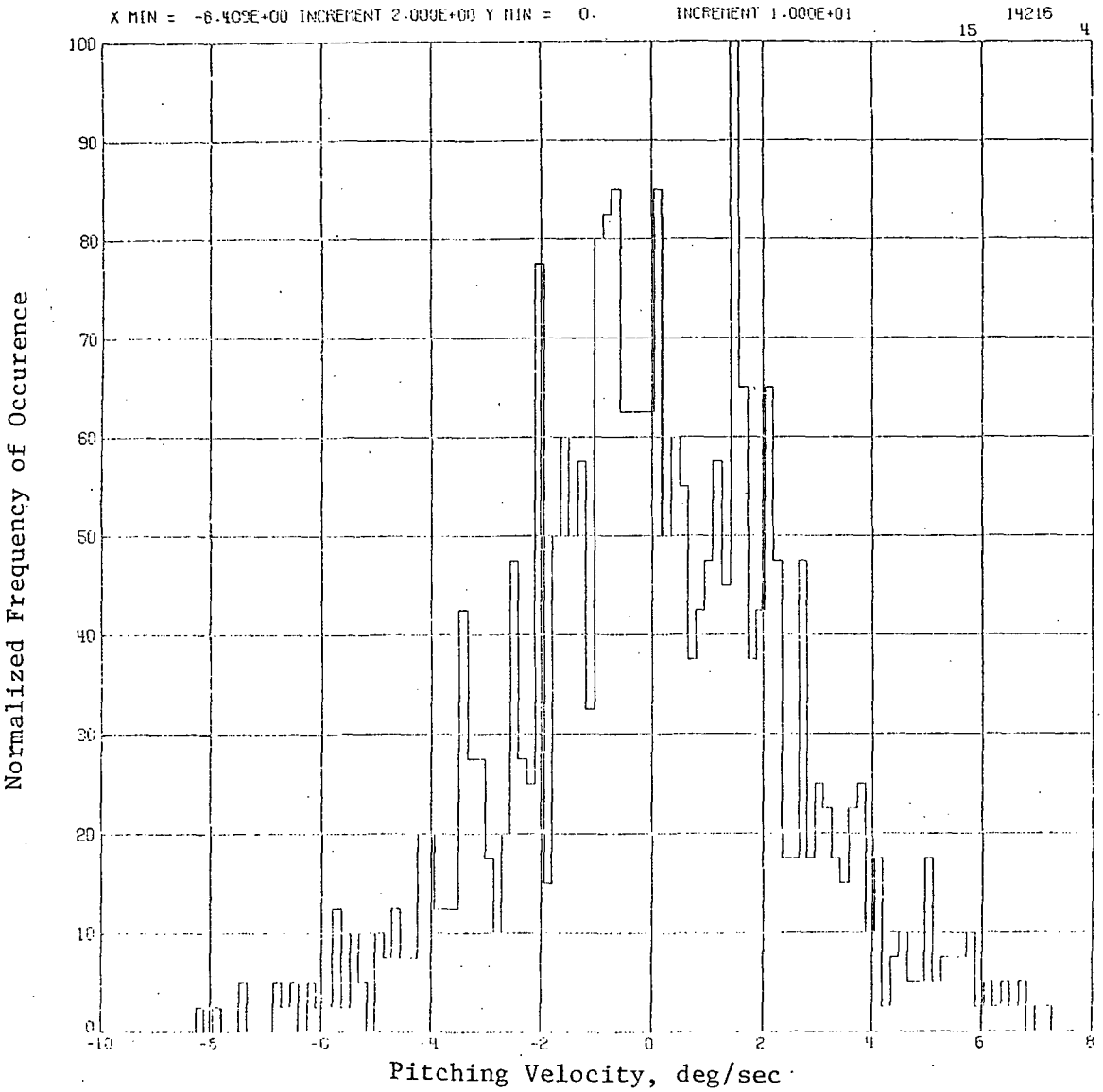

(b) Pitching velocity histogram
(RMS-pitching velocity 2.4632 deg/sec)

FIGURE 4. Continued.

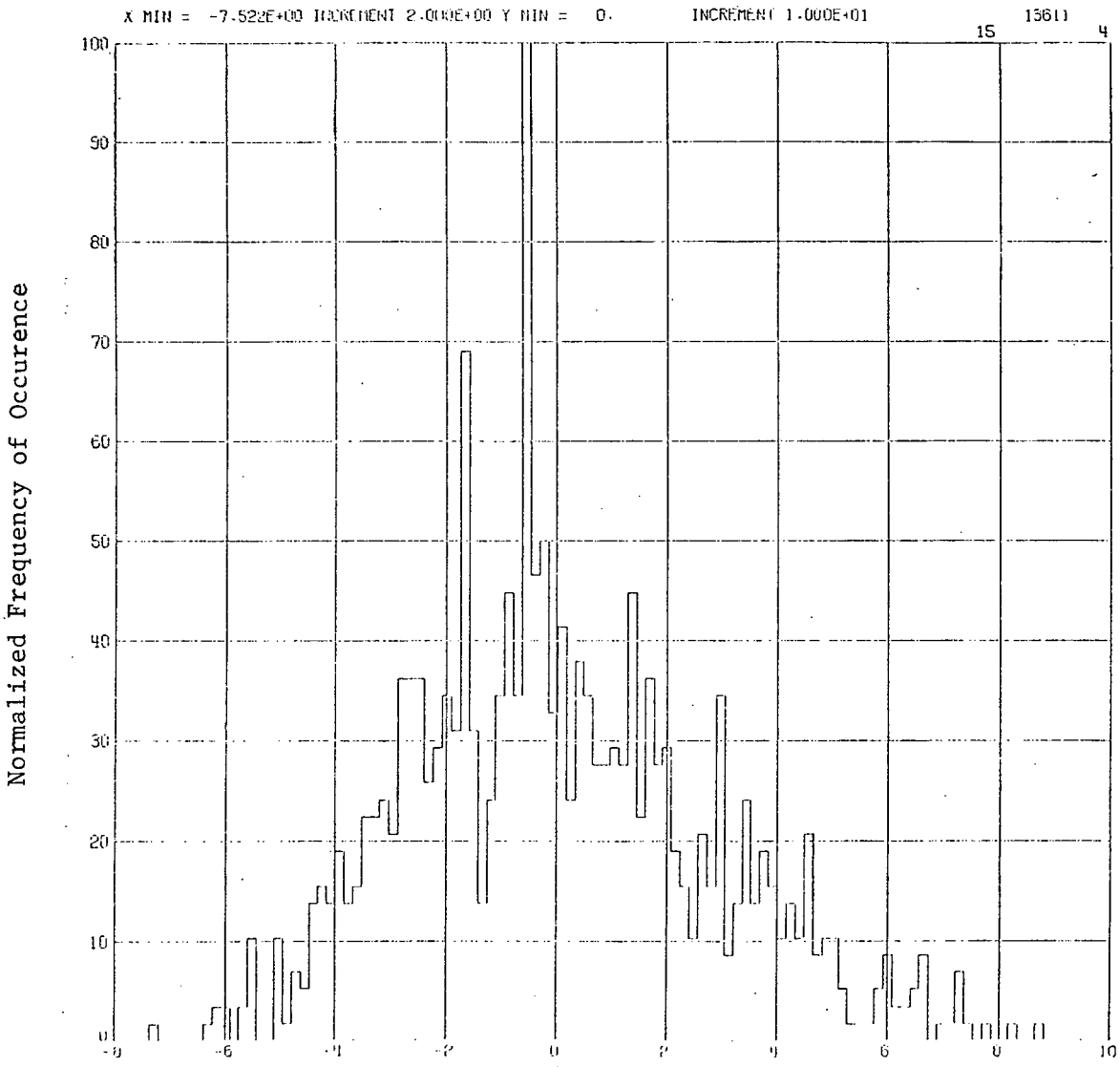

(b) Pitching velocity histogram
(RMS-pitching velocity 2.8574 deg/sec)

FIGURE 4. Continued.

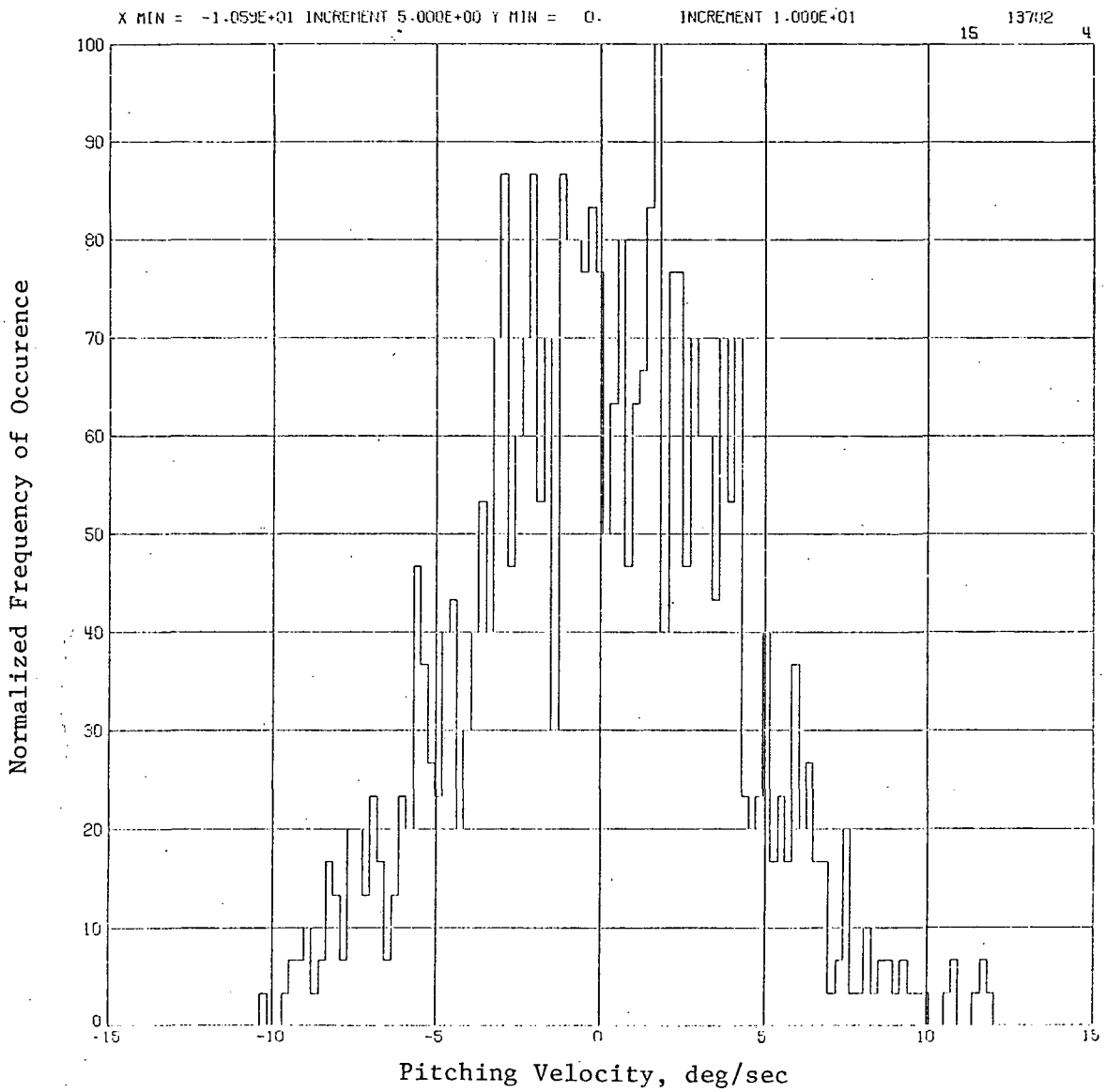

(b) Pitching velocity histogram
(RMS-pitching velocity 3.6558 deg/sec)

FIGURE 4. Continued.

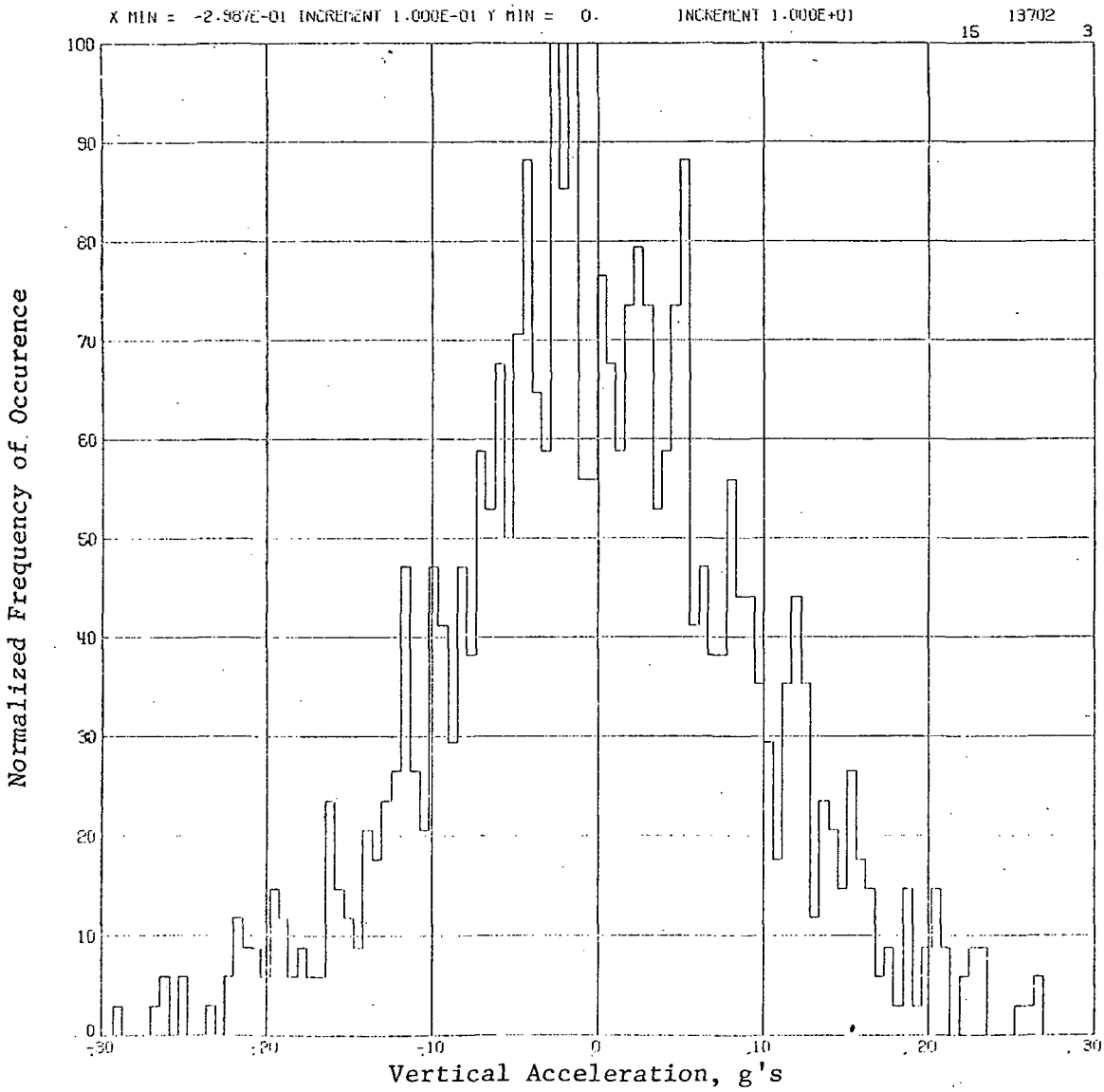

(c) Vertical acceleration histogram
(RMS-vertical acceleration 0.0720 g's)

FIGURE 4. Continued.

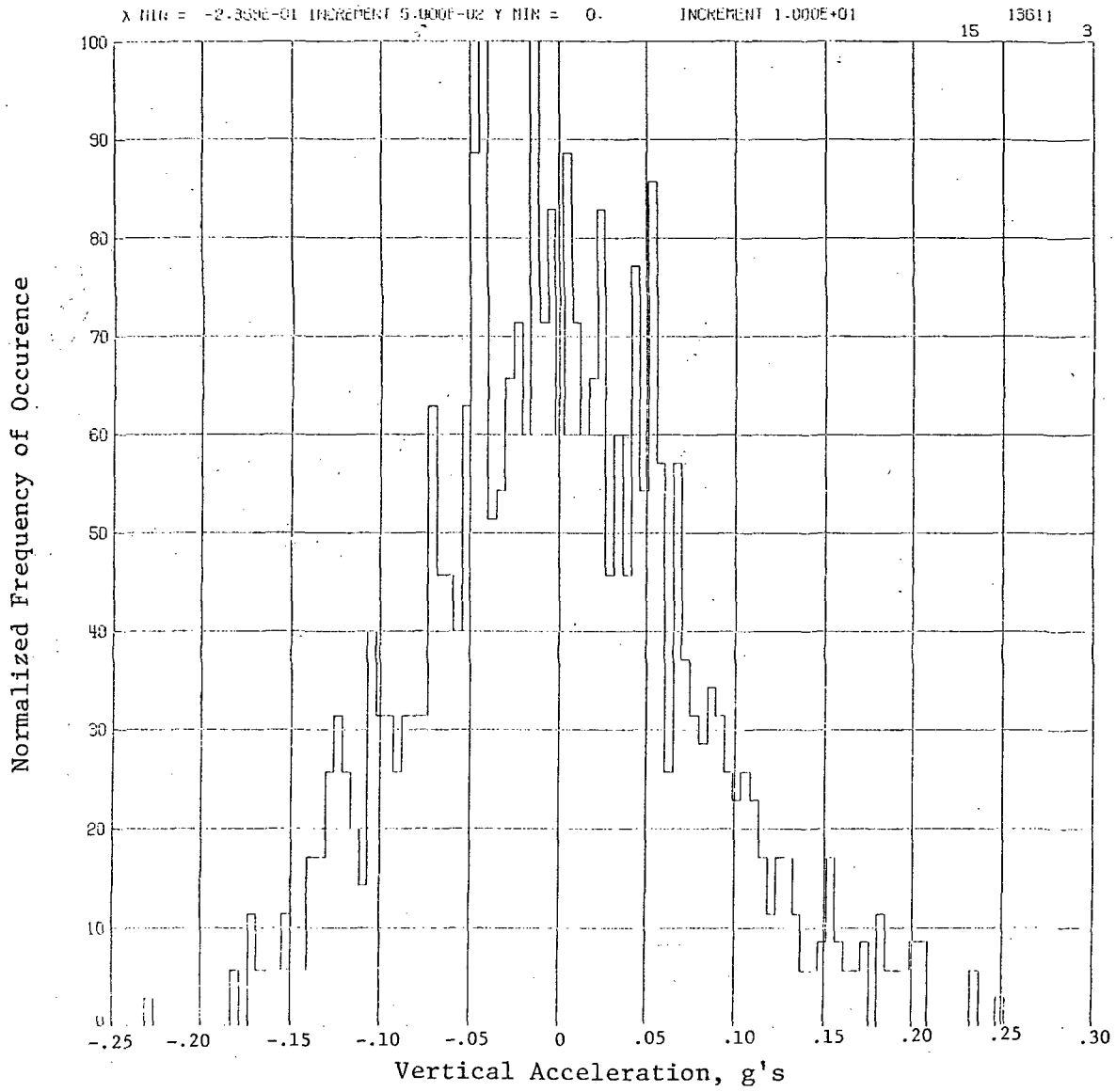

(c) Vertical acceleration histogram
(RMS-vertical acceleration 0.0762 g's)

FIGURE 4. Continued.

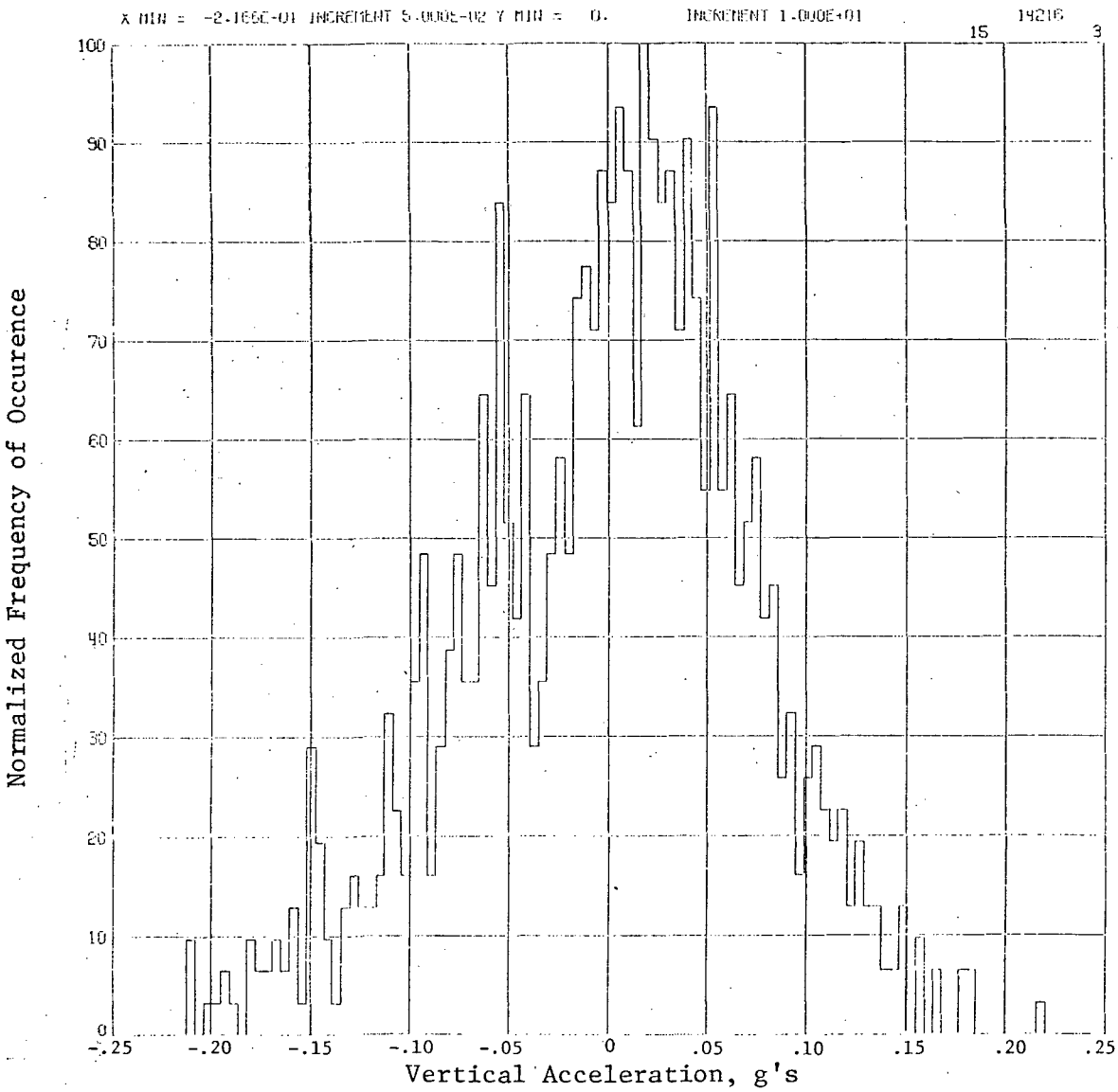

(c) Vertical acceleration histogram
(RMS-vertical acceleration 0.0892 g's)

FIGURE 4. Continued.

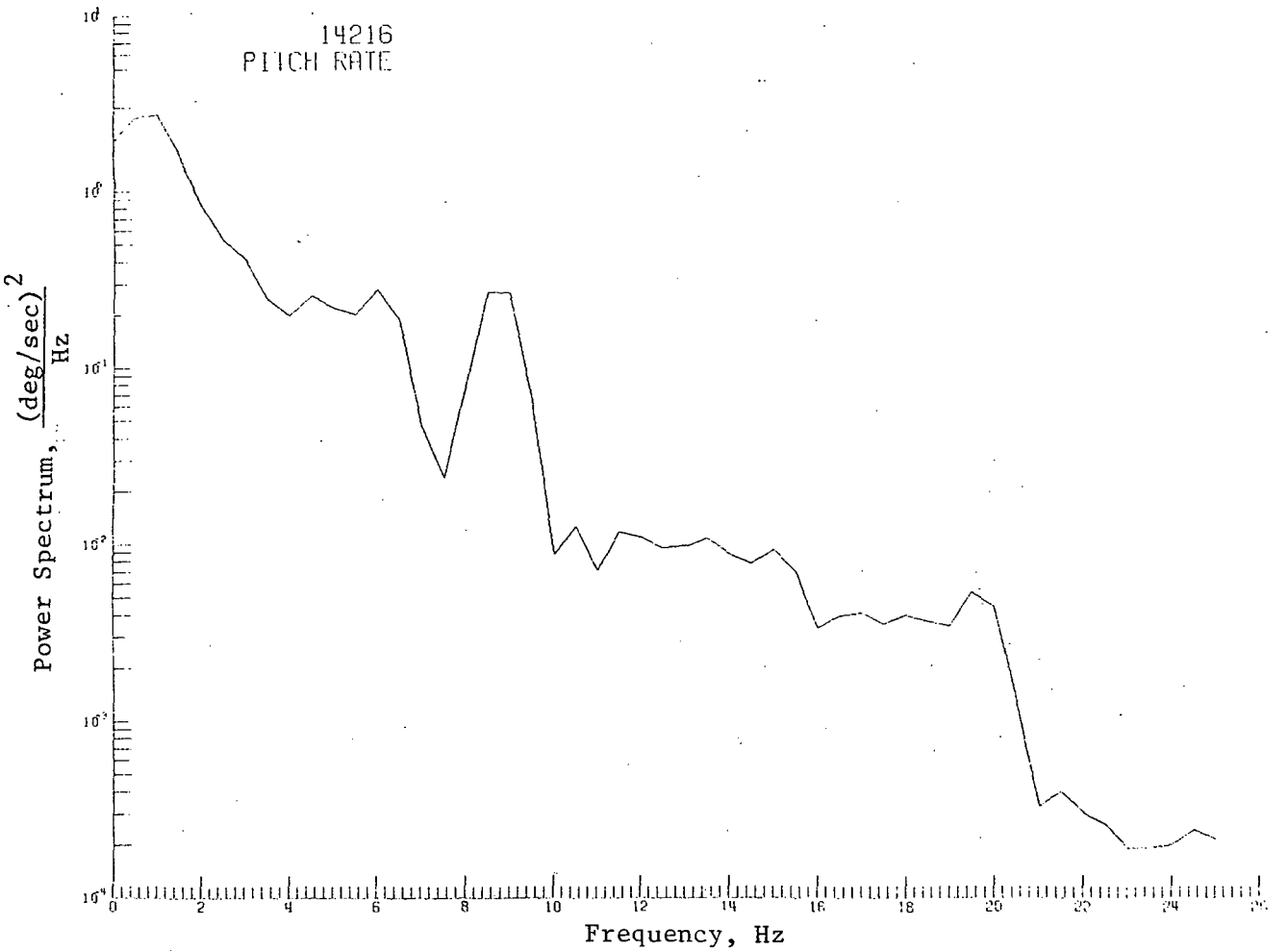

(d) Pitching velocity power spectrum
(RMS-pitching velocity 2.4632 deg/sec)

FIGURE 4. Continued.

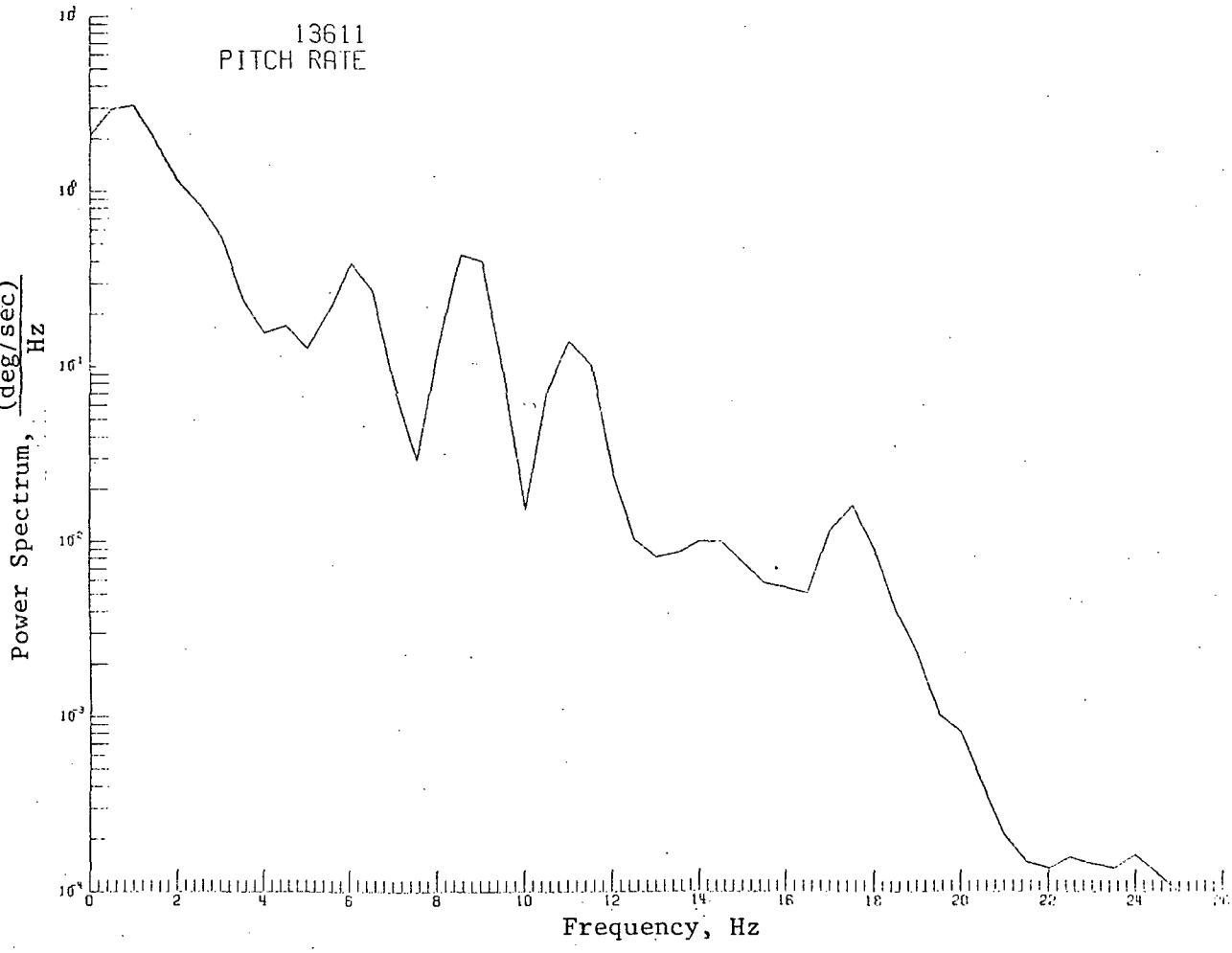

(d) Pitching velocity power spectrum
(RMS-pitching velocity 2.8574 deg/sec)

FIGURE 4. Continued.

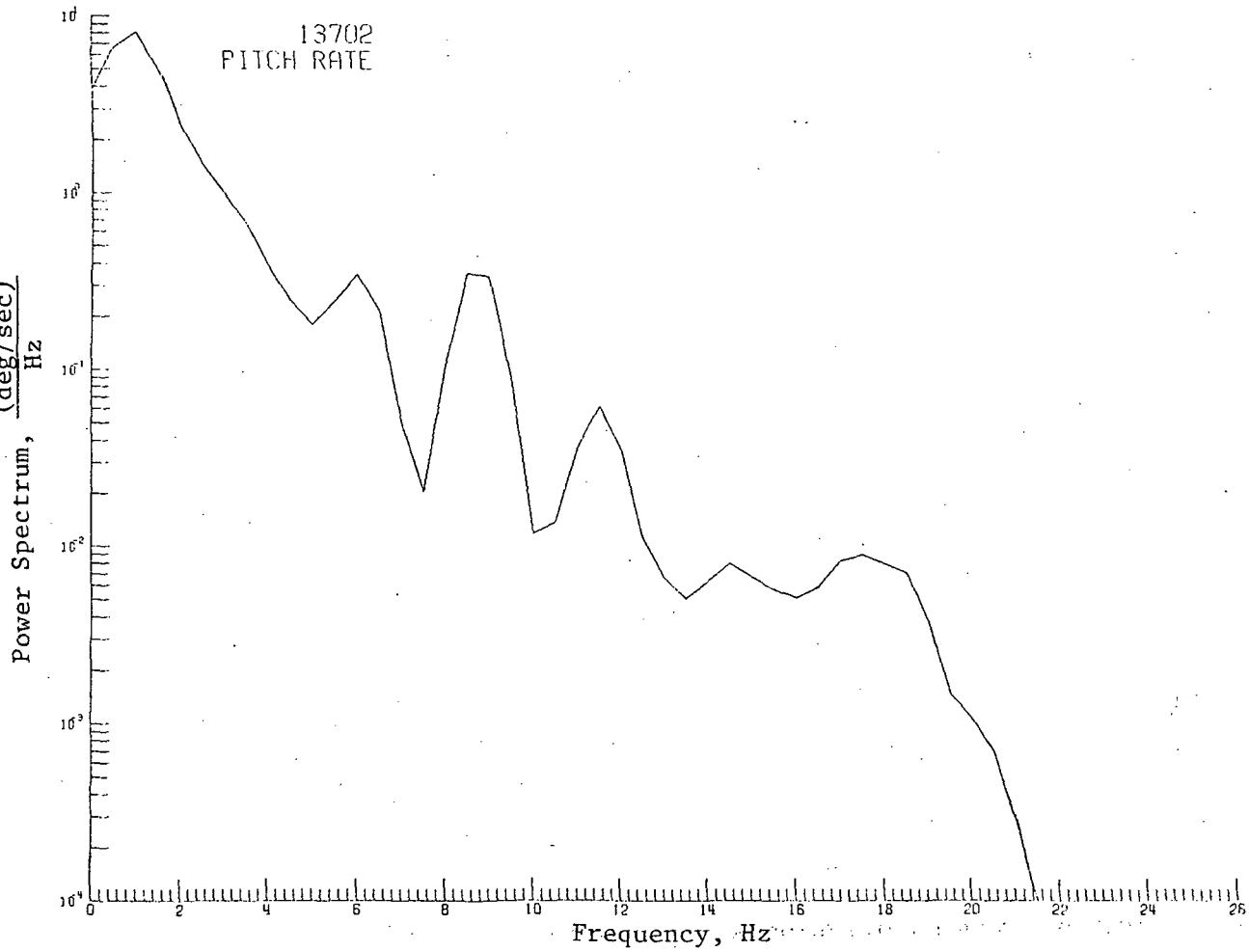

(d) Pitching velocity power spectrum
(RMS-pitching velocity 3.6558 deg/sec)

FIGURE 4. Continued.

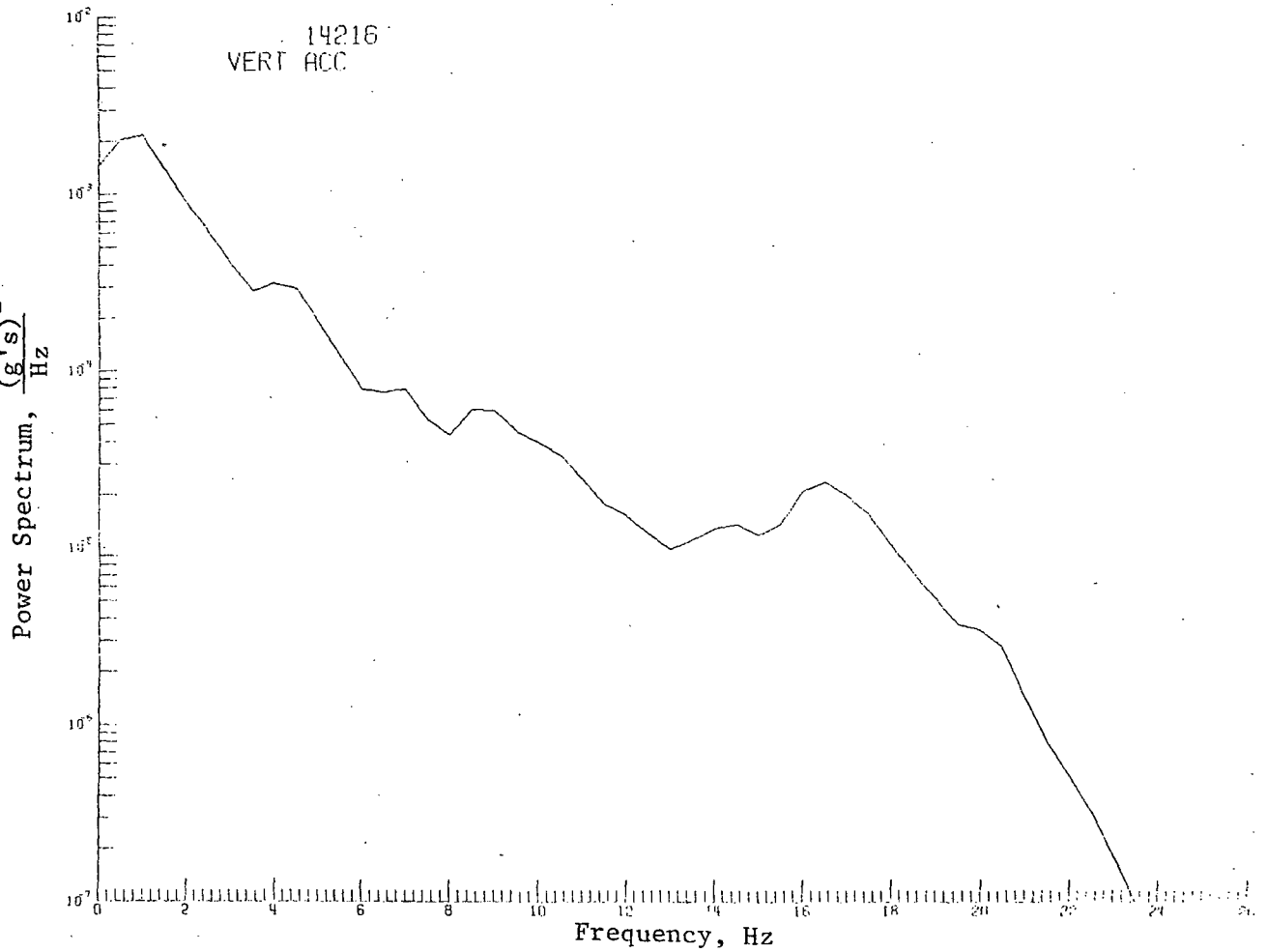

(e) Vertical Acceleration power spectrum
(RMS-vertical acceleration 0.0720 g's)

FIGURE 4. Continued.

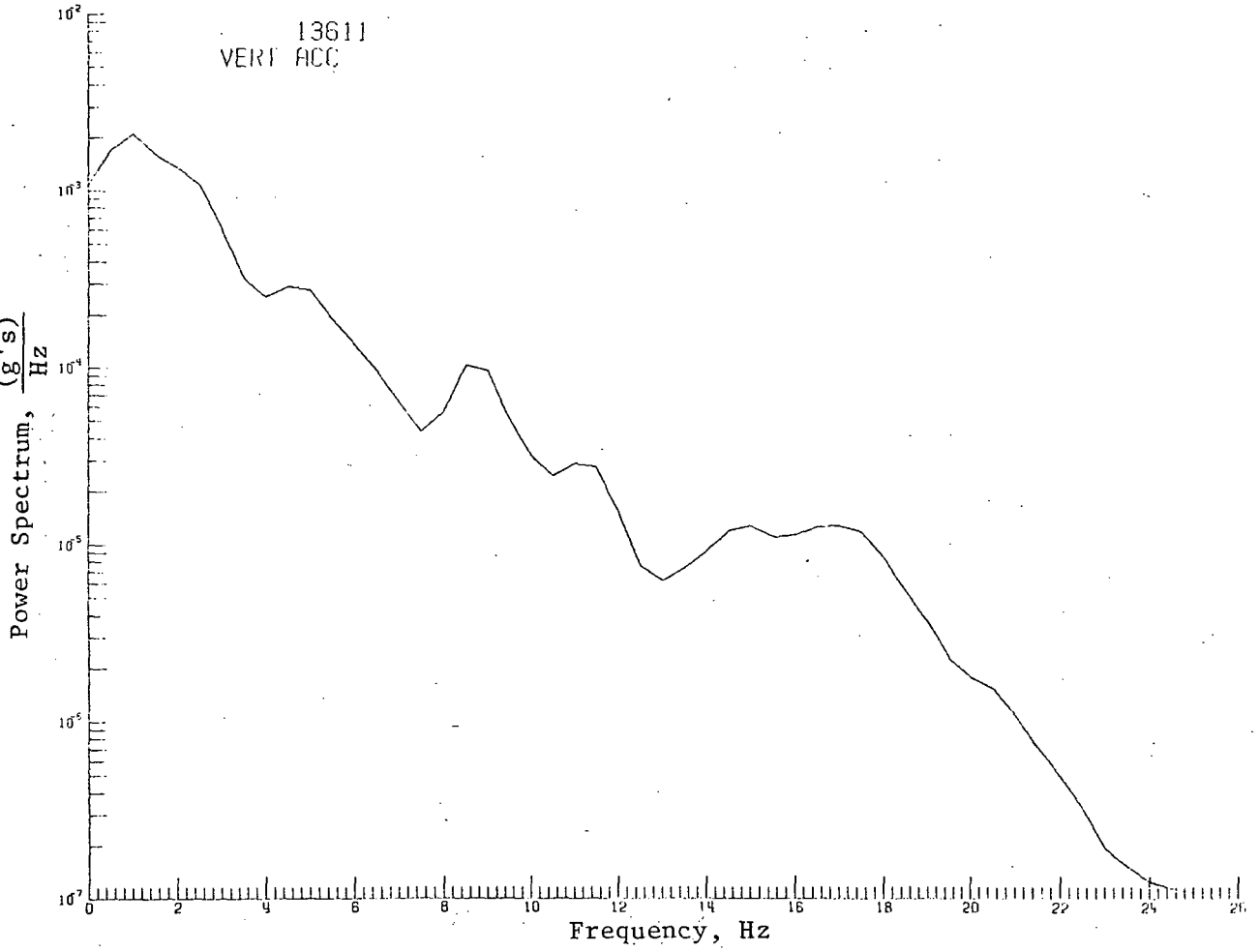

(e) Vertical acceleration power spectrum
(RMS-vertical acceleration 0.0762 g's)

FIGURE 4. Continued.

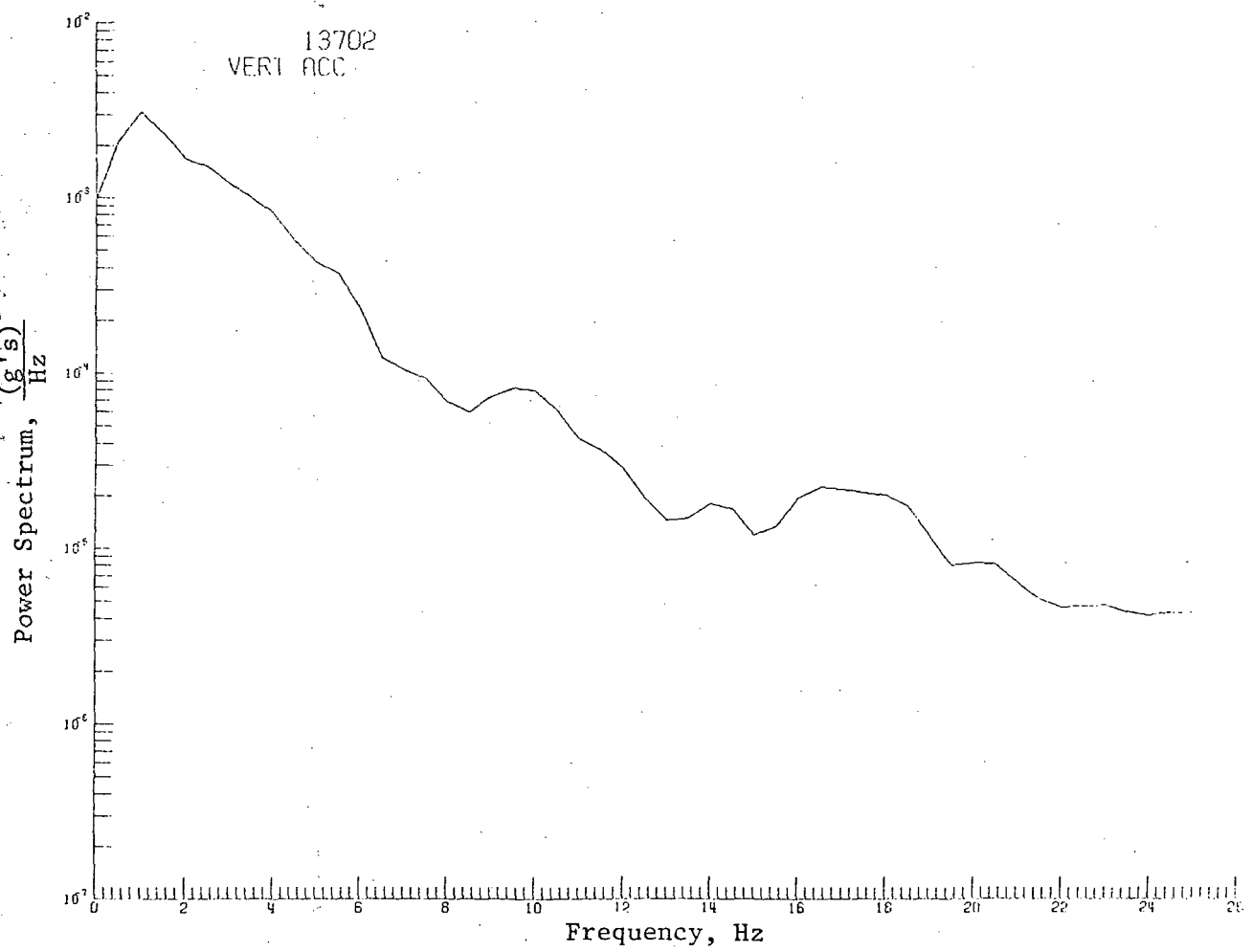

(e) Vertical acceleration power spectrum
(RMS-vertical acceleration 0.0892 g's)

FIGURE 4. Concluded.

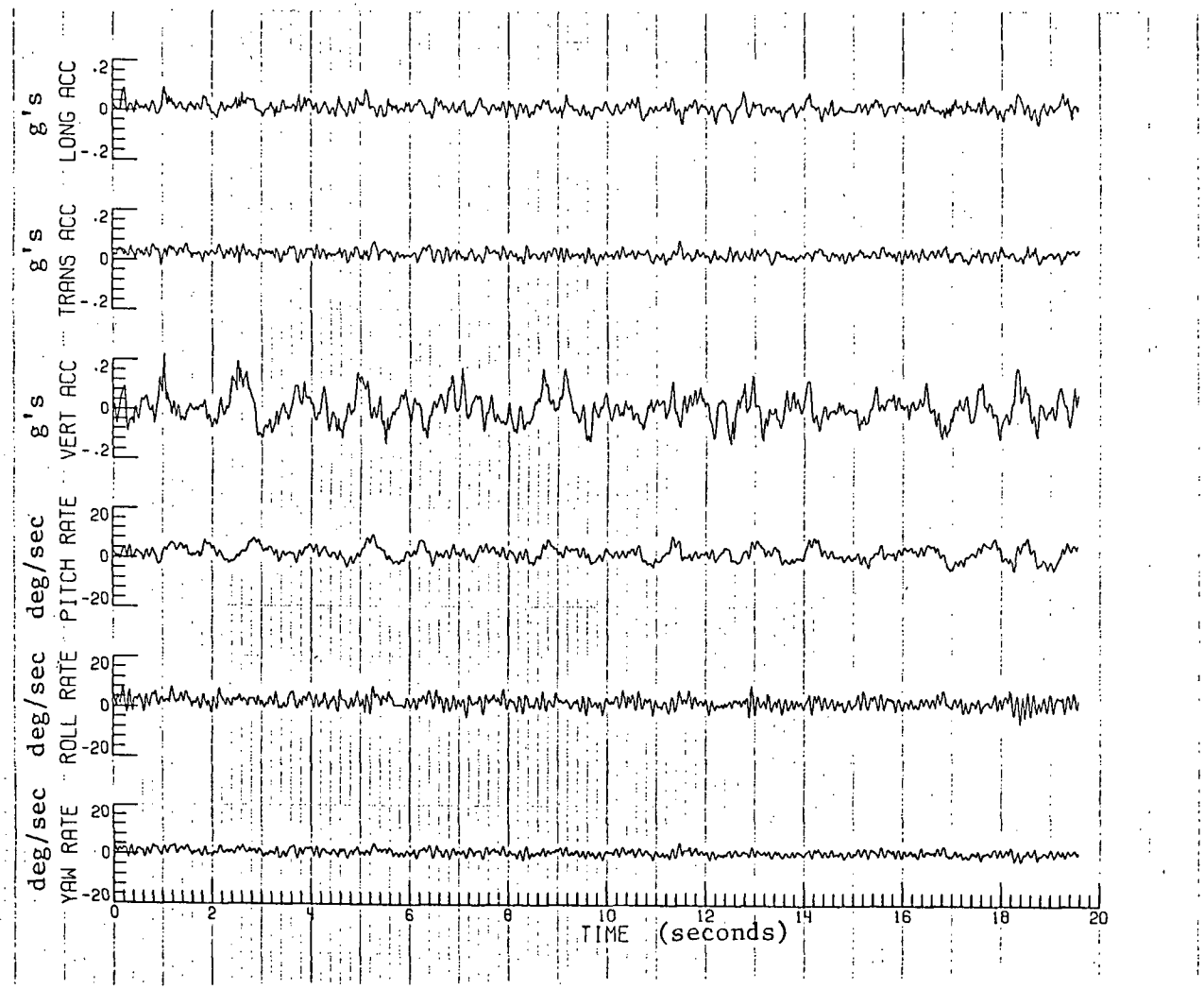

(a) Time histories (RMS-vertical acceleration 0.0563 g's; RMS-pitching velocity 2.4538 deg/sec)

FIGURE 5. MEASURED MOTION CHARACTERISTICS USING AN APPROXIMATELY CONSTANT RMS-PITCHING VELOCITY WITH A VARIABLE RMS-VERTICAL ACCELERATION

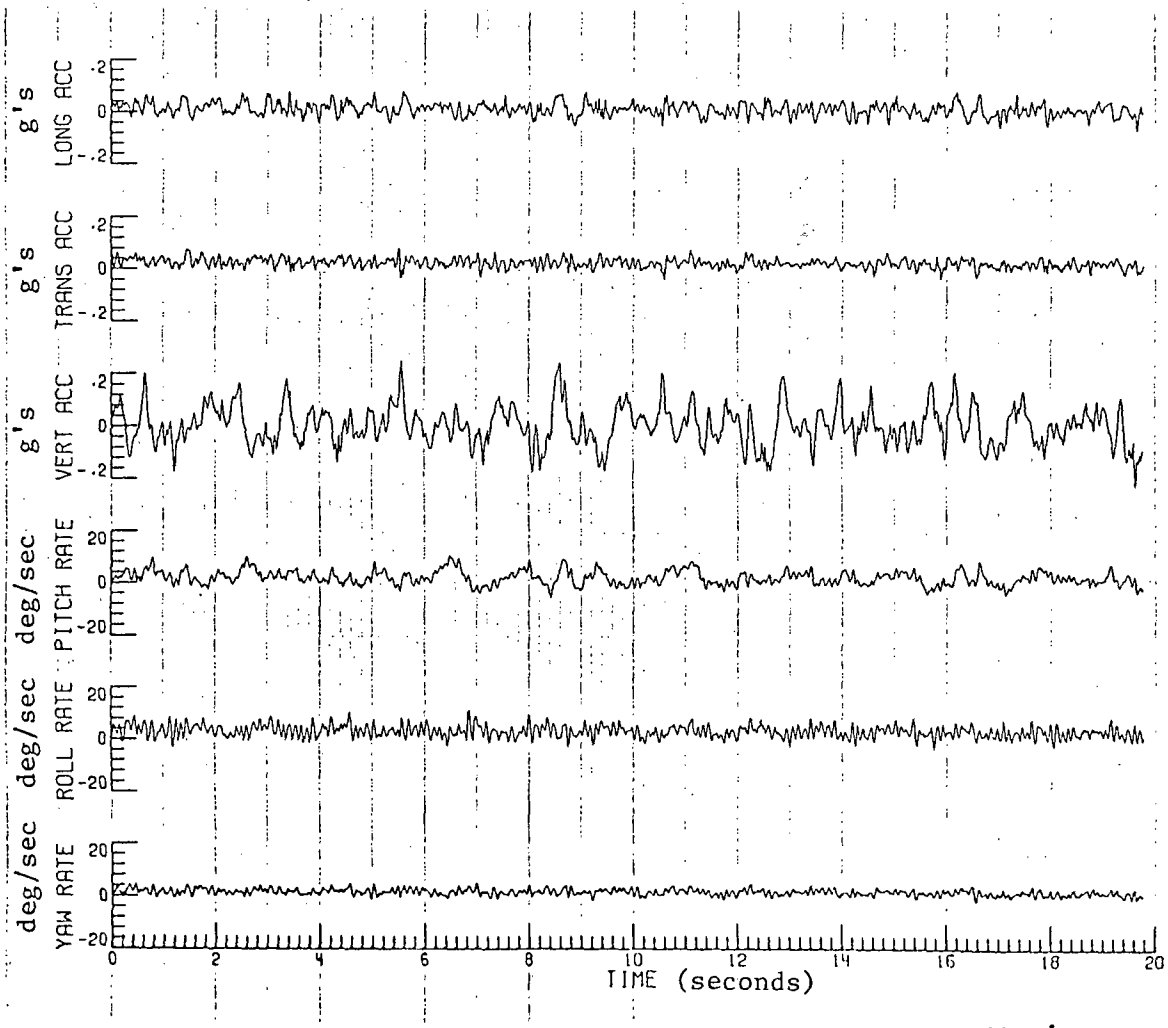

(a) Time histories (RMS-vertical acceleration 0.0762 g's; RMS-pitching velocity 2.8574 deg/sec)

FIGURE 5. Continued.

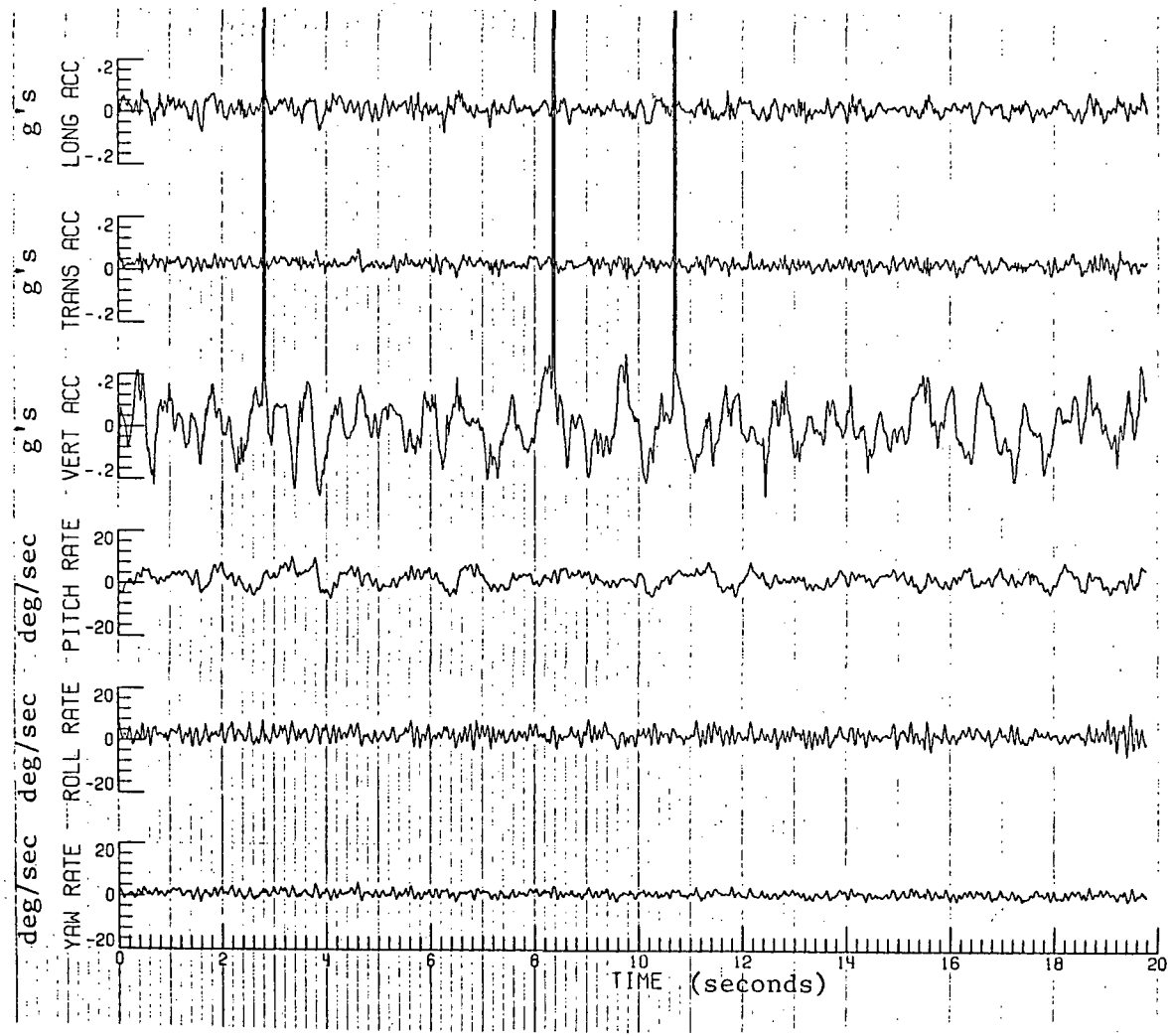

(a) Time histories (RMS-vertical acceleration 0.0948 g's; RMS-pitching velocity 3.0594 deg/sec)

FIGURE 5. Continued.

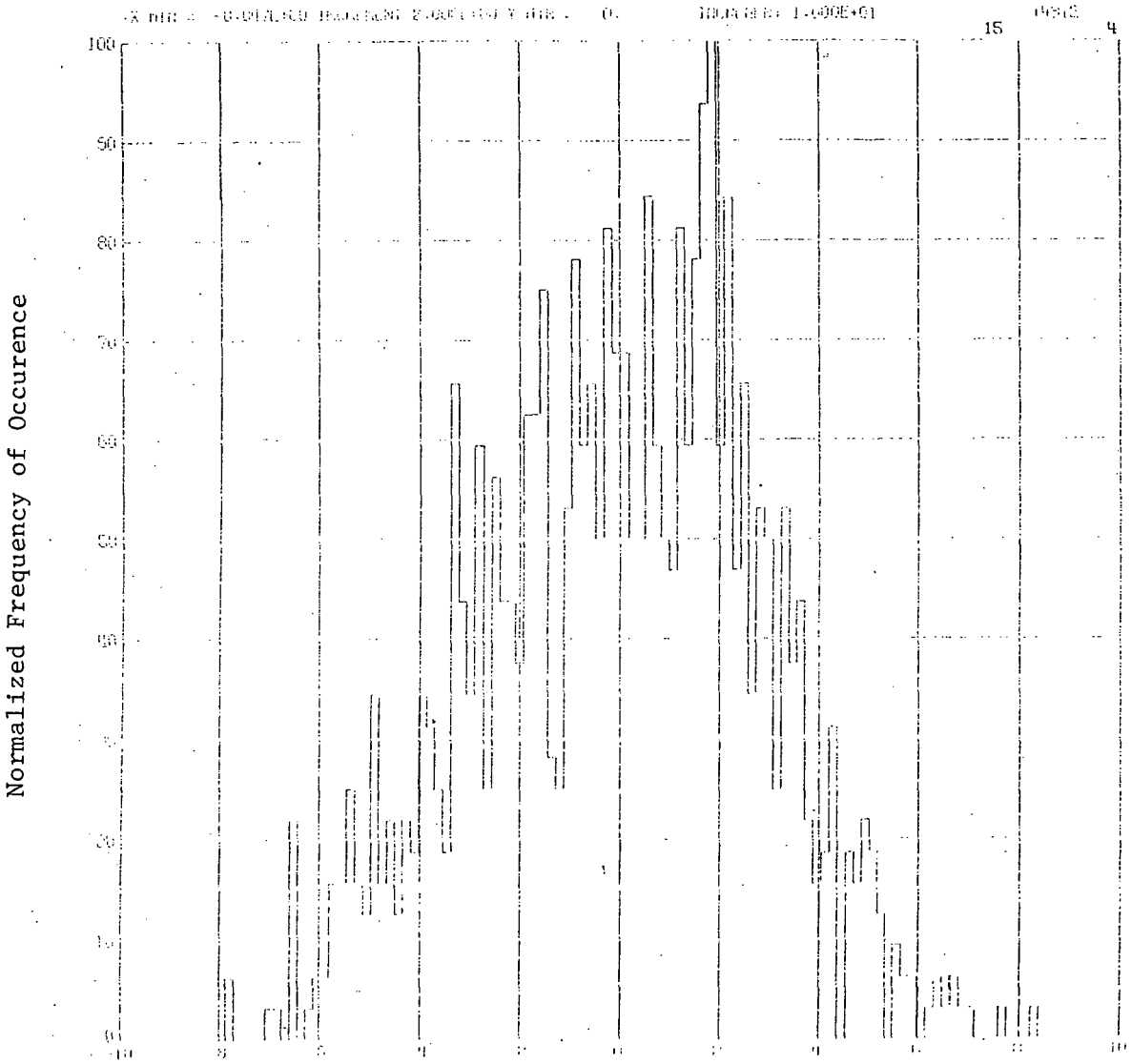

(b) Pitching velocity histogram
(RMS-pitching velocity 2.4538 deg/sec)

FIGURE 5. Continued.

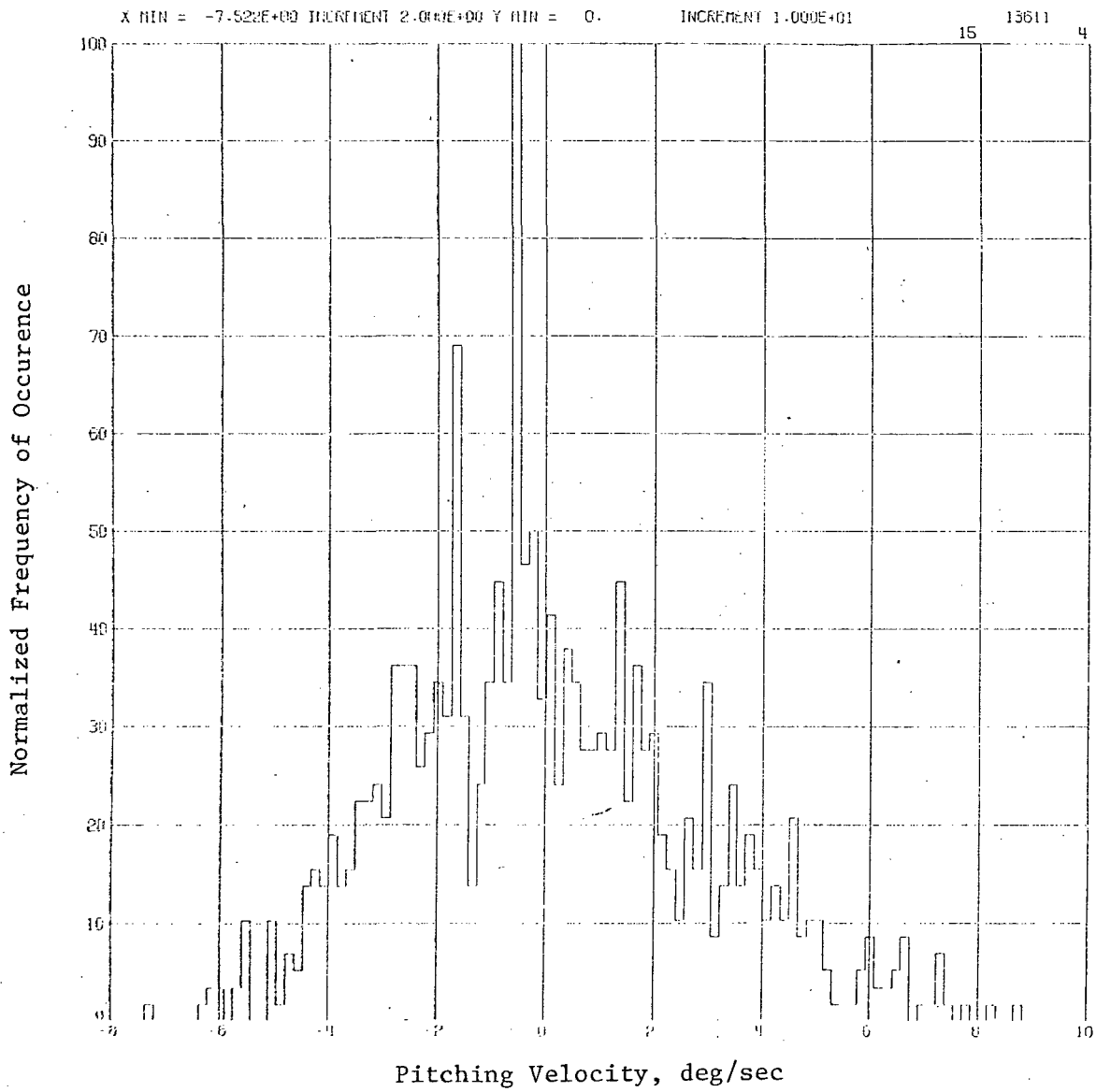

(b) Pitching velocity histogram
(RMS-pitching velocity 2.8574 deg/sec)

FIGURE 5. Continued.

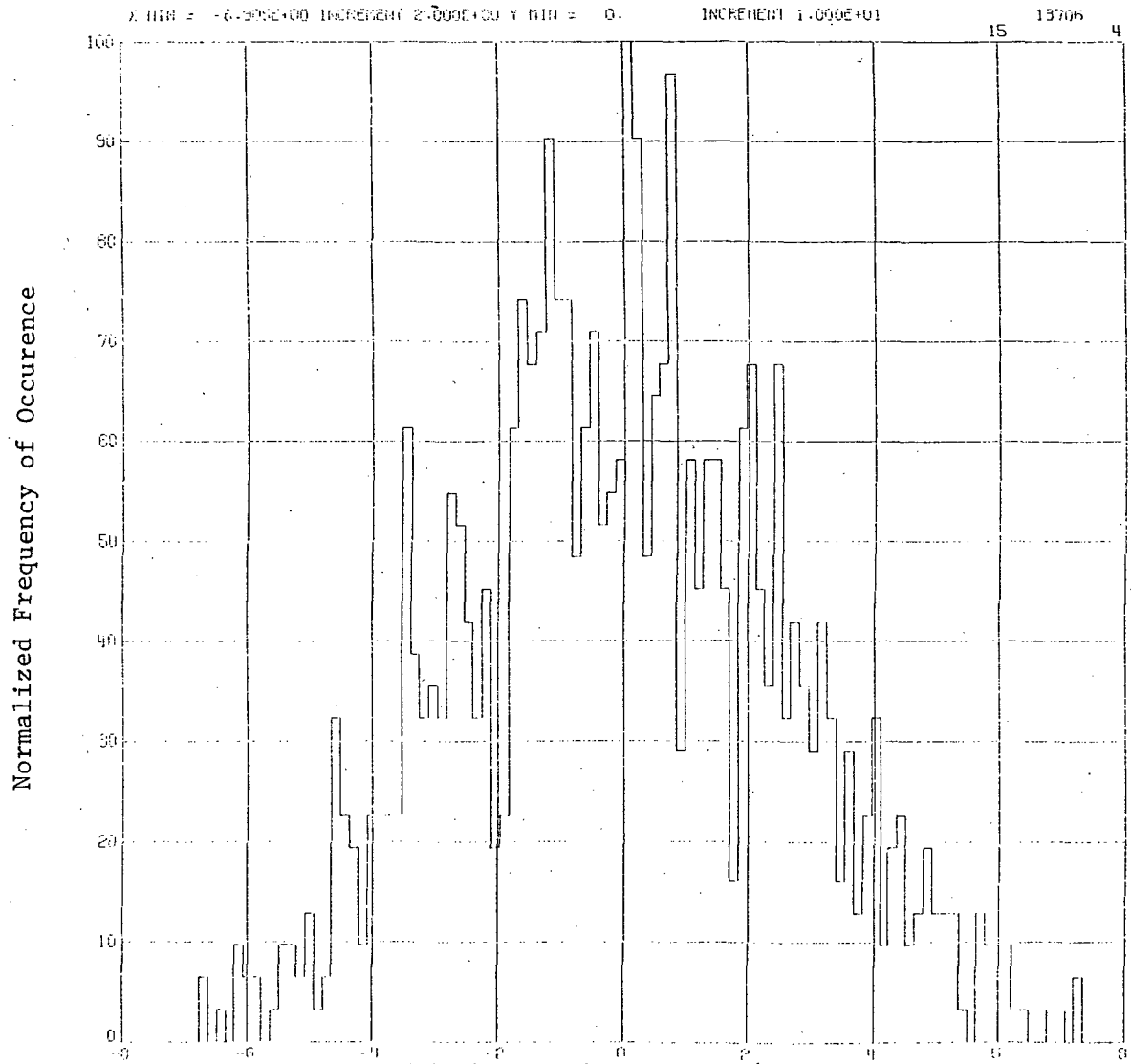

(b) Pitching velocity histogram
(RMS-pitching velocity 3.0594 deg/sec)

FIGURE 5. Continued.

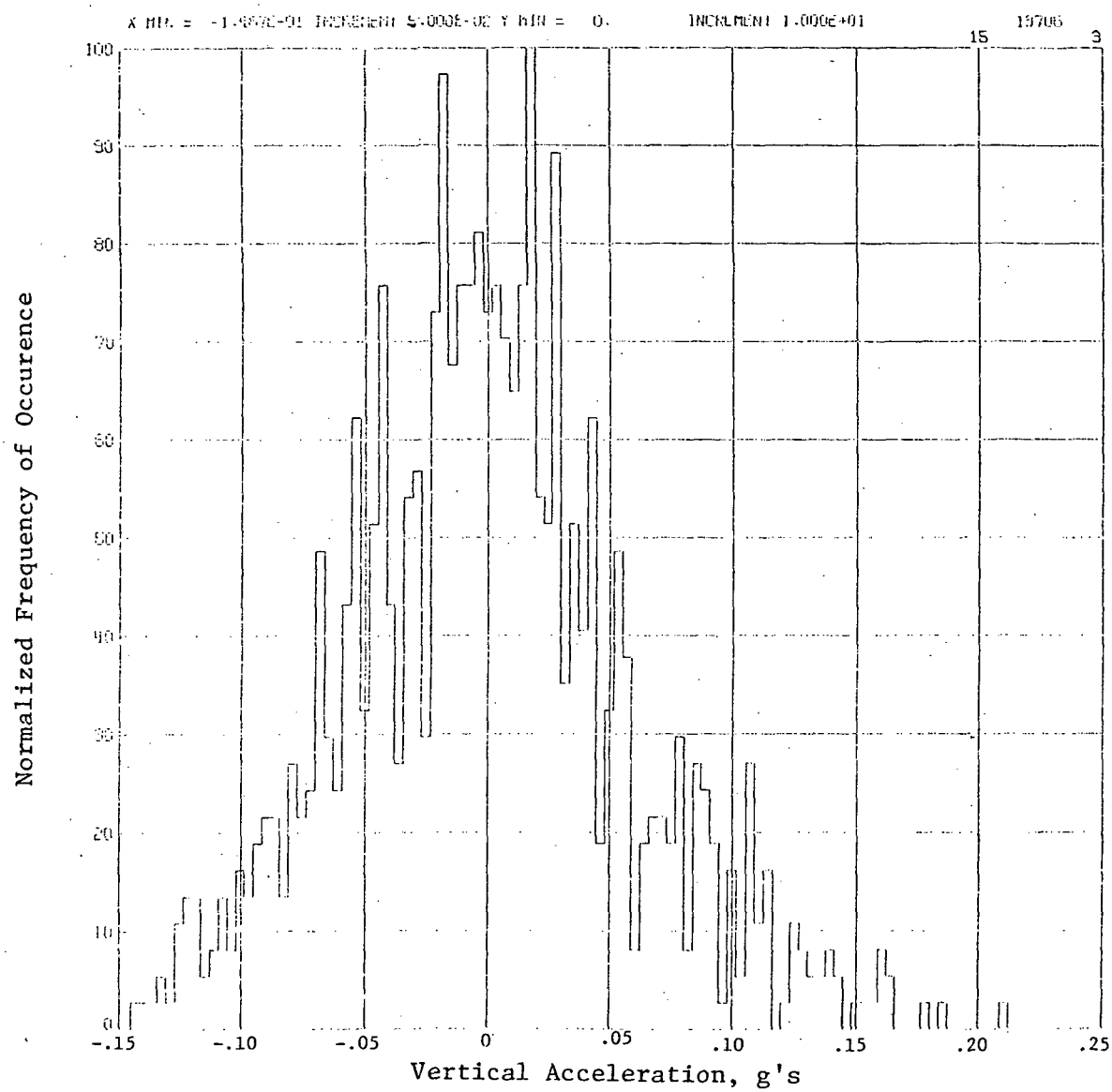

(c) Vertical acceleration histogram
(RMS-vertical acceleration 0.0563 g's)

FIGURE 5. Continued.

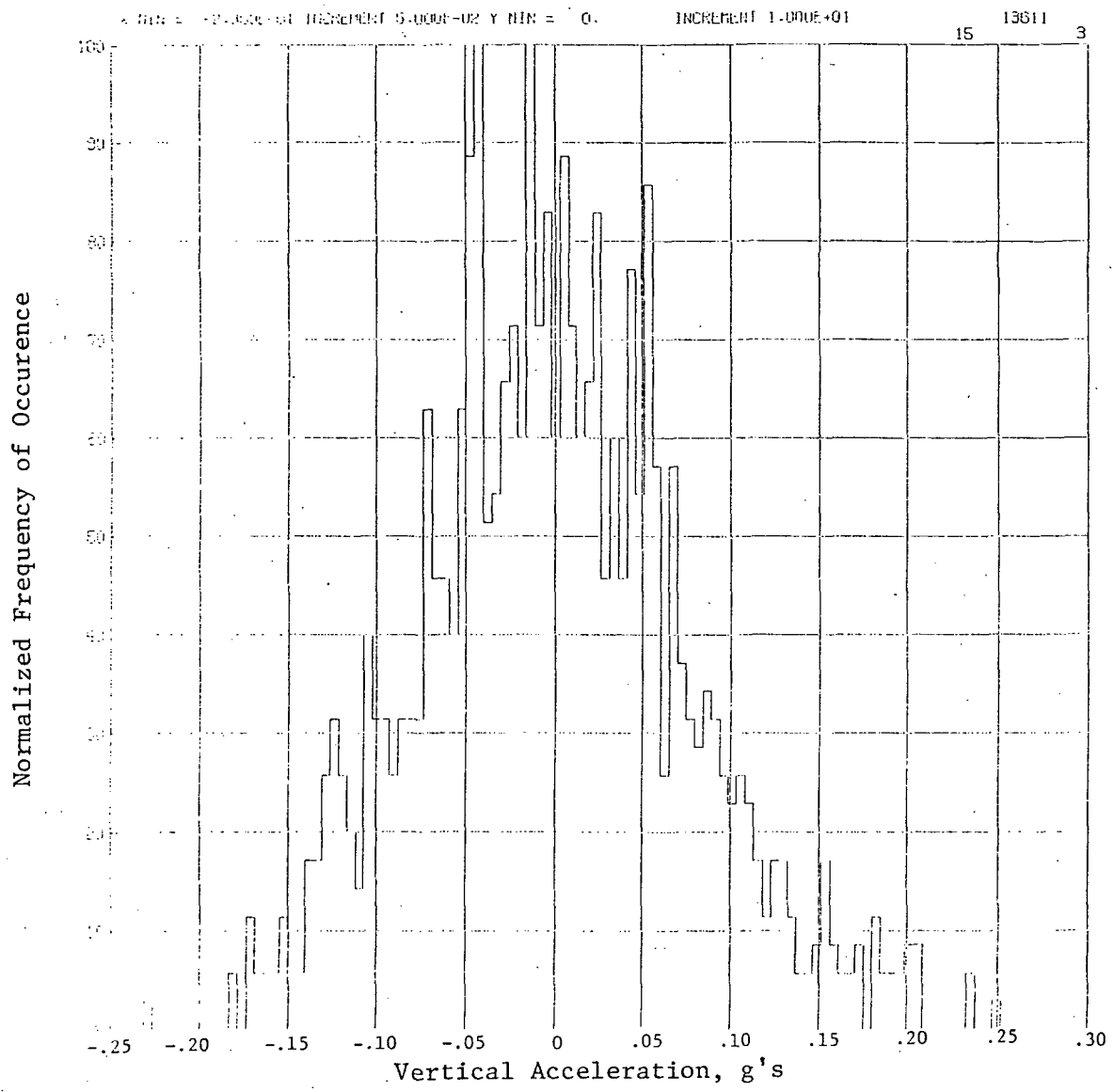

(c) Vertical acceleration histogram
(RMS-vertical acceleration 0.0762 g's)

FIGURE 5. Continued.

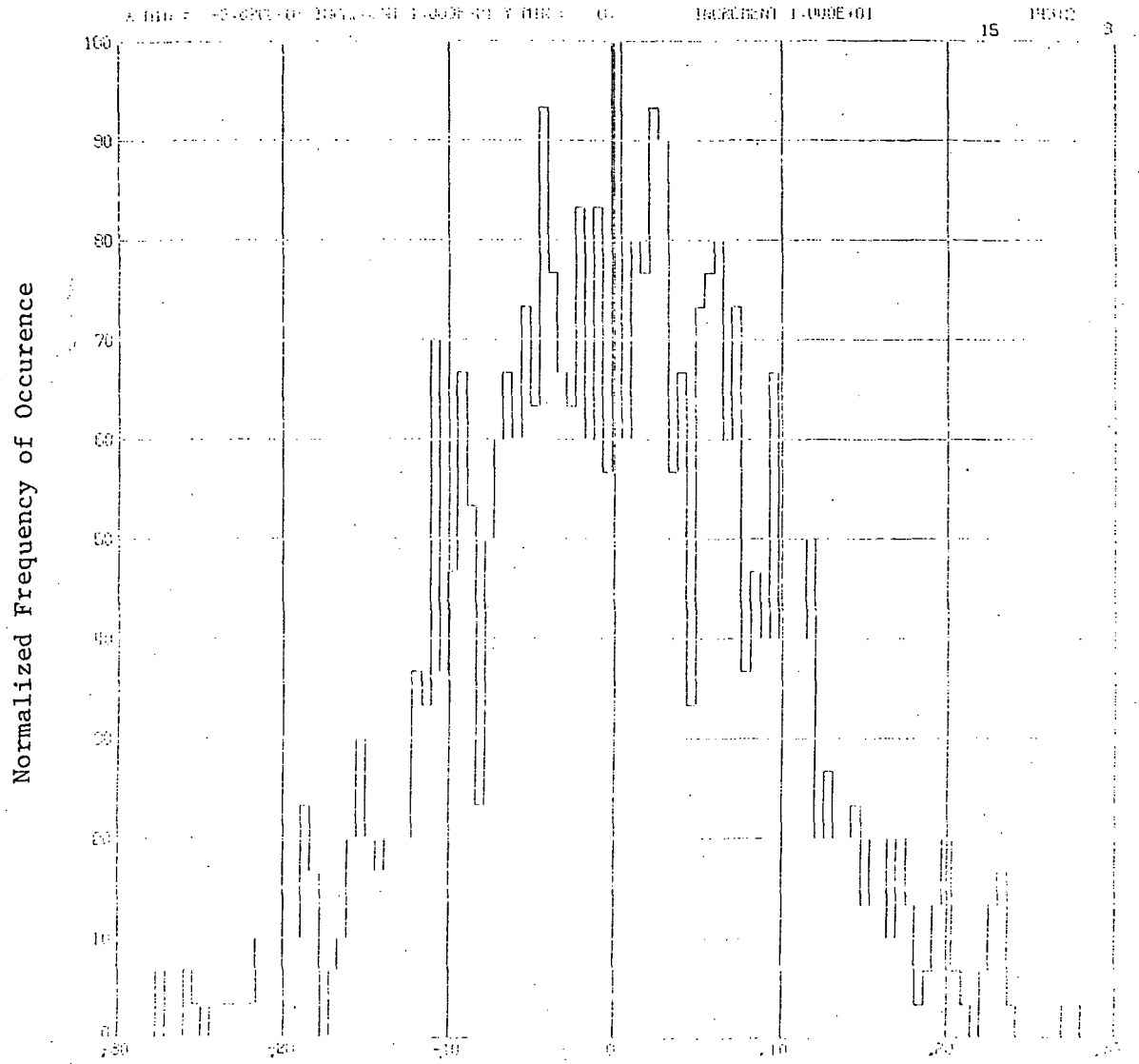

(c) Vertical acceleration histogram
(RMS-vertical acceleration 0.0948 g's)

FIGURE 5. Continued.

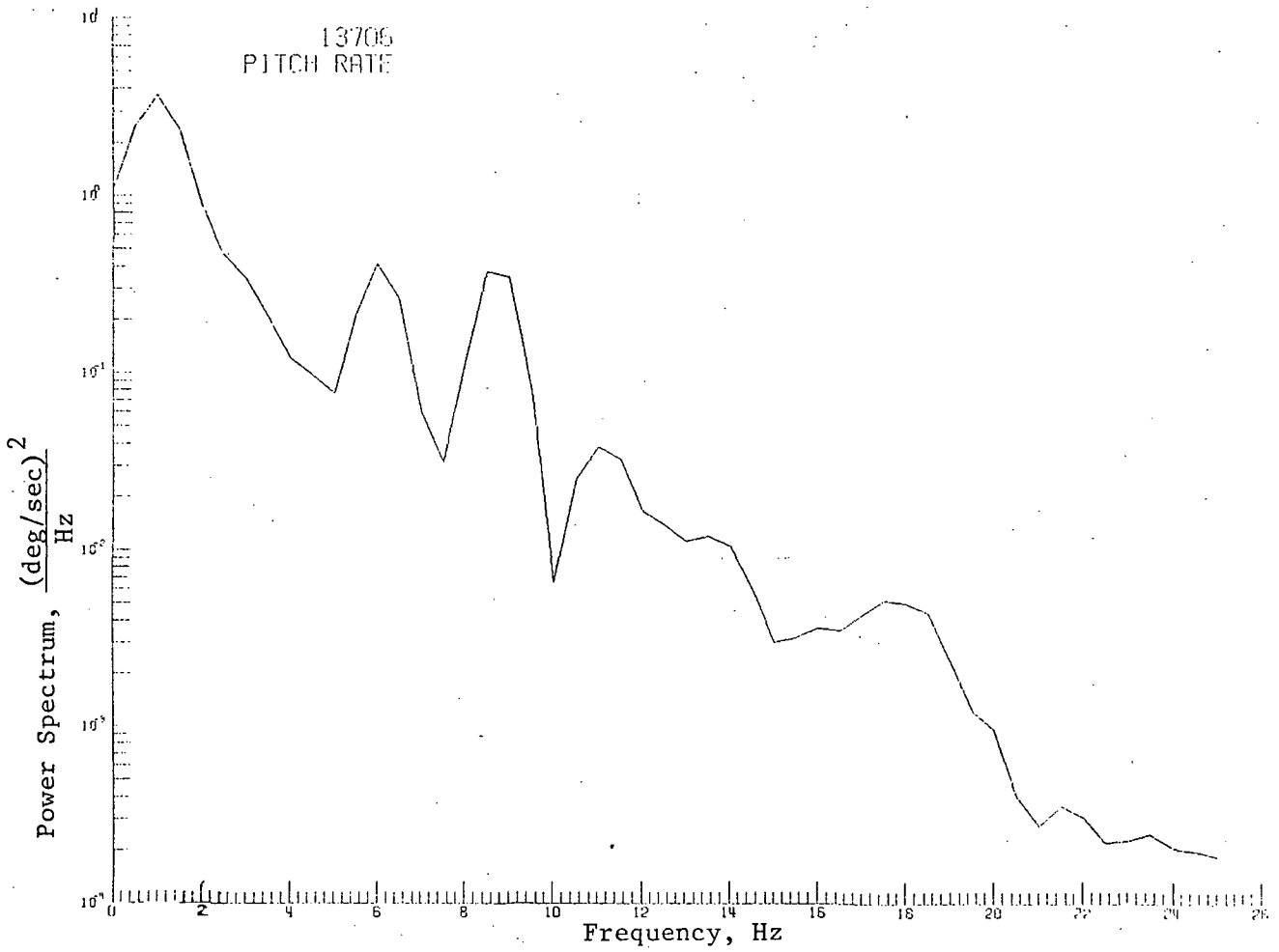

(d) Pitching velocity power spectrum
(RMS-pitching velocity 2.4538 deg/sec)

FIGURE 5. Continued.

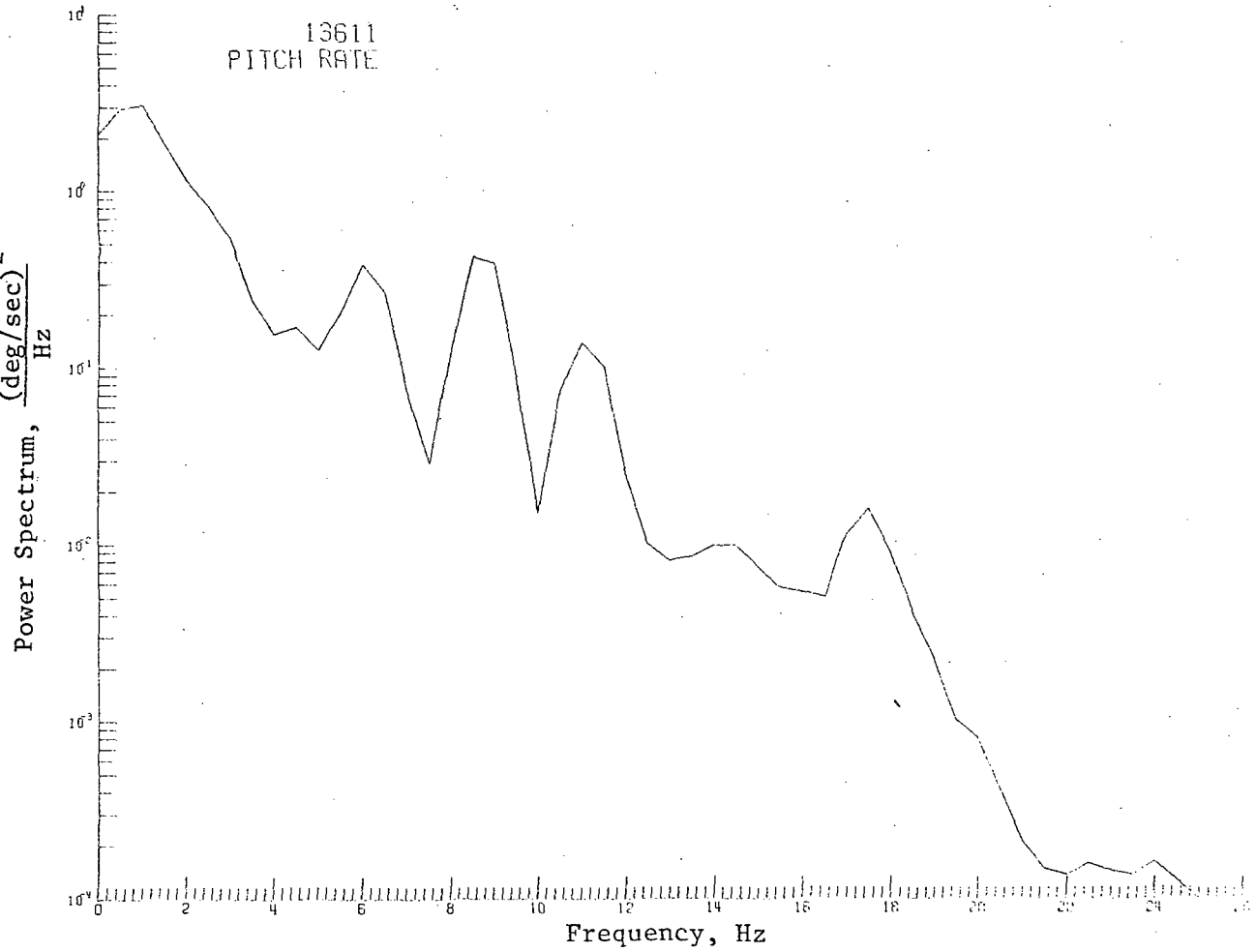

(d) Pitching velocity power spectrum
(RMS-pitching velocity 2.8574 deg/sec)

FIGURE 5. Continued.

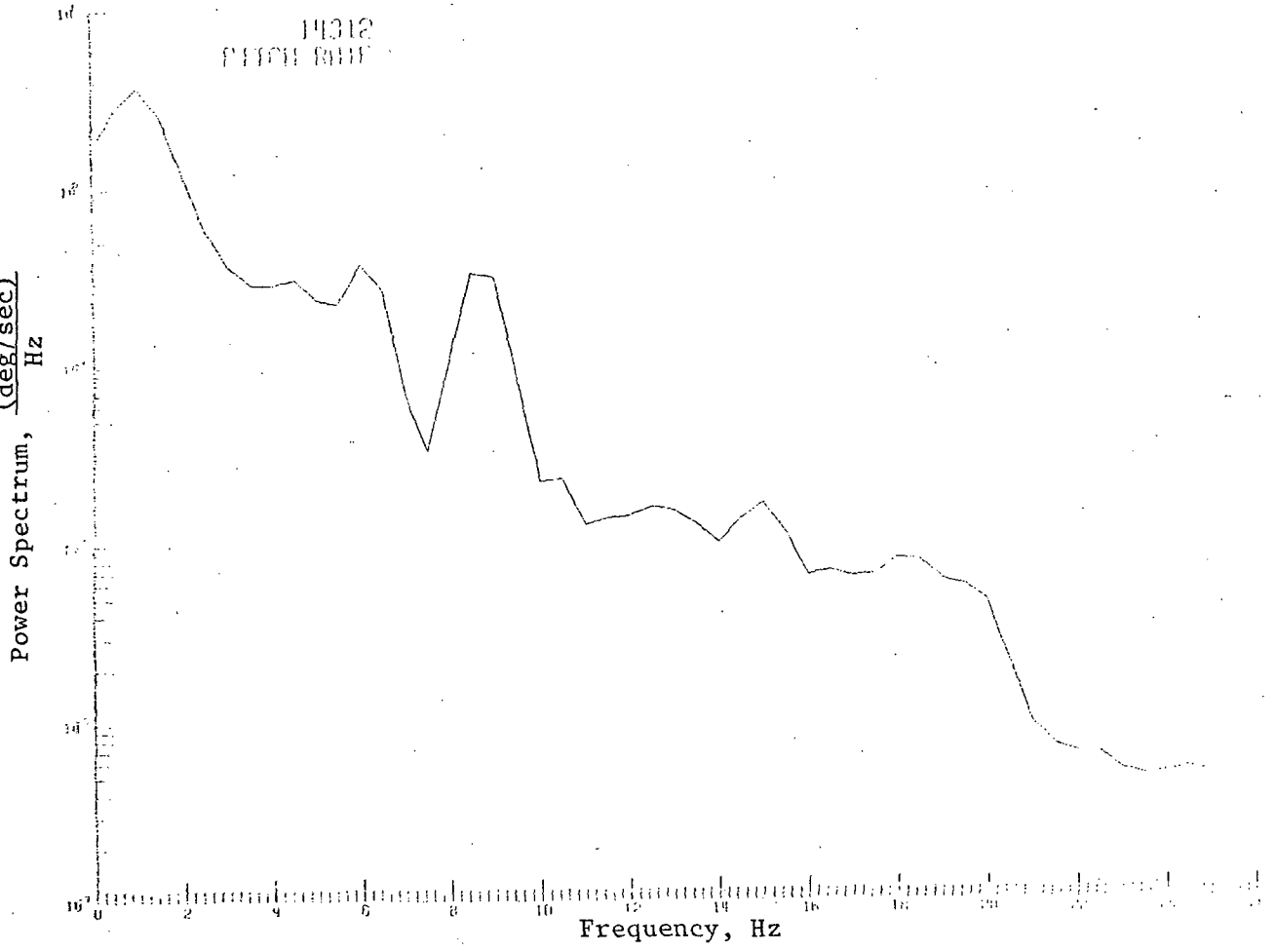

(d) Pitching velocity power spectrum
(RMS-pitching velocity 3.0594 deg/sec)

FIGURE 5. Continued.

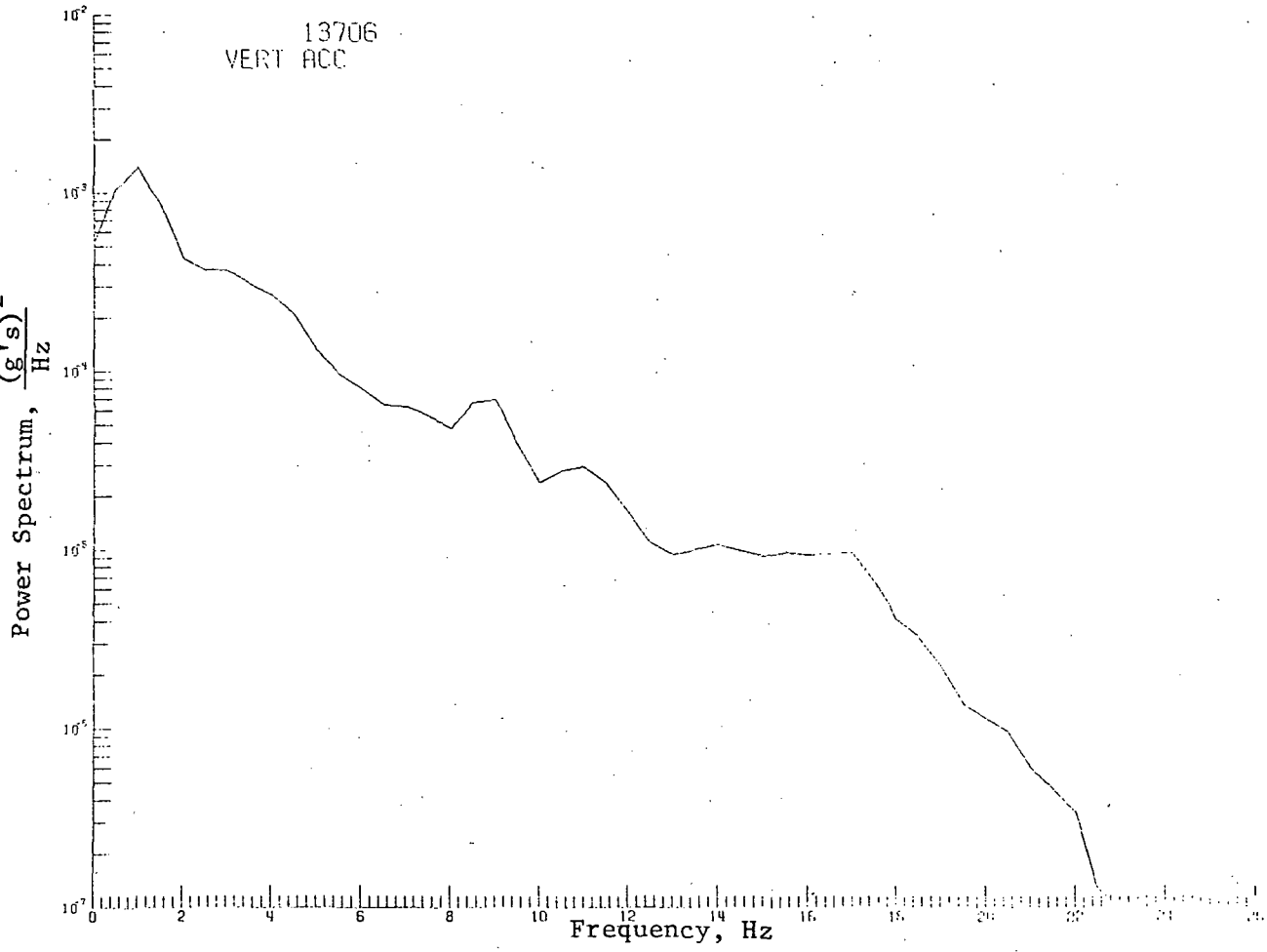

(e) Vertical acceleration power spectrum
(RMS-vertical acceleration 0.0563 g's)

FIGURE 5. Continued.

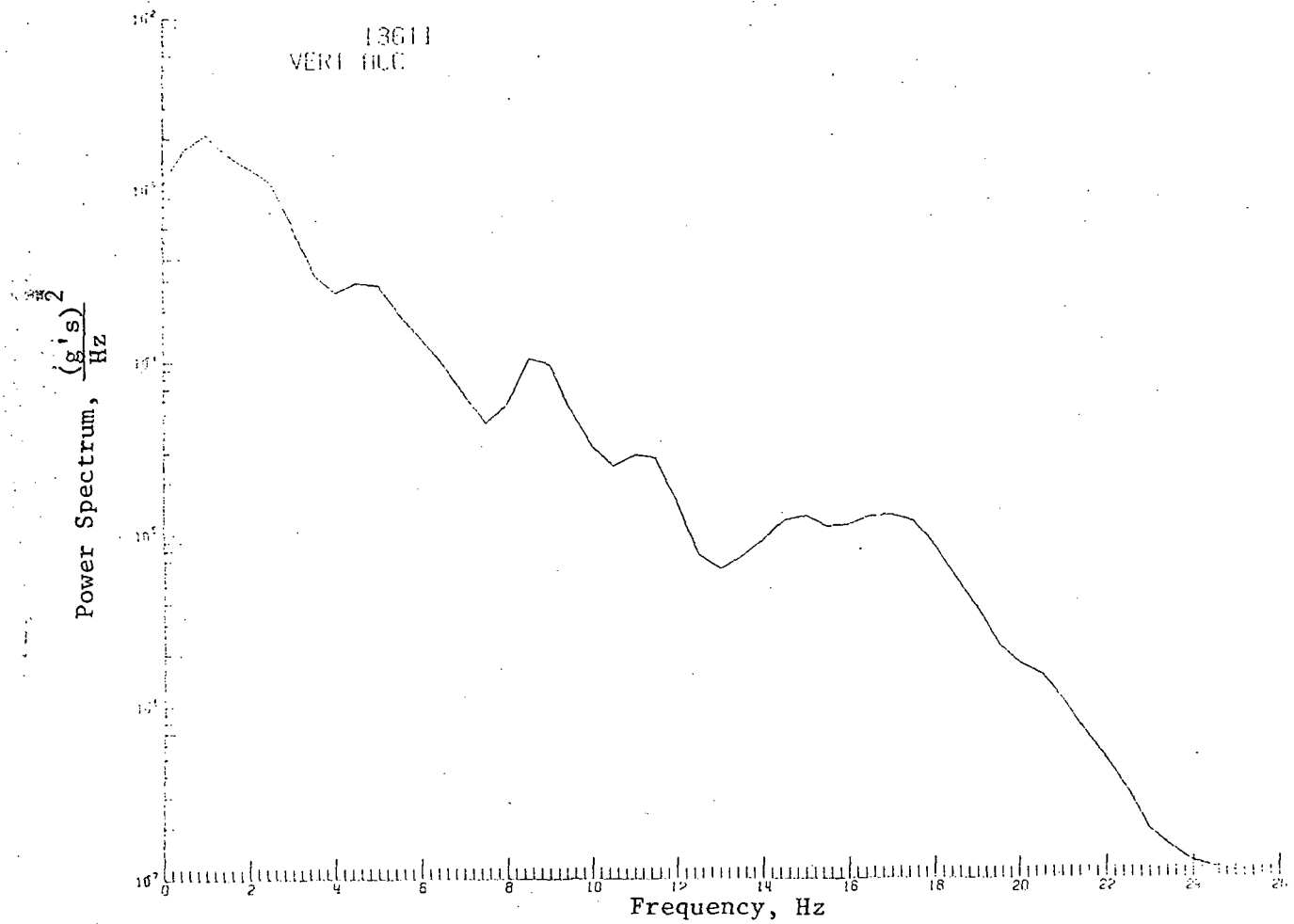

(e) Vertical acceleration power spectrum
(RMS-vertical acceleration 0.0762 g's)

FIGURE 5. Continued.

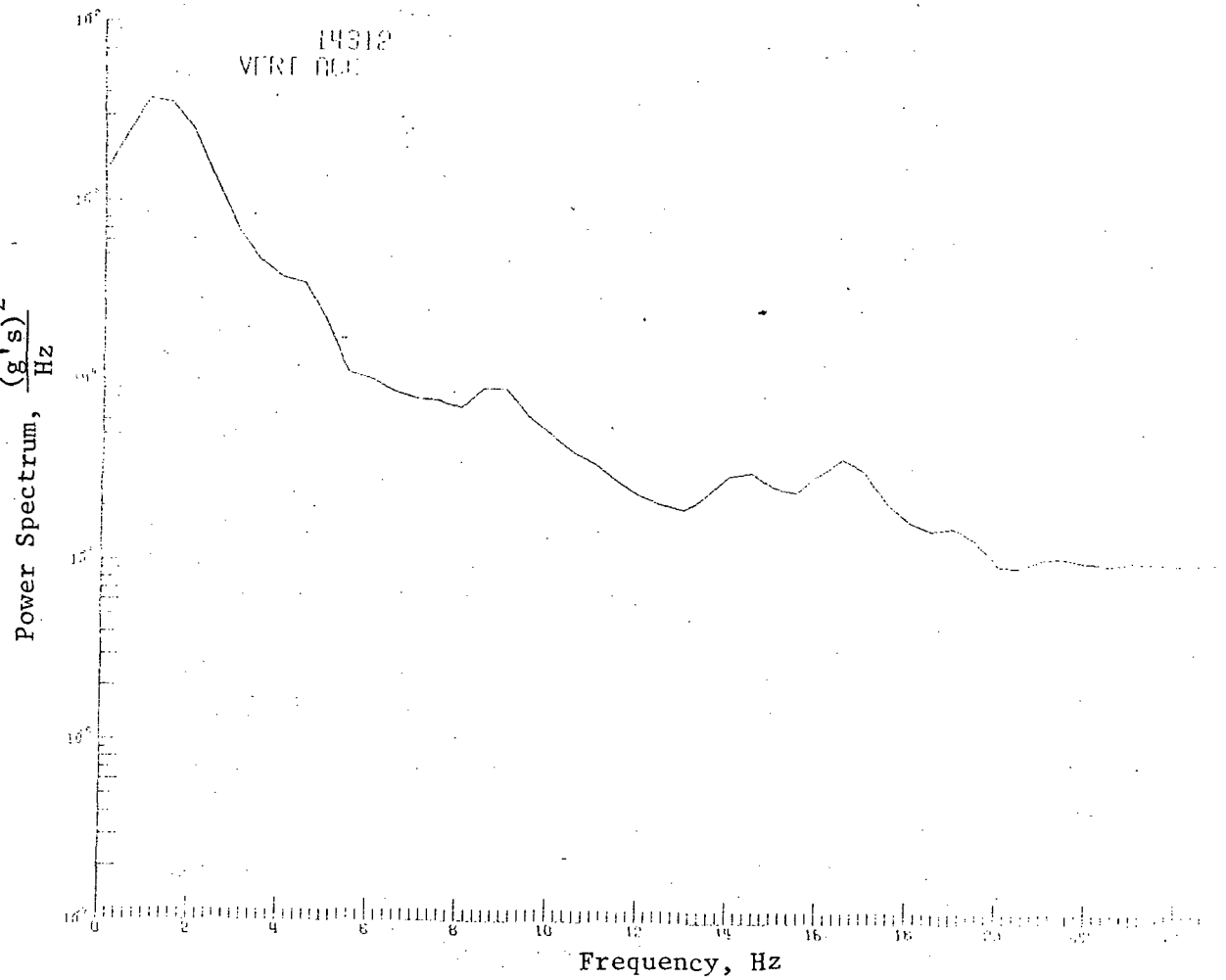

(e) Vertical acceleration power spectrum
(RMS-vertical acceleration 0.0948 g's)

FIGURE 5. Concluded.

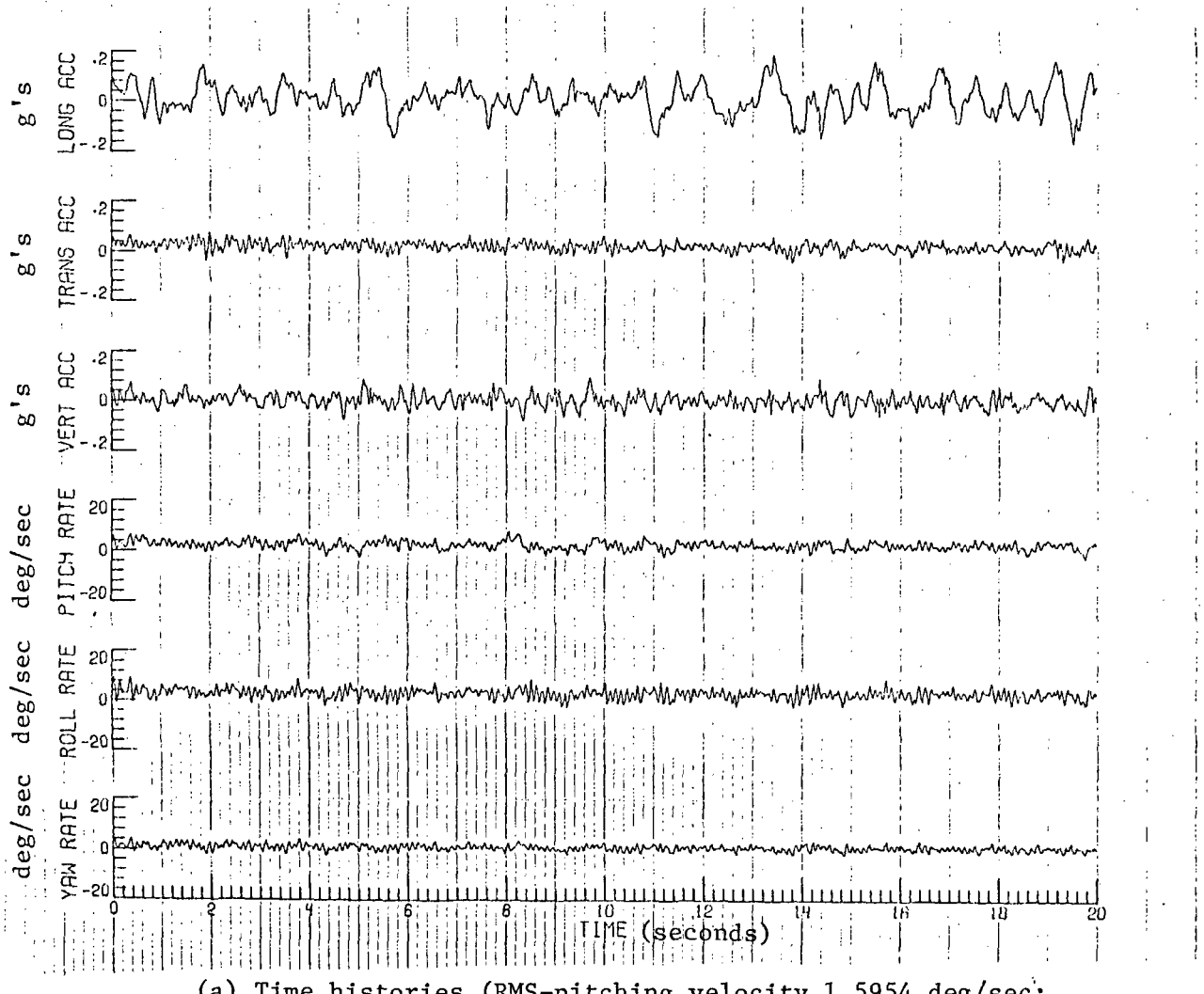

(a) Time histories (RMS-pitching velocity 1.5954 deg/sec; RMS-longitudinal acceleration 0.0603 g's)

FIGURE 6. MEASURED MOTION CHARACTERISTICS USING AN APPROXIMATELY CONSTANT RMS-LONGITUDINAL ACCELERATION WITH A VARIABLE RMS-PITCHING VELOCITY

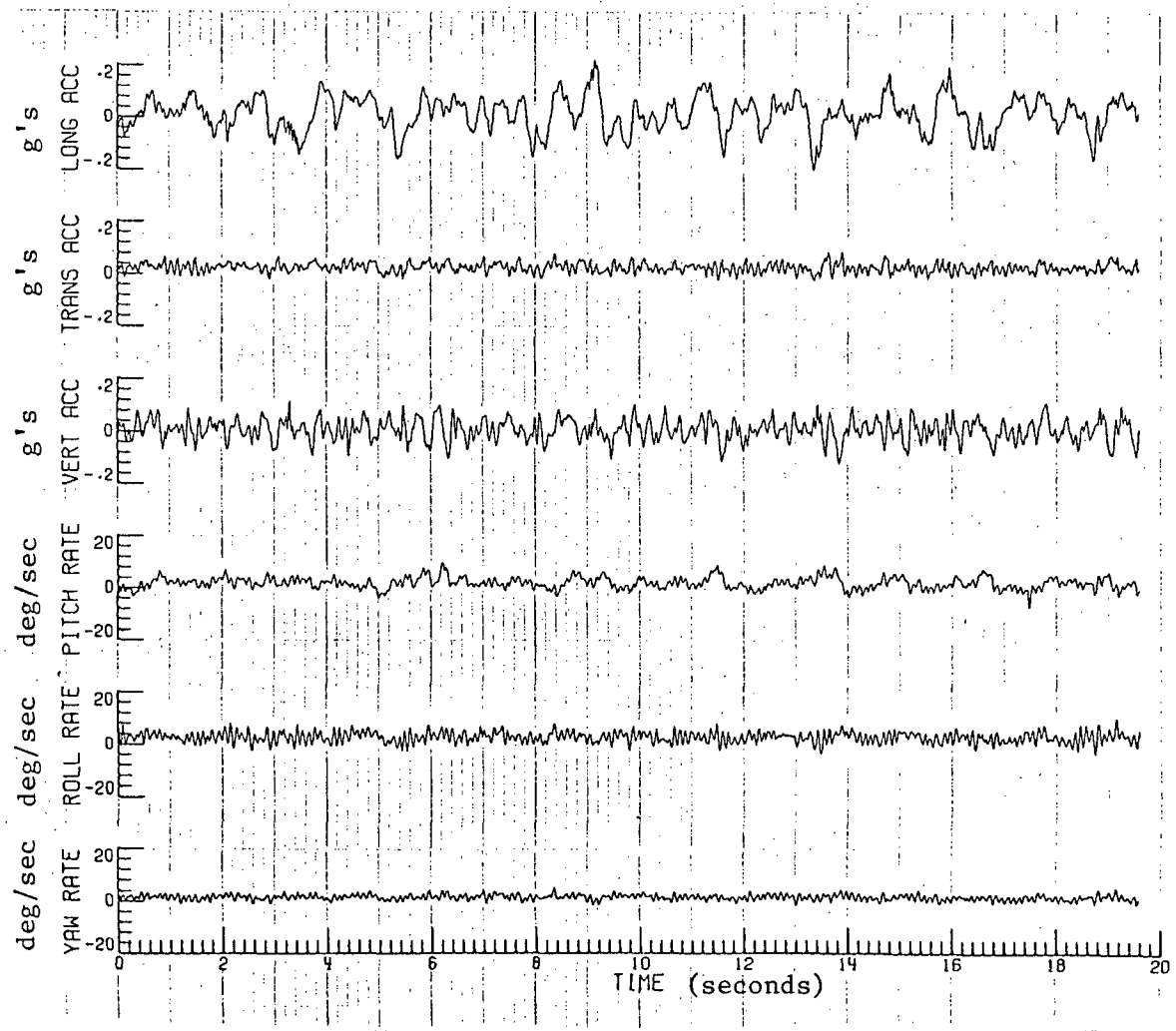

(a) Time histories (RMS-pitching velocity 2.4617 deg/sec; RMS-longitudinal acceleration 0.0678 g's)

FIGURE 6. Continued.

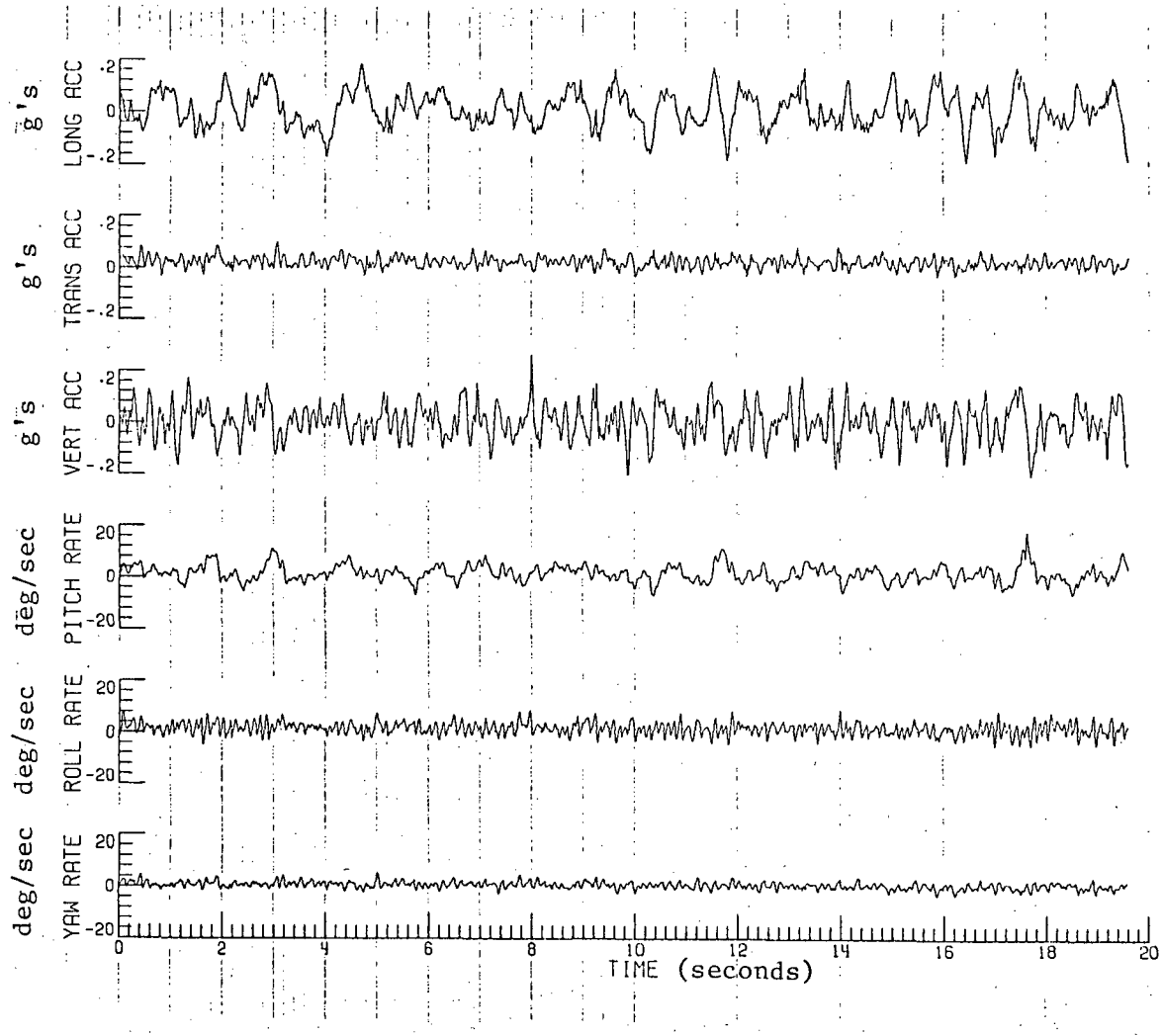

(a) Time histories (RMS-pitching velocity 3.1371 deg/sec; RMS-longitudinal acceleration 0.0723 g's)

FIGURE 6. Continued.

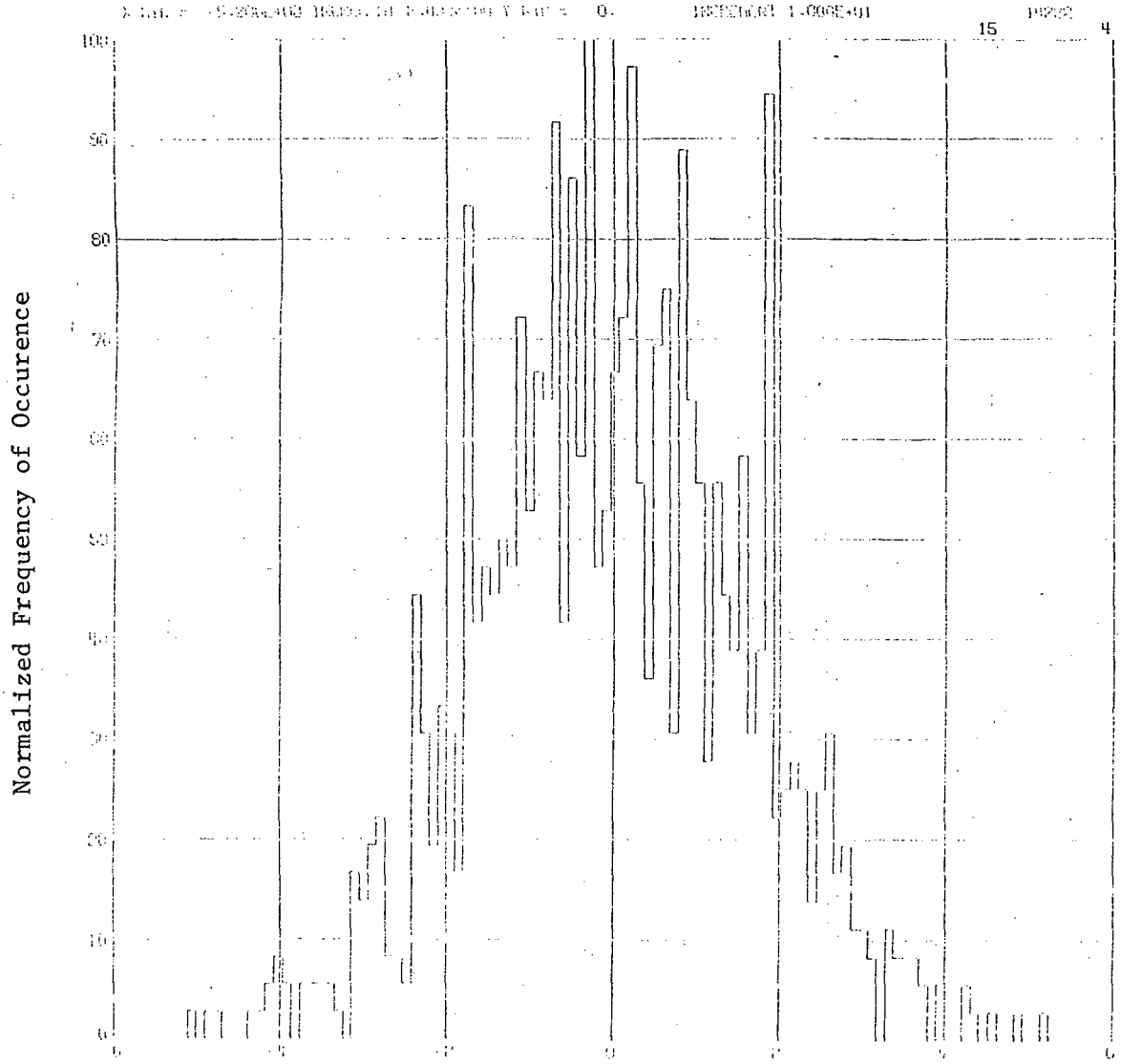

(b) Pitching velocity histogram
(RMS-pitching velocity 1.5954 deg/sec)

FIGURE 6. Continued.

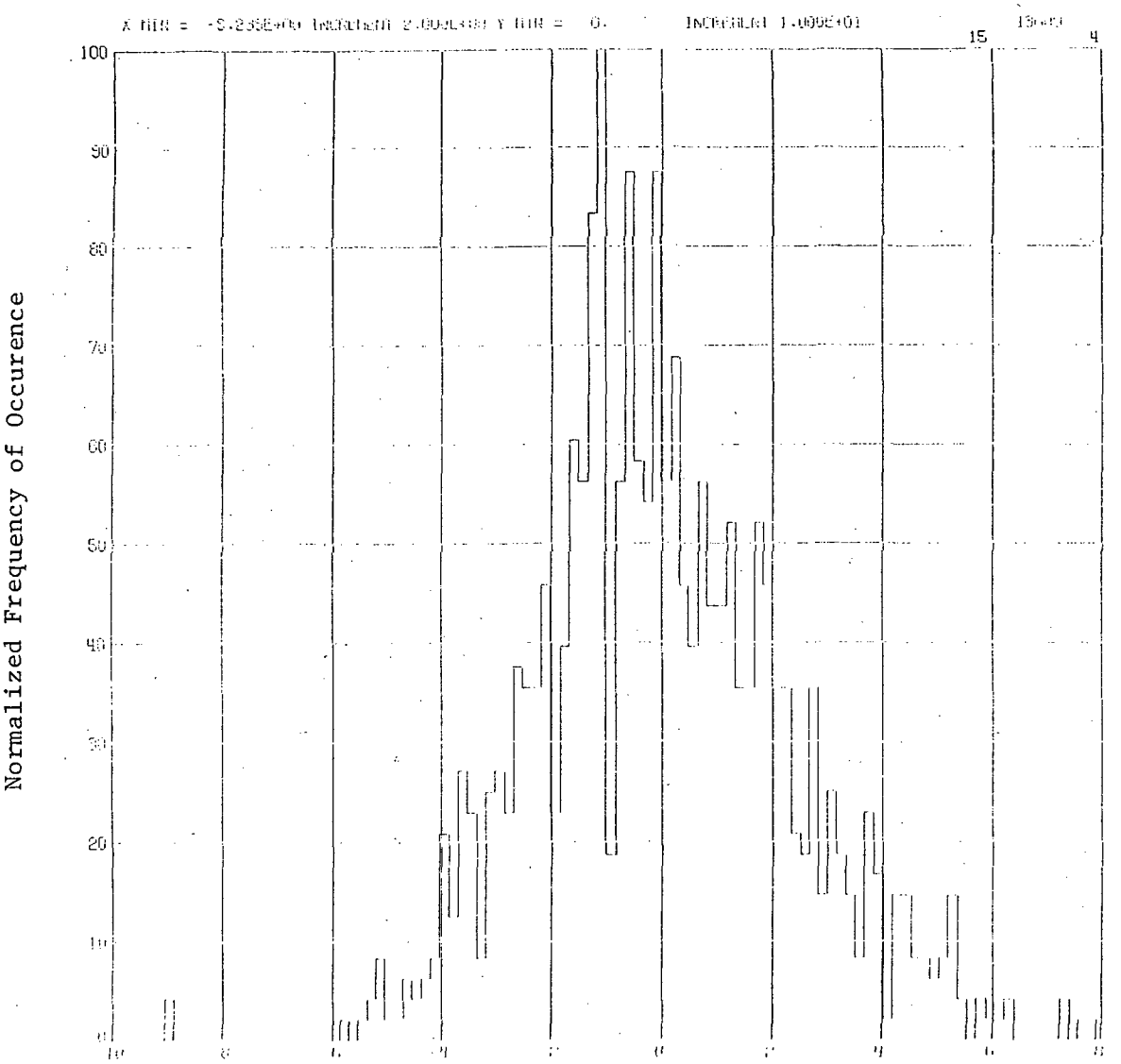

Pitching Velocity, deg/sec

(b) Pitching velocity histogram
(RMS-pitching velocity 2.4617 deg/sec)

FIGURE 6. Continued.

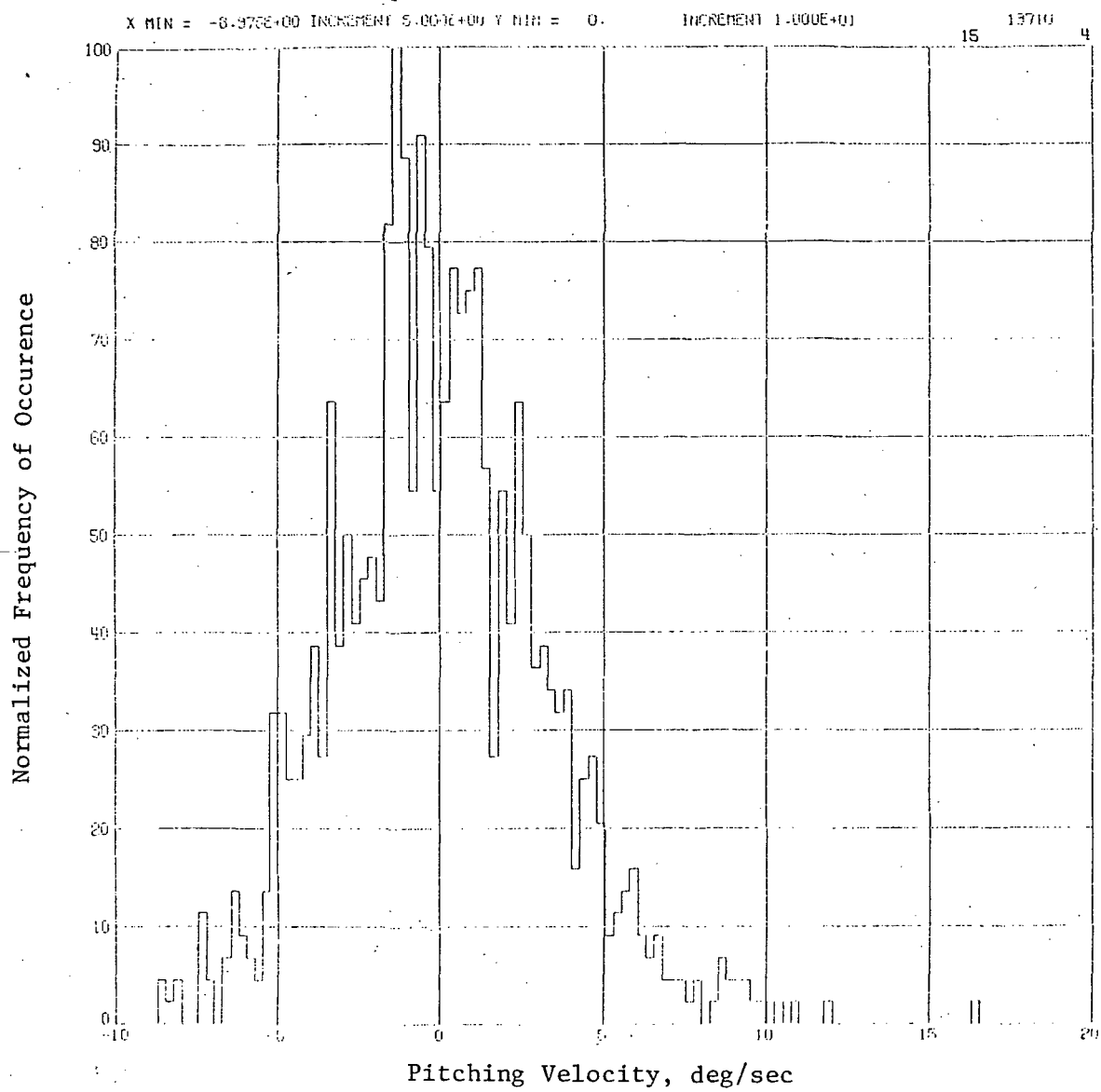

(b) Pitching velocity histogram
(RMS-pitching velocity 3.1371 deg/sec)

FIGURE 6. Continued.

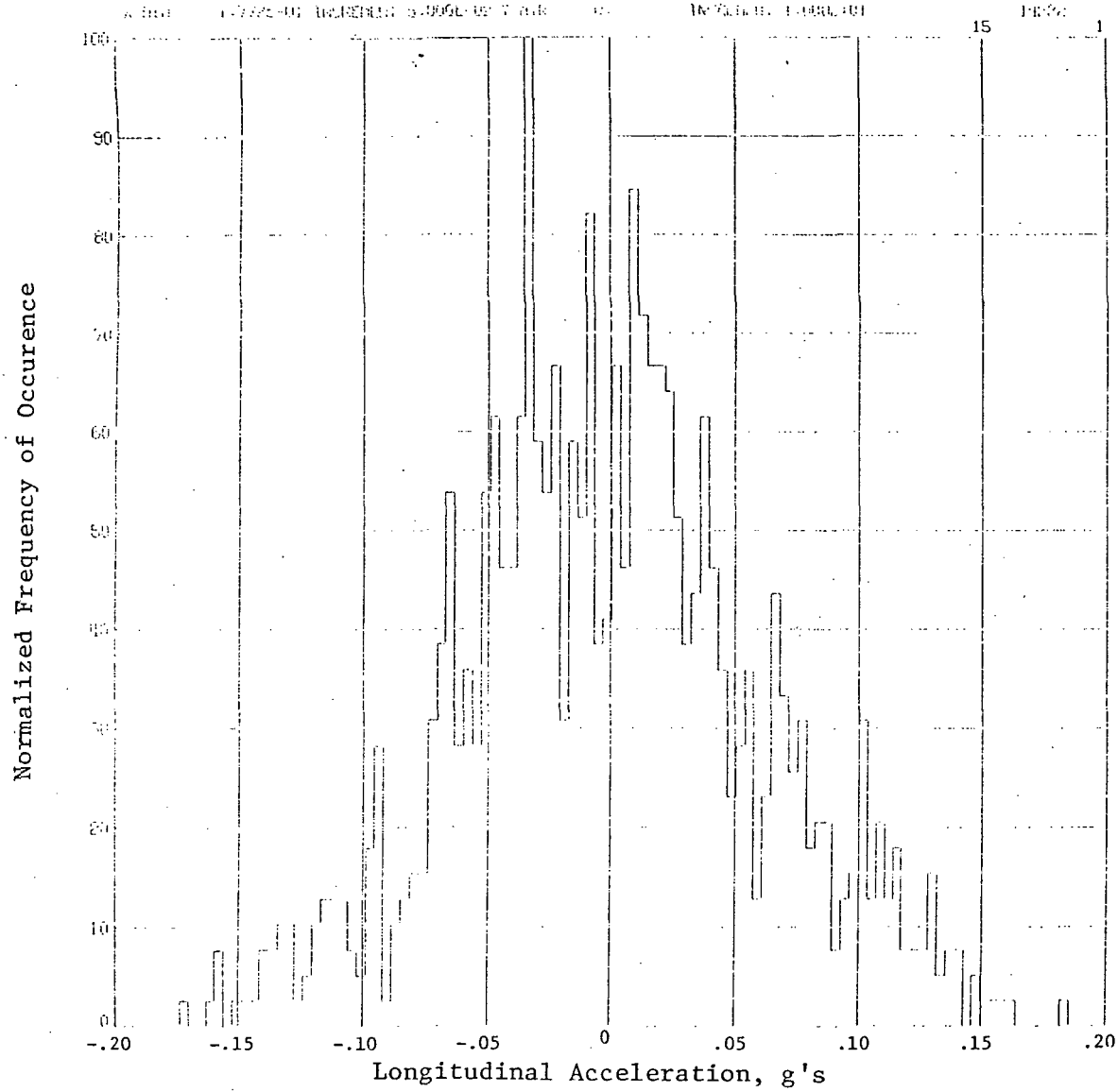

(c) Longitudinal acceleration histogram
(RMS-longitudinal acceleration 0.0603 g's)

FIGURE 6. Continued.

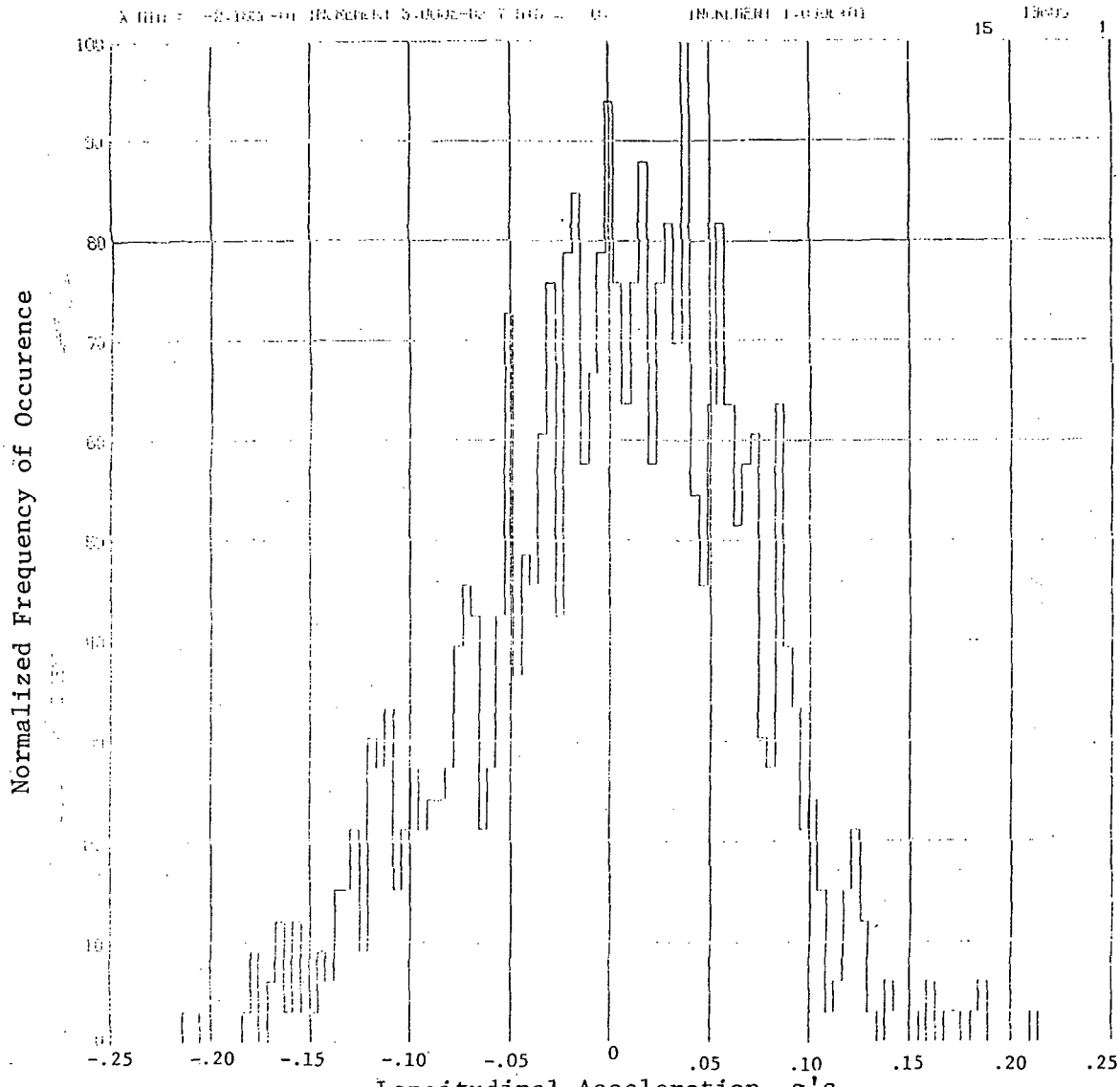

(c) Longitudinal acceleration histogram
(RMS-longitudinal acceleration 0.0678 g's)

FIGURE 6. Continued.

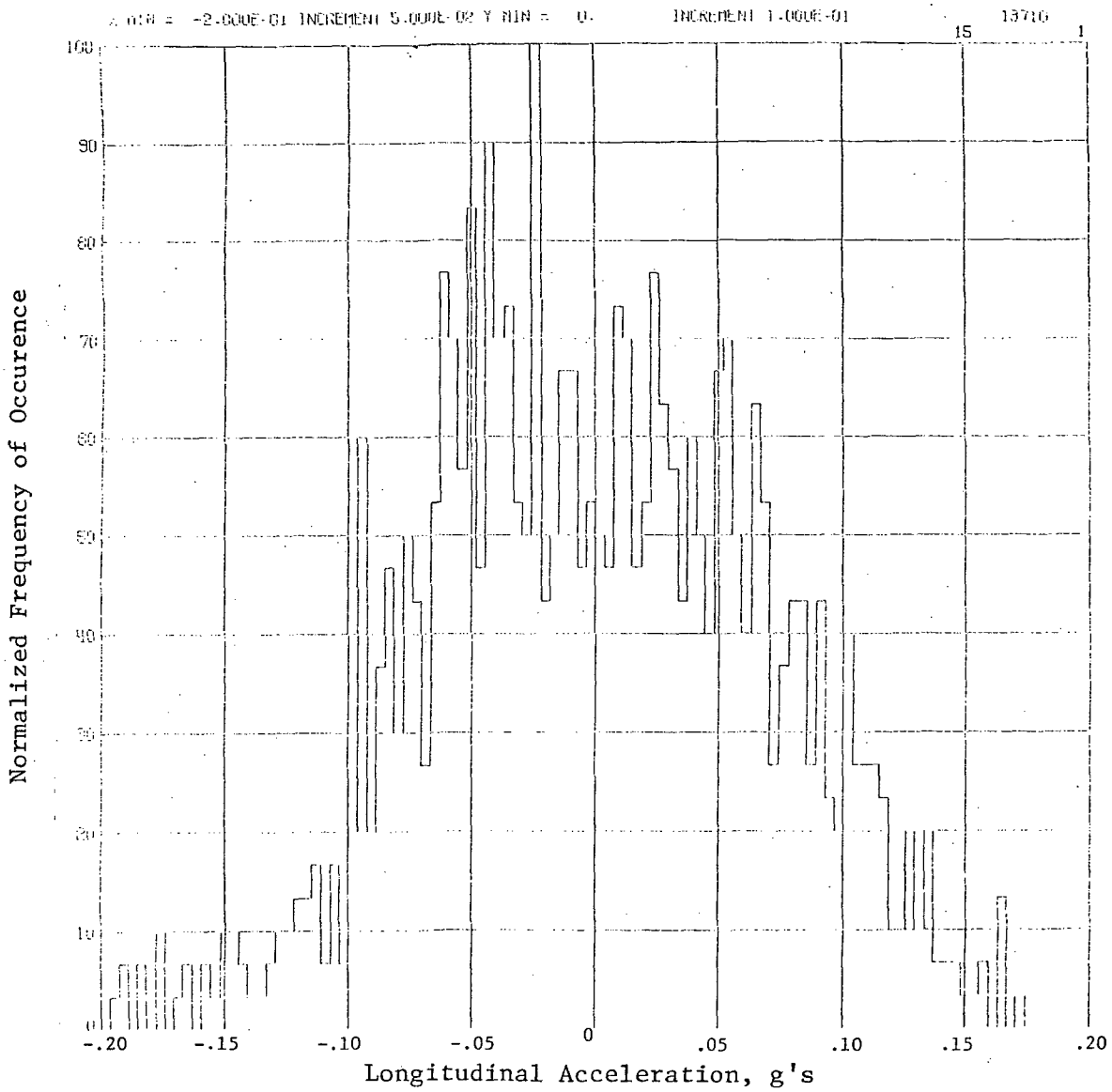

(c) Longitudinal acceleration histogram
(RMS-longitudinal acceleration 0.0723 g's)

FIGURE 6. Continued.

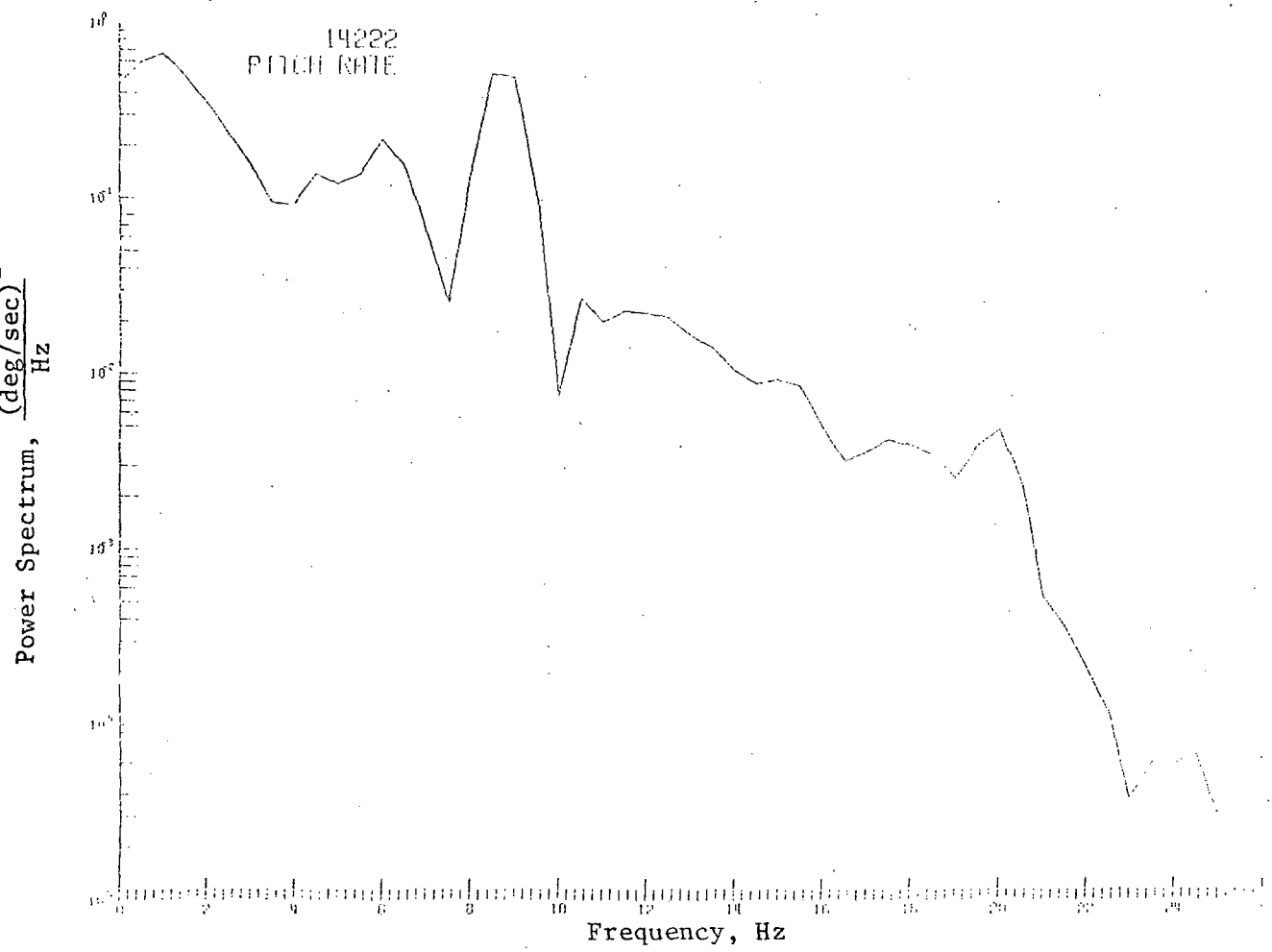

(d) Pitching velocity power spectrum
(RMS-pitching velocity 1.5954 deg/sec)

FIGURE 6. Continued.

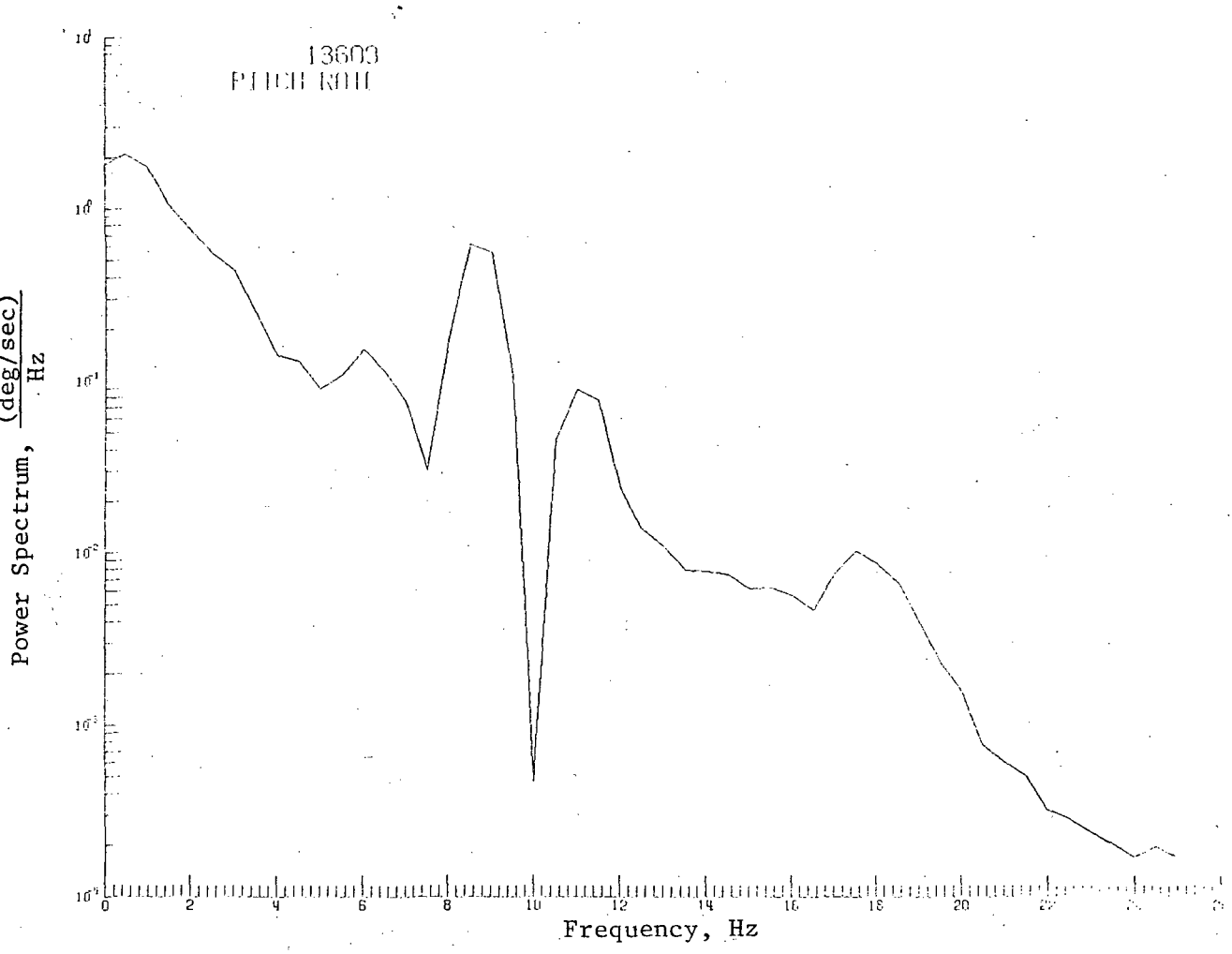

(d) Pitching velocity power spectrum
(RMS-pitching velocity 2.4617 deg/sec)

FIGURE 6. Continued.

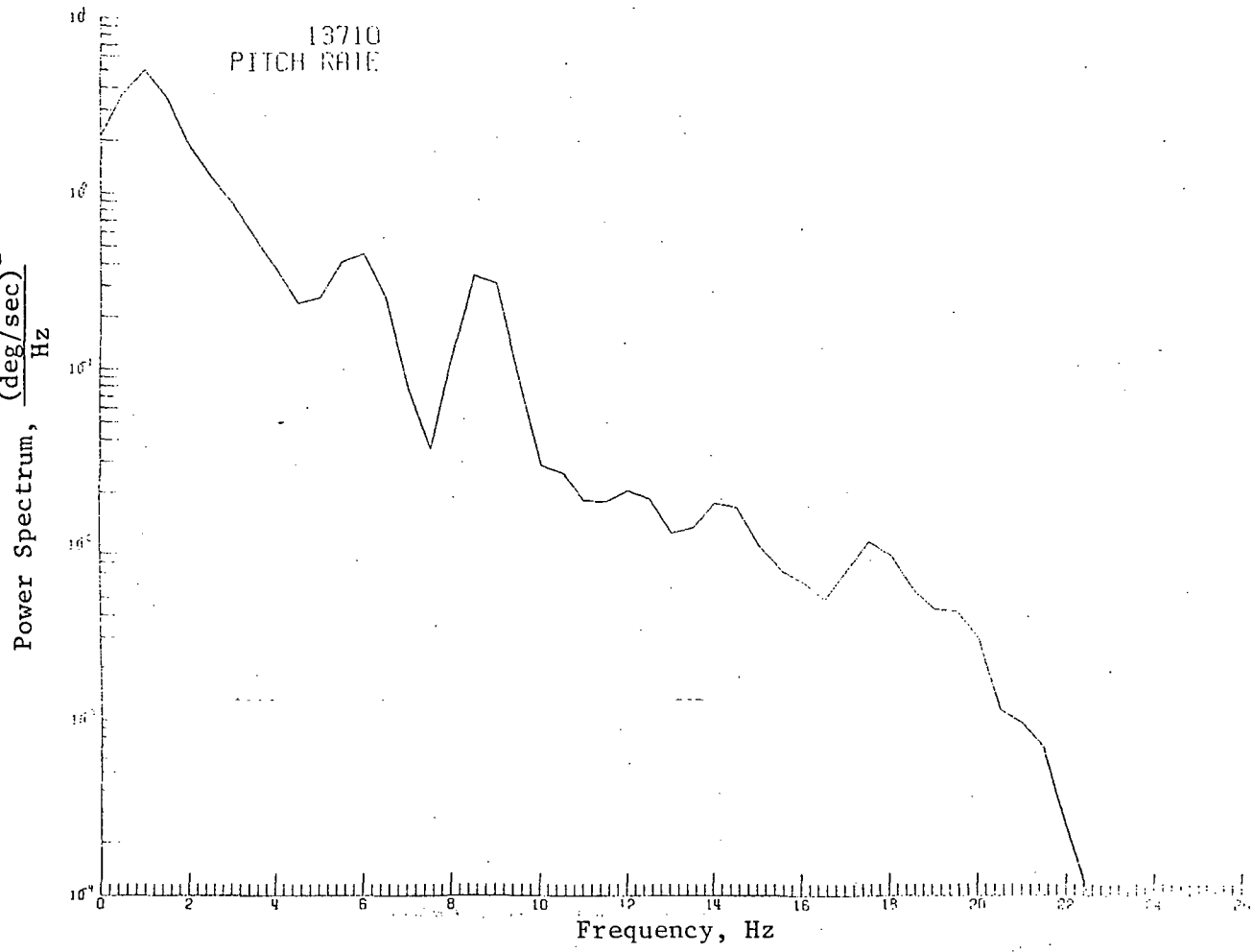

(d) Pitching velocity power spectrum
(RMS-pitching velocity 3.1371 deg/sec)

FIGURE 6. Continued.

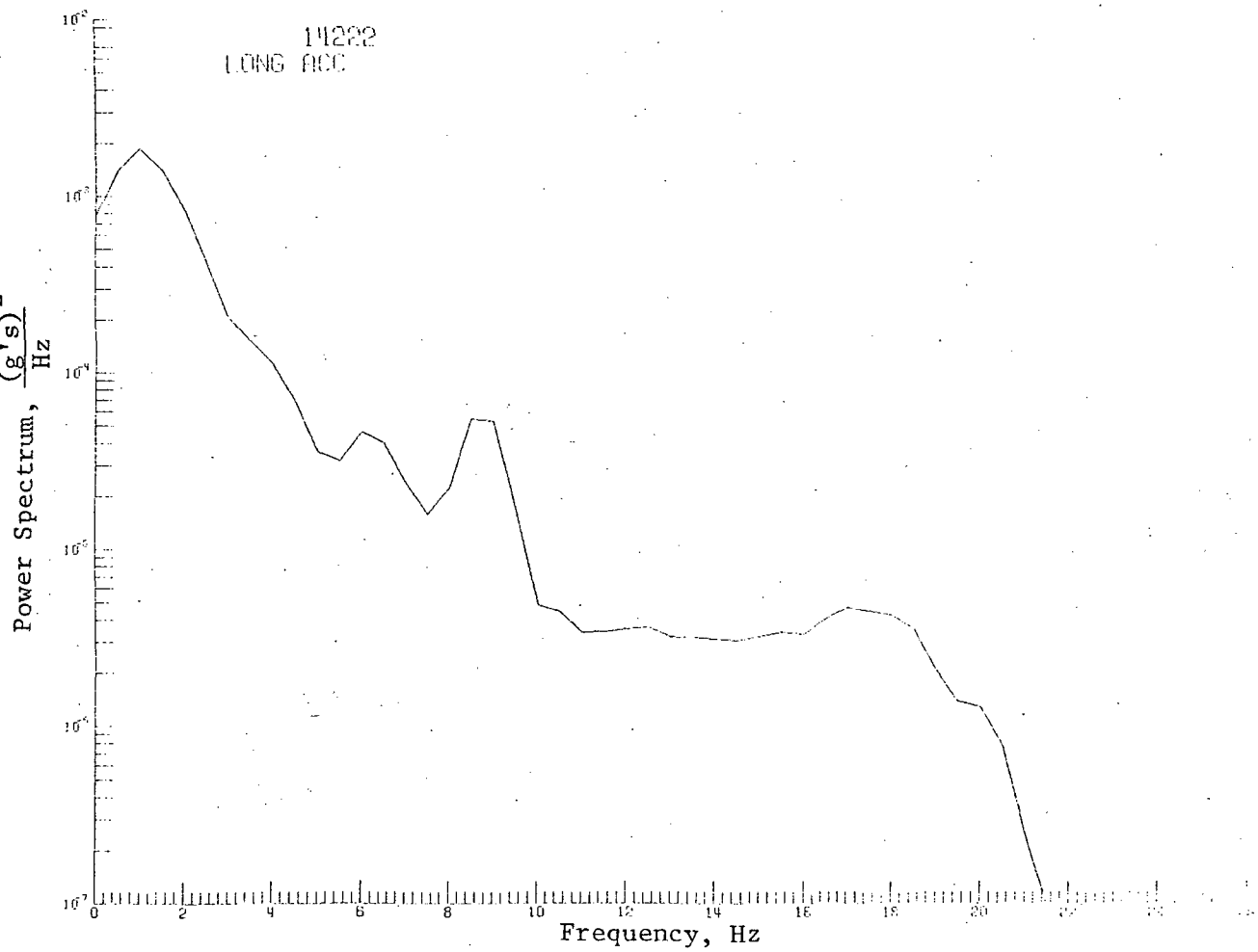

(e) Longitudinal acceleration power spectrum
(RMS-longitudinal acceleration 0.0603 g's)

FIGURE 6. Continued.

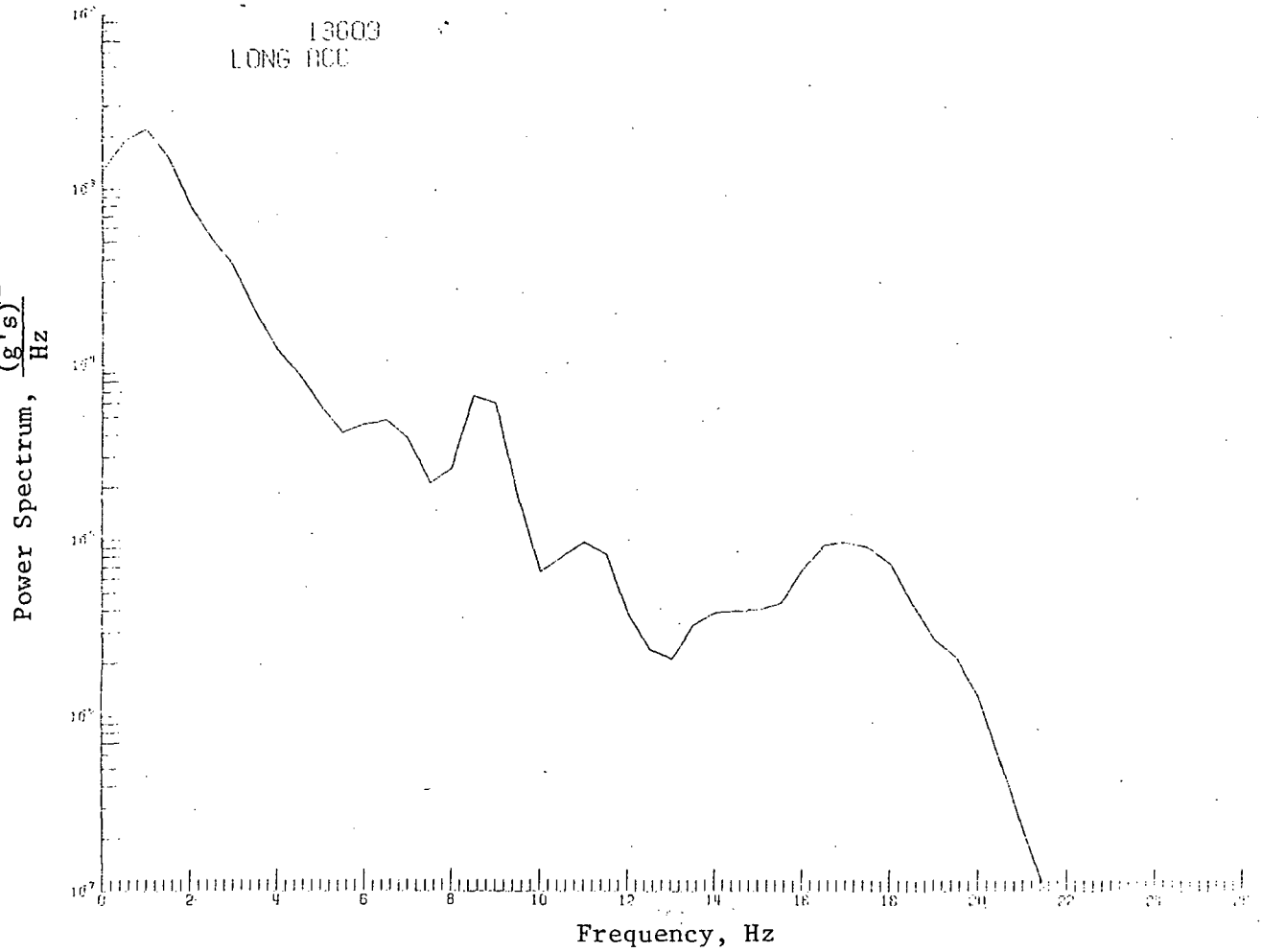

(e) Longitudinal acceleration power spectrum
(RMS-longitudinal acceleration 0.0678 g's)

FIGURE 6. Continued.

(e) Longitudinal acceleration power spectrum
(RMS-longitudinal acceleration 0.0723 g's)

FIGURE 6. Concluded.

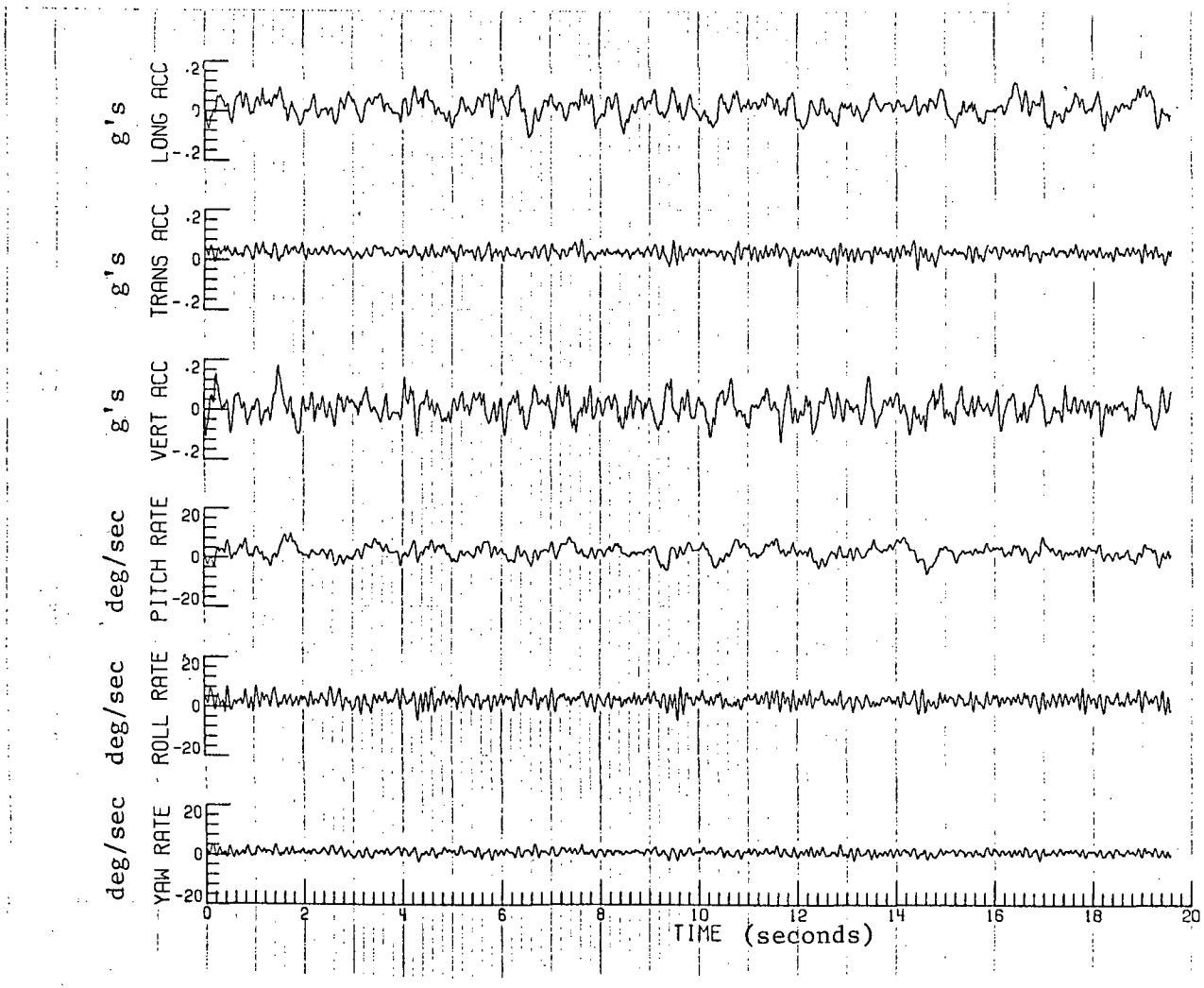

(a) Time histories (RMS-pitching velocity 2.4551 deg/sec; RMS-longitudinal acceleration 0.0382 g's)

FIGURE 7. MEASURED MOTION CHARACTERISTICS USING AN APPROXIMATELY CONSTANT RMS-PITCHING VELOCITY WITH A VARIABLE RMS-LONGITUDINAL ACCELERATION

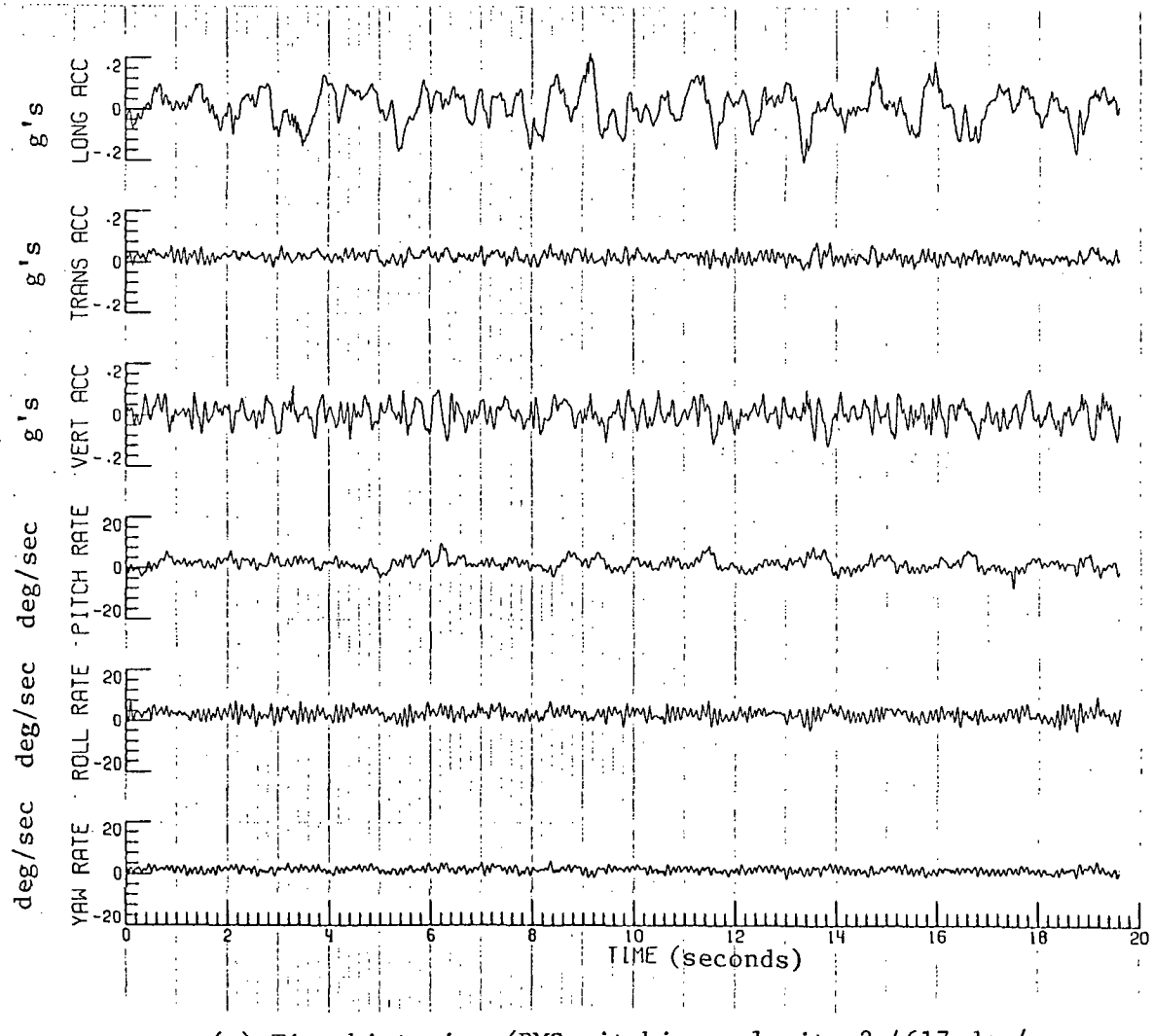

(a) Time histories (RMS-pitching velocity 2.4617 deg/sec; RMS-longitudinal acceleration 0.0678 g's)

FIGURE 7. Continued.

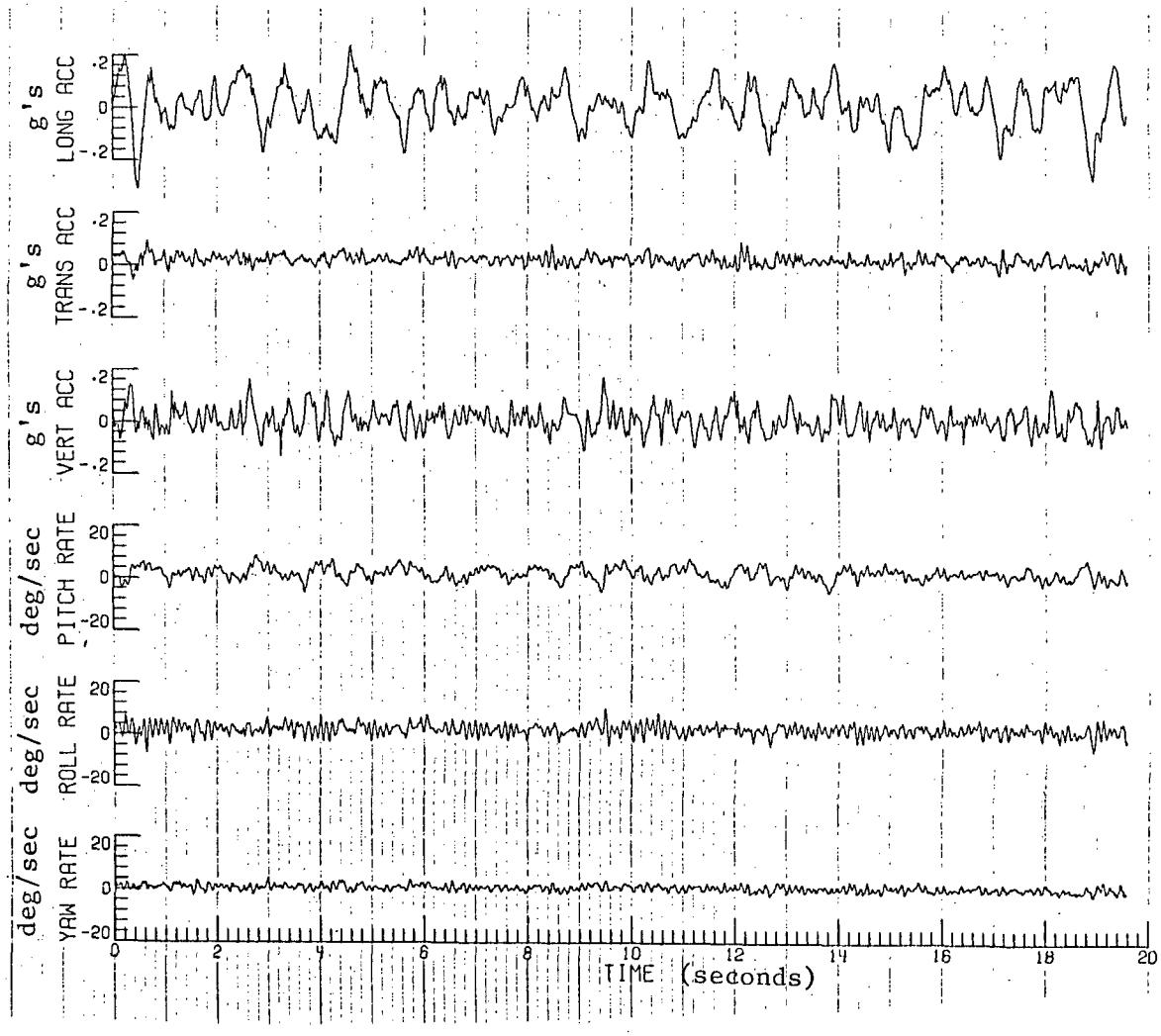

(a) Time histories (RMS-pitching velocity 2.7677 deg/sec; RMS-longitudinal acceleration 0.0846 g's)

FIGURE 7. Continued.

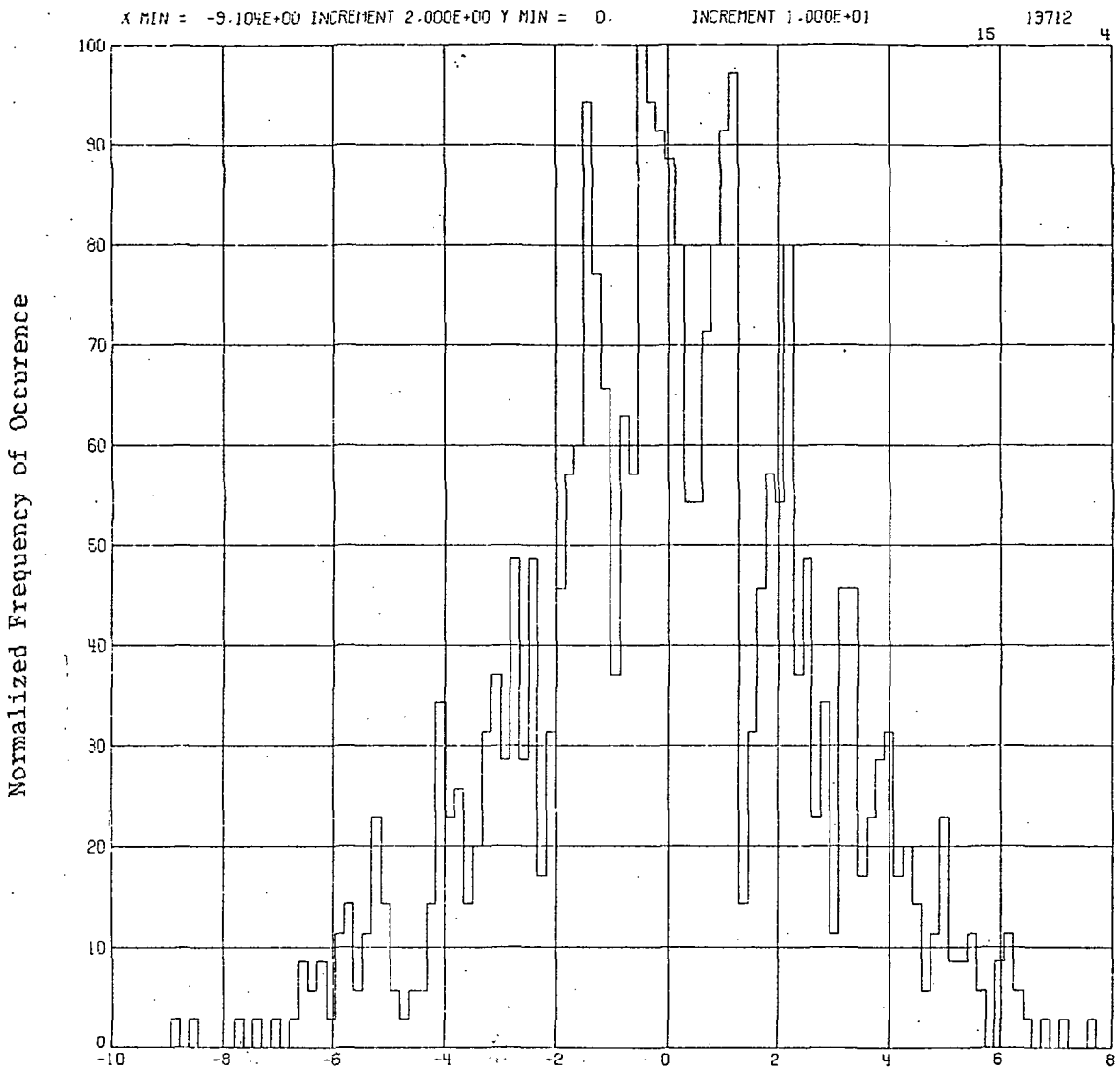

(b) Pitching velocity histogram
(RMS-pitching velocity 2.4551 deg/sec)

FIGURE 7. Continued.

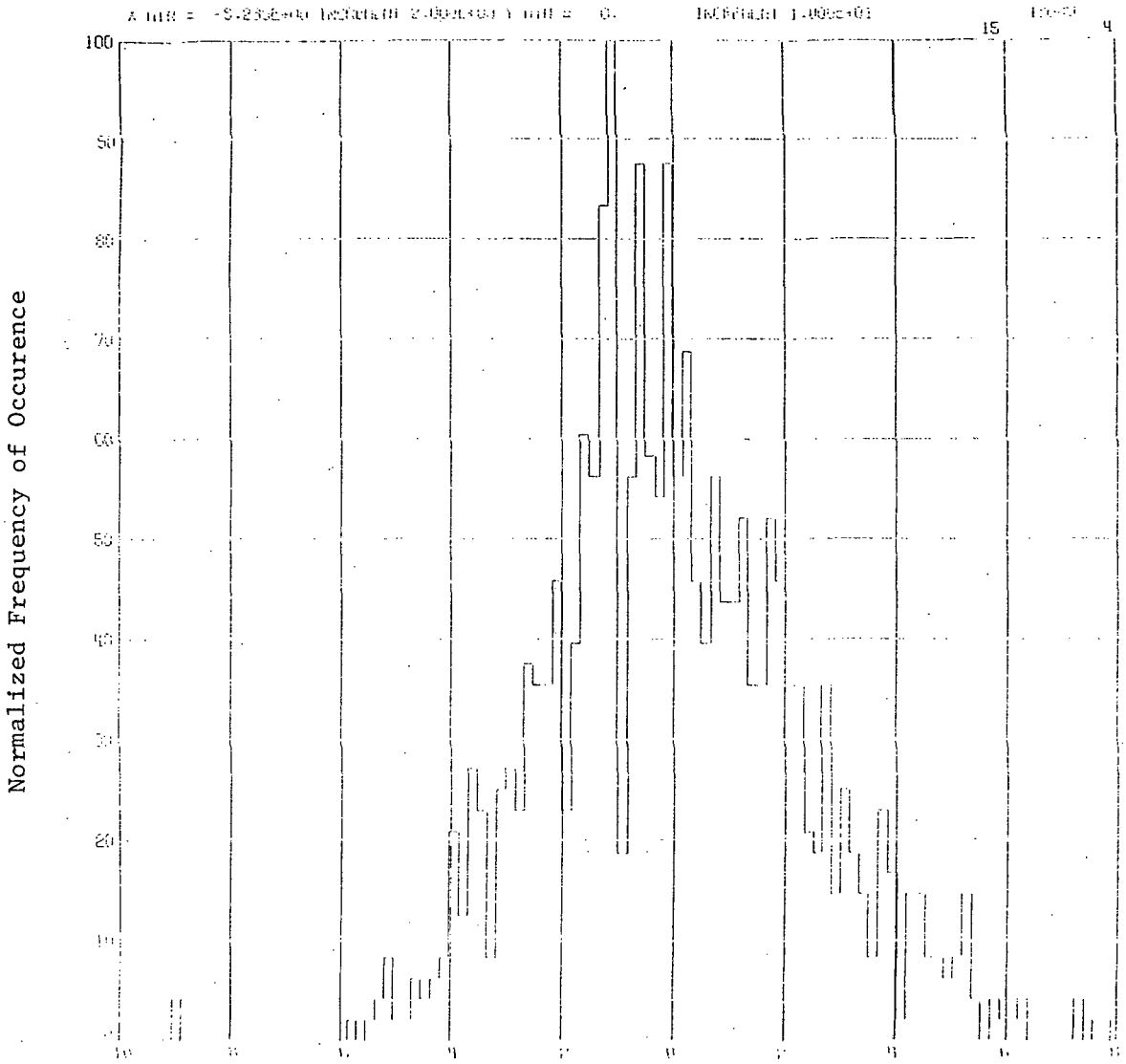

(b) Pitching velocity histogram
(RMS-pitching velocity 2.4617 deg/sec)

FIGURE 7. Continued.

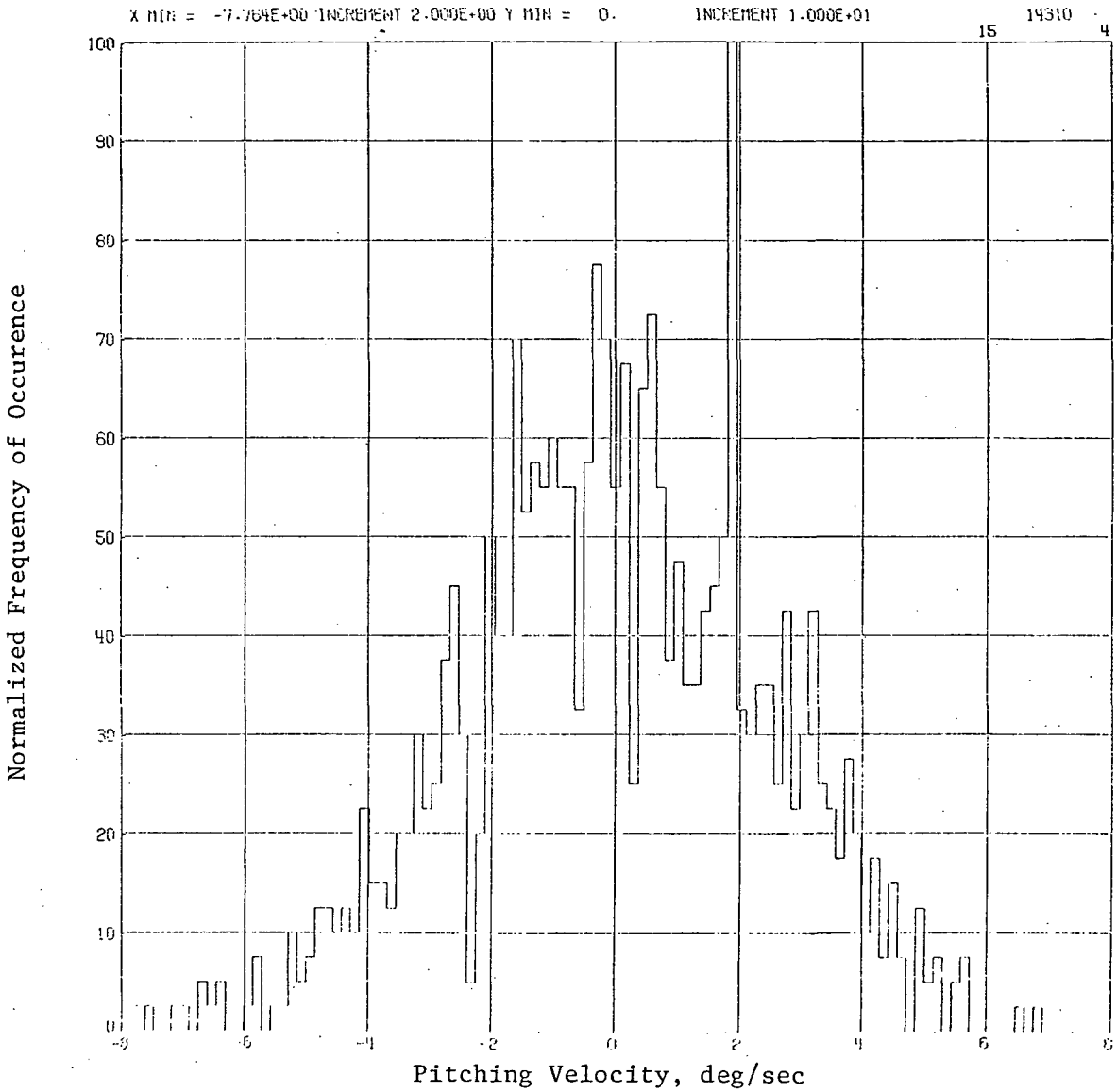

(b) Pitching velocity histogram
(RMS-pitching velocity 2.7677 deg/sec)

FIGURE 7. Continued.

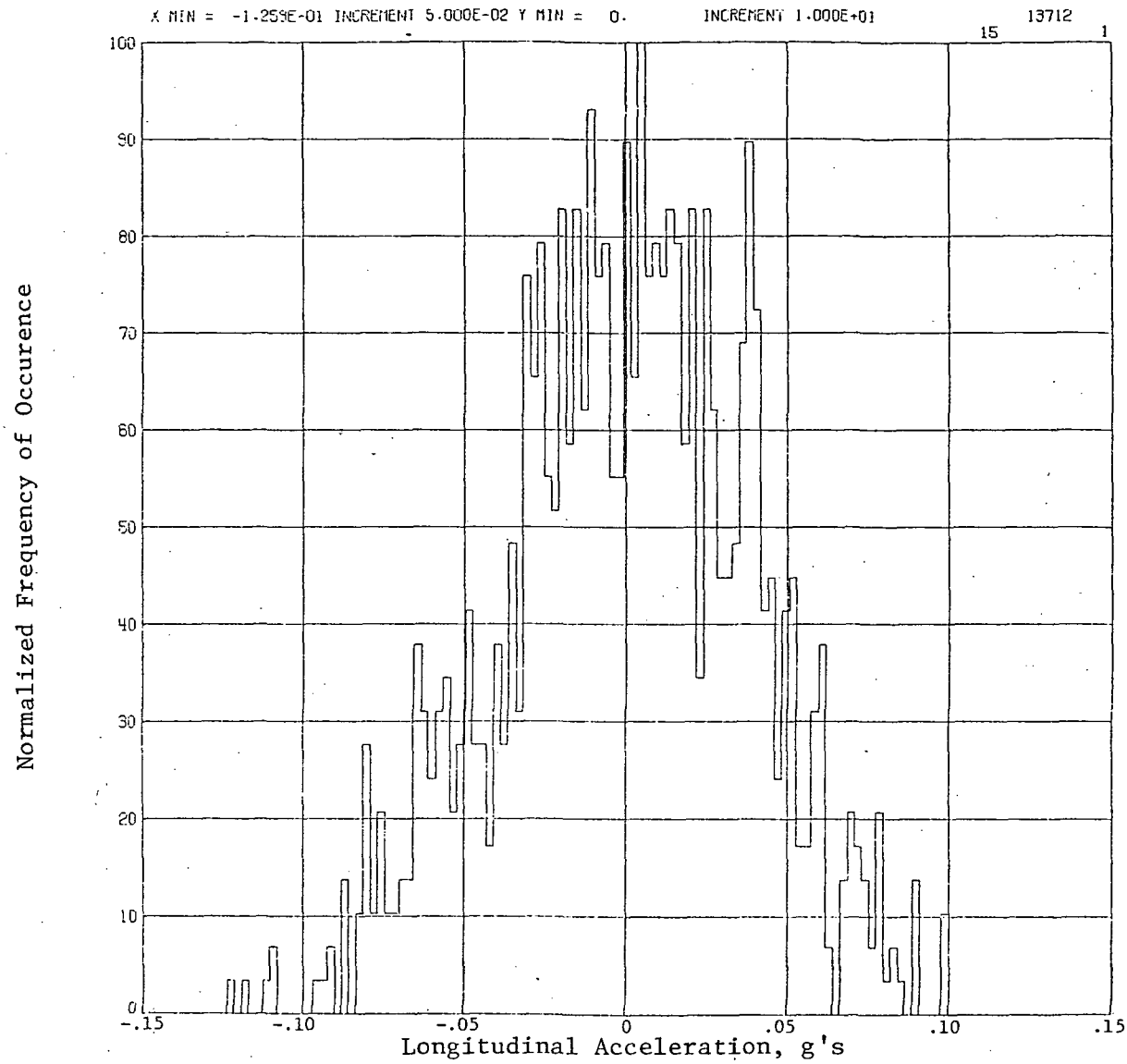

(c) Longitudinal acceleration histogram
(RMS-longitudinal acceleration 0.0382 g's)

FIGURE 7. Continued.

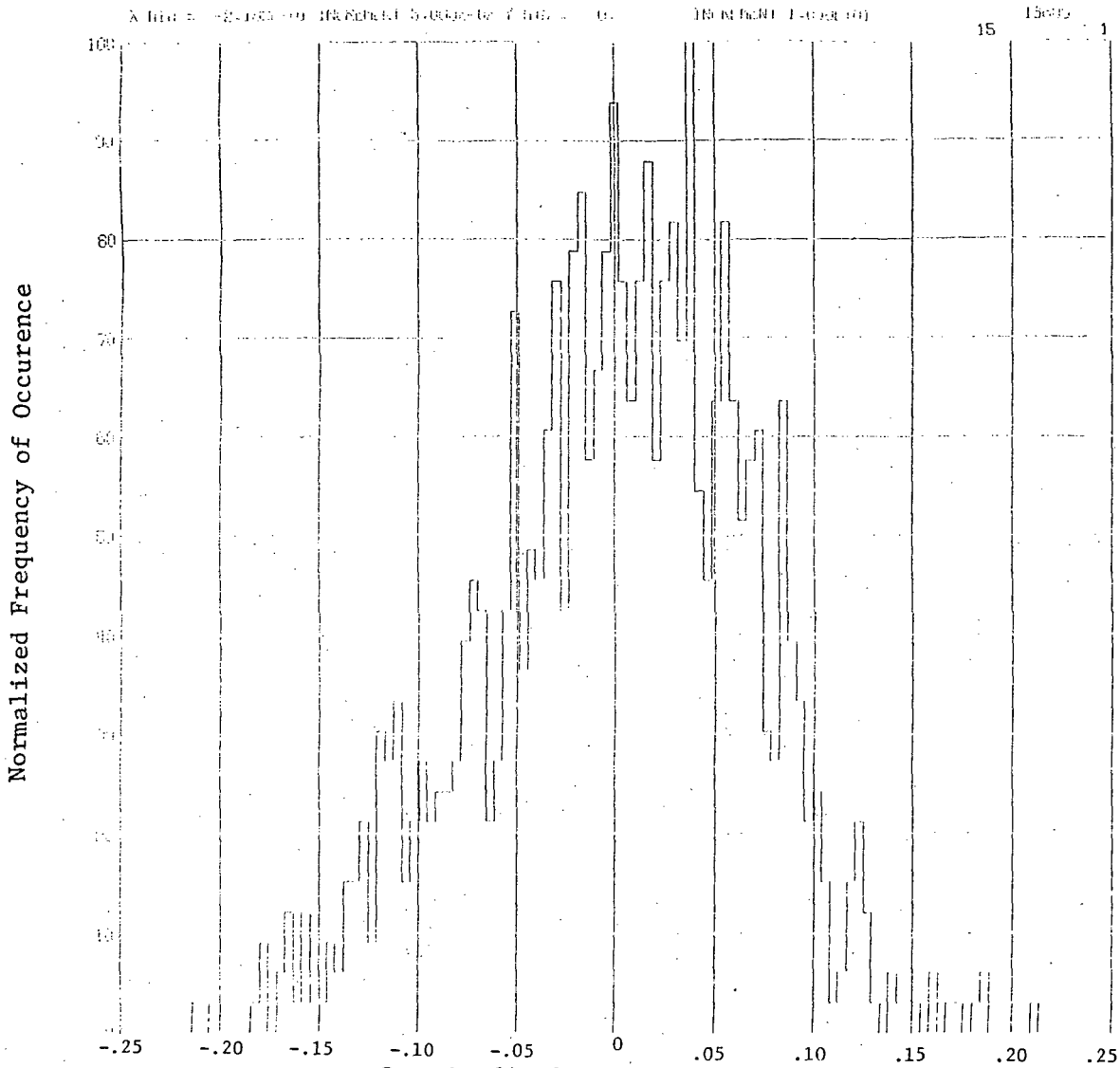

(c) Longitudinal acceleration histogram
(RMS-longitudinal acceleration 0.0678 g's)

FIGURE 7. Continued.

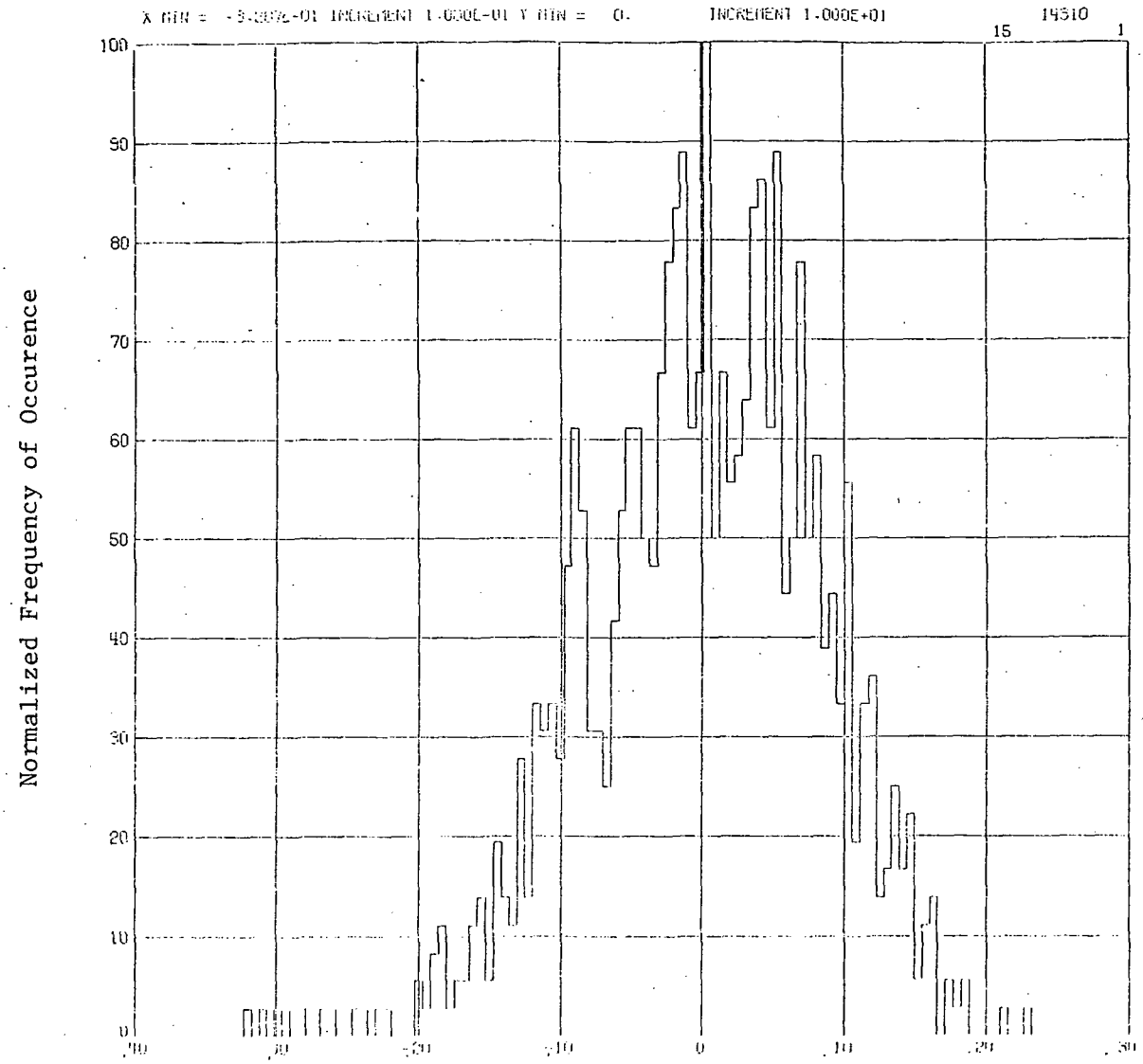

(c) Longitudinal acceleration histogram
(RMS-longitudinal acceleration 0.0846 g's)

FIGURE 7. Continued.

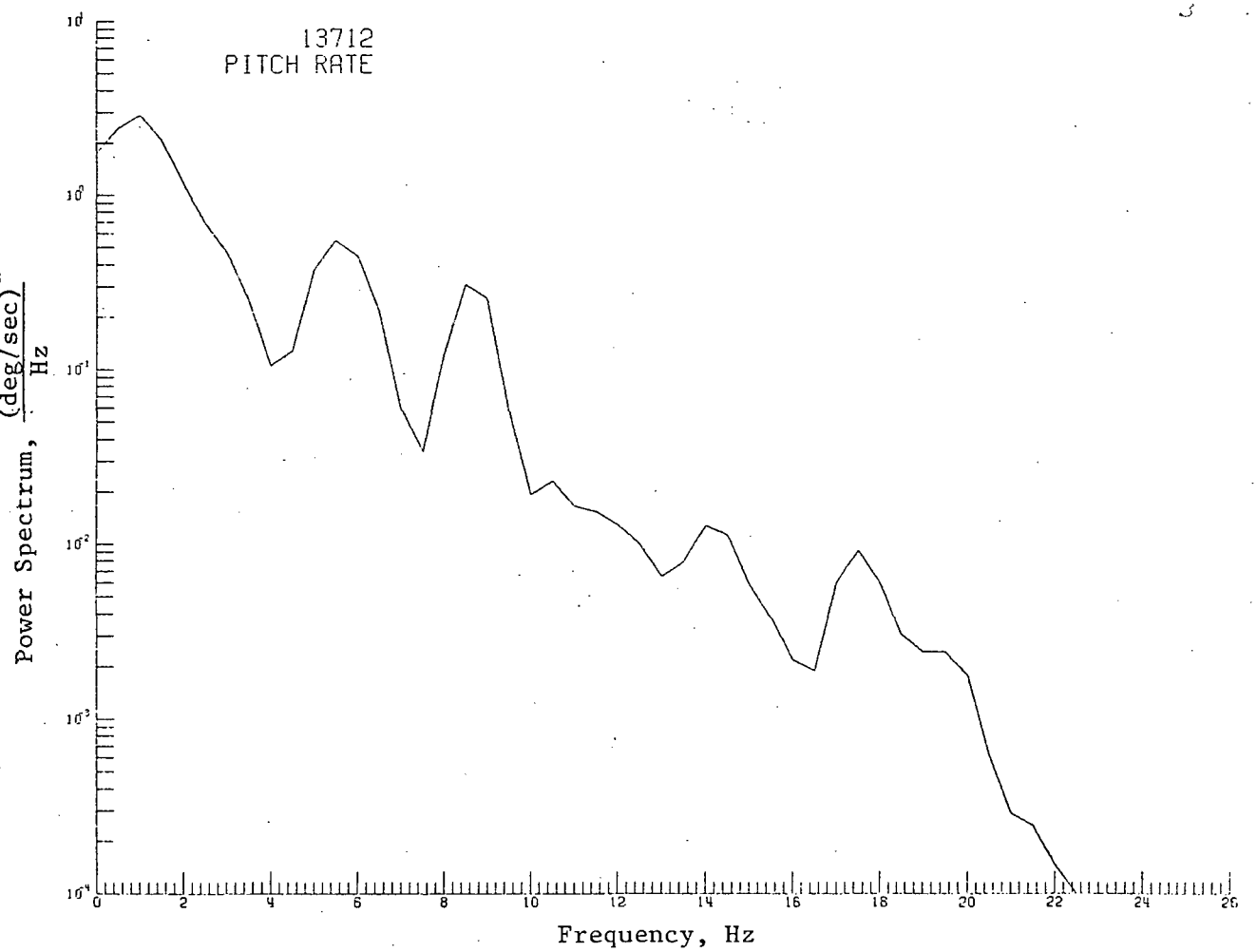

(d) Pitching velocity power spectrum
(RMS-pitching velocity 2.4551 deg/sec)

FIGURE 7. Continued.

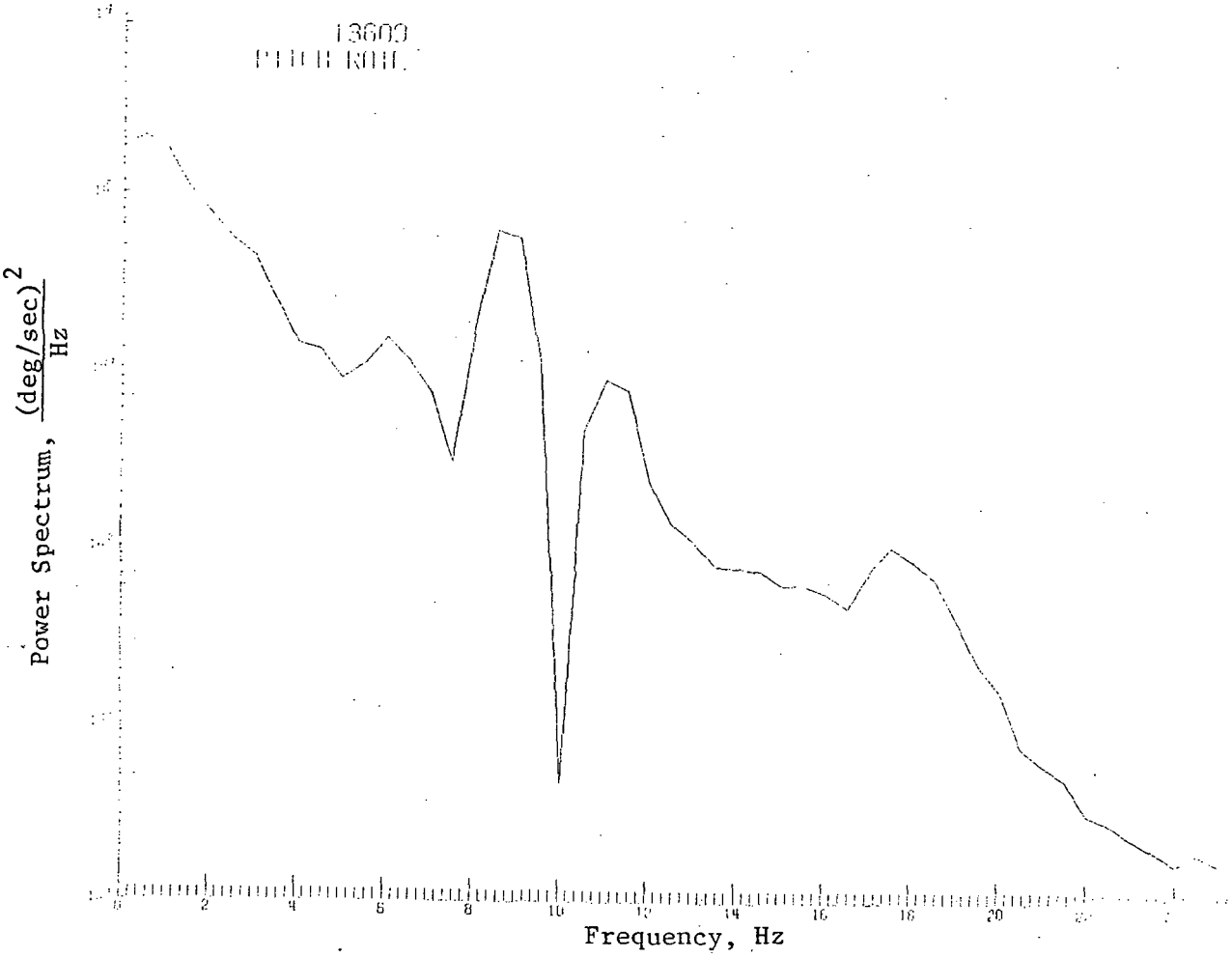

(d) Pitching velocity power spectrum
(RMS-pitching velocity 2.4617 deg/sec)

FIGURE 7. Continued.

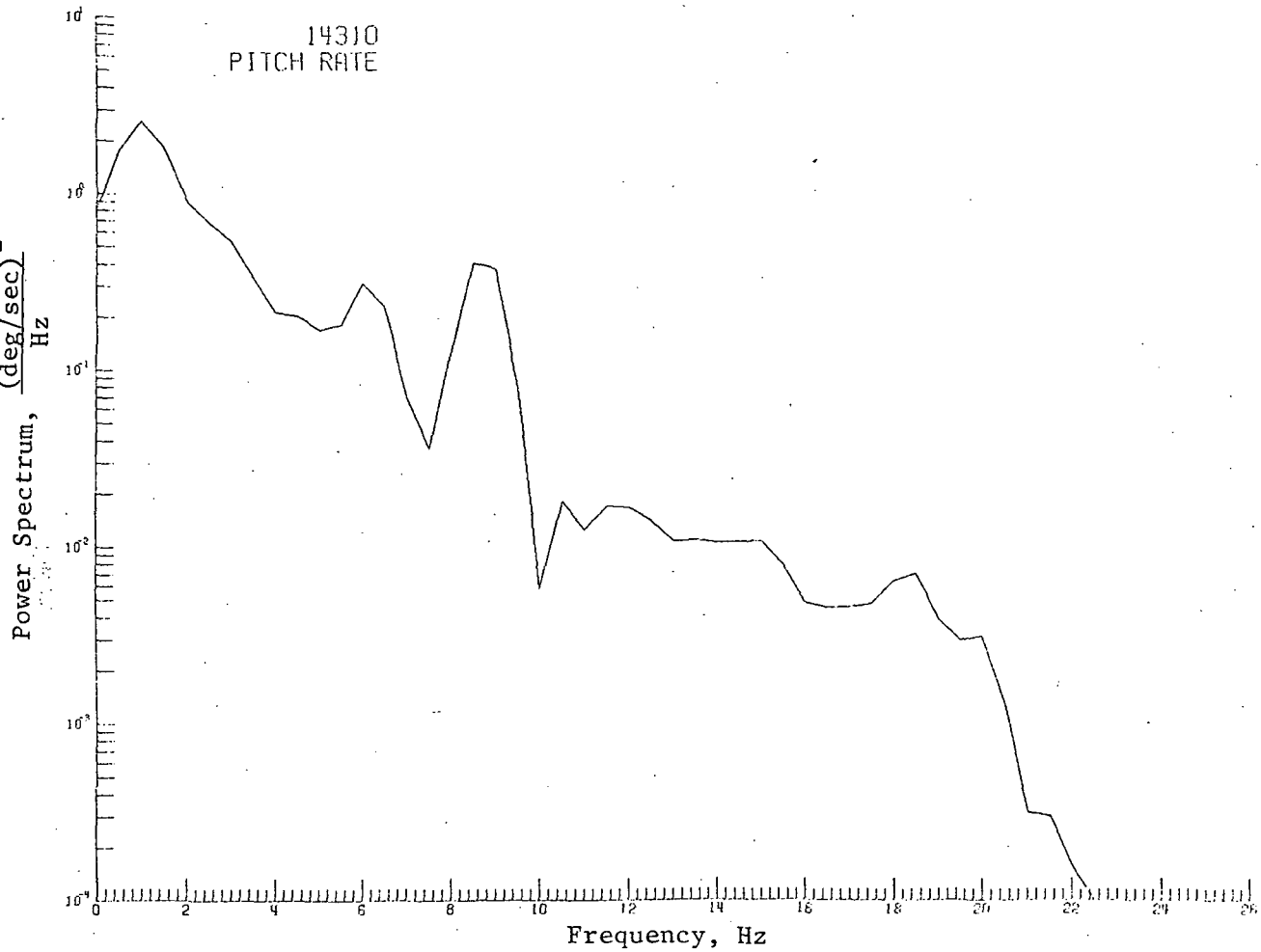

(d) Pitching velocity power spectrum
(RMS-pitching velocity 2.7677 deg/sec)

FIGURE 7. Continued.

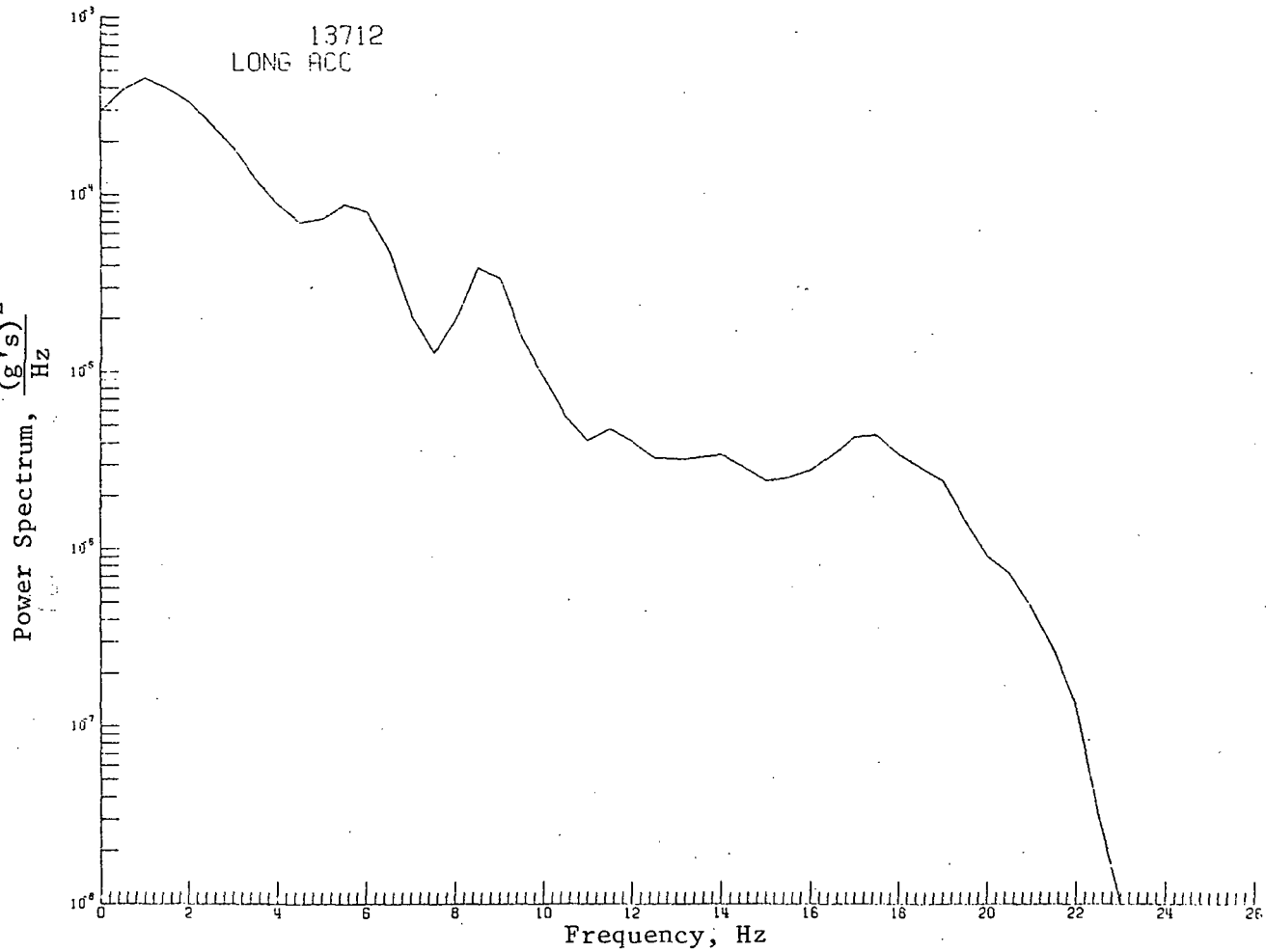

(e) Longitudinal acceleration power spectrum
(RMS-longitudinal acceleration 0.0382 g's)

FIGURE 7. Continued.

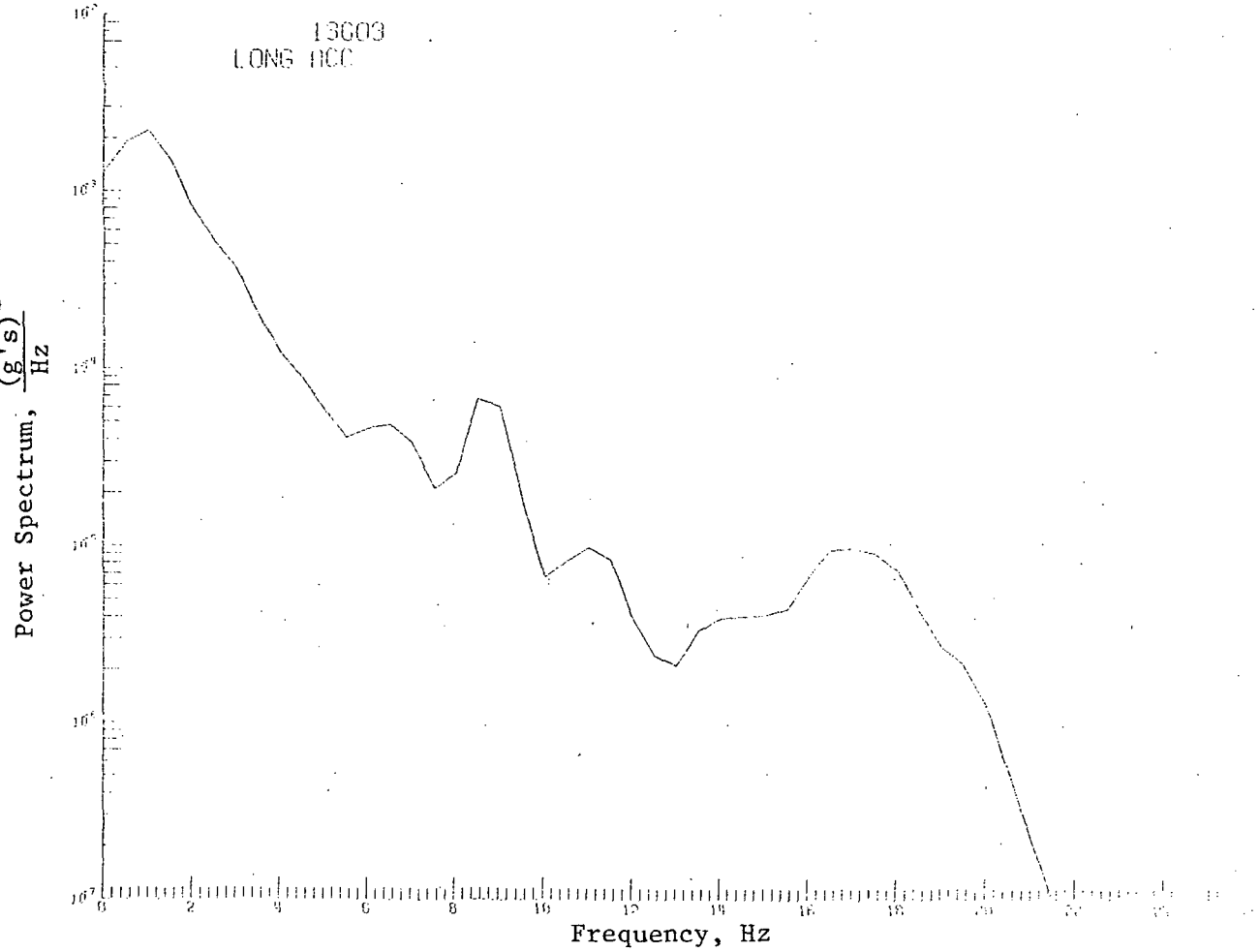

(e) Longitudinal acceleration power spectrum
(RMS-longitudinal acceleration 0.0687 g's)

FIGURE 7. Continued.

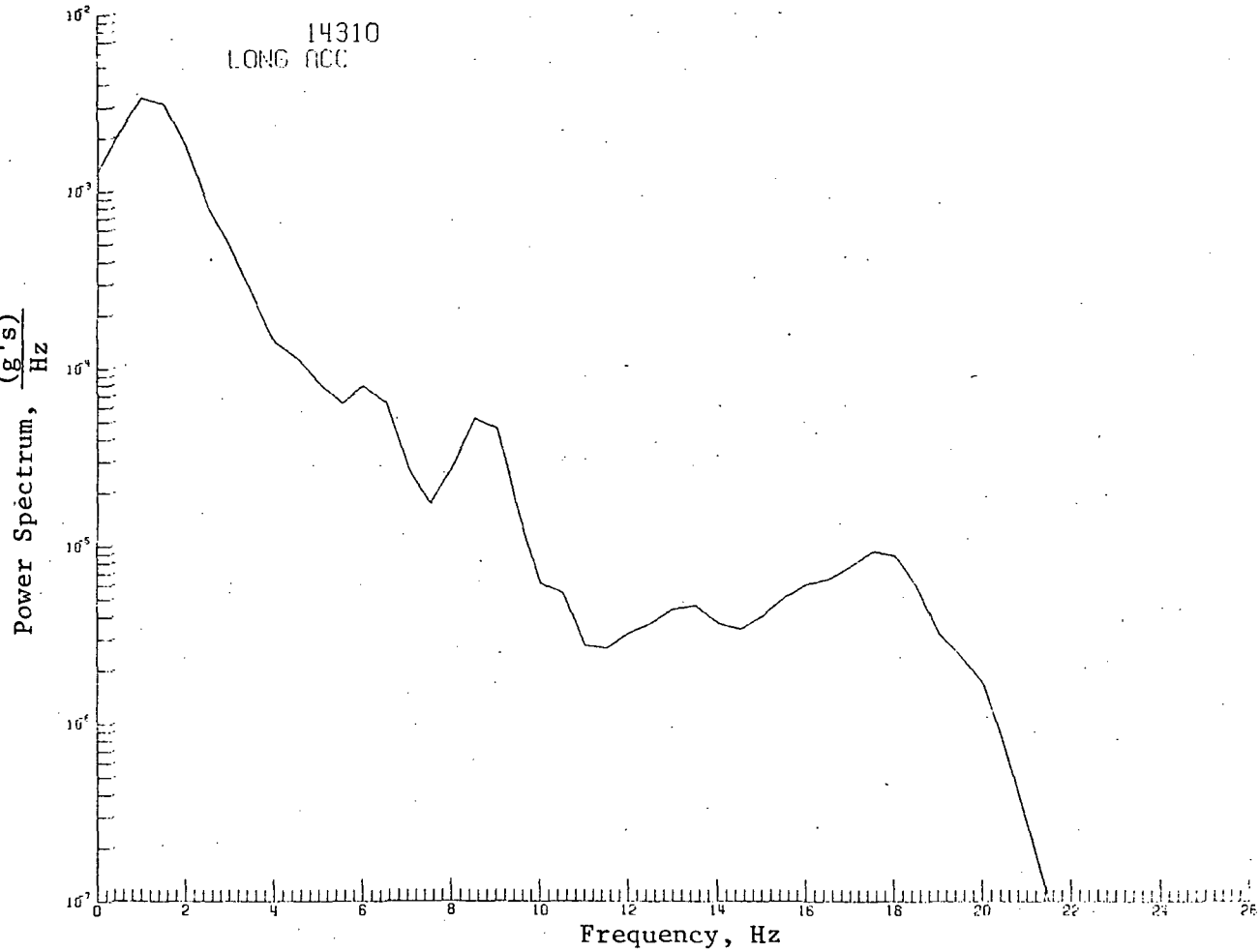

(e) Longitudinal acceleration power spectrum
(RMS-longitudinal acceleration 0.0846 g's)

FIGURE 7. Concluded.

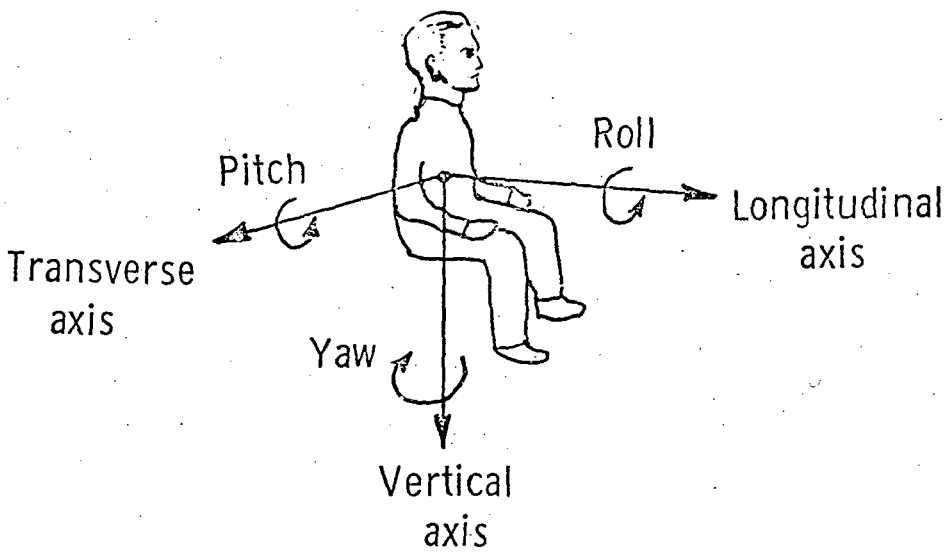

Figure 8 – Reference axes.

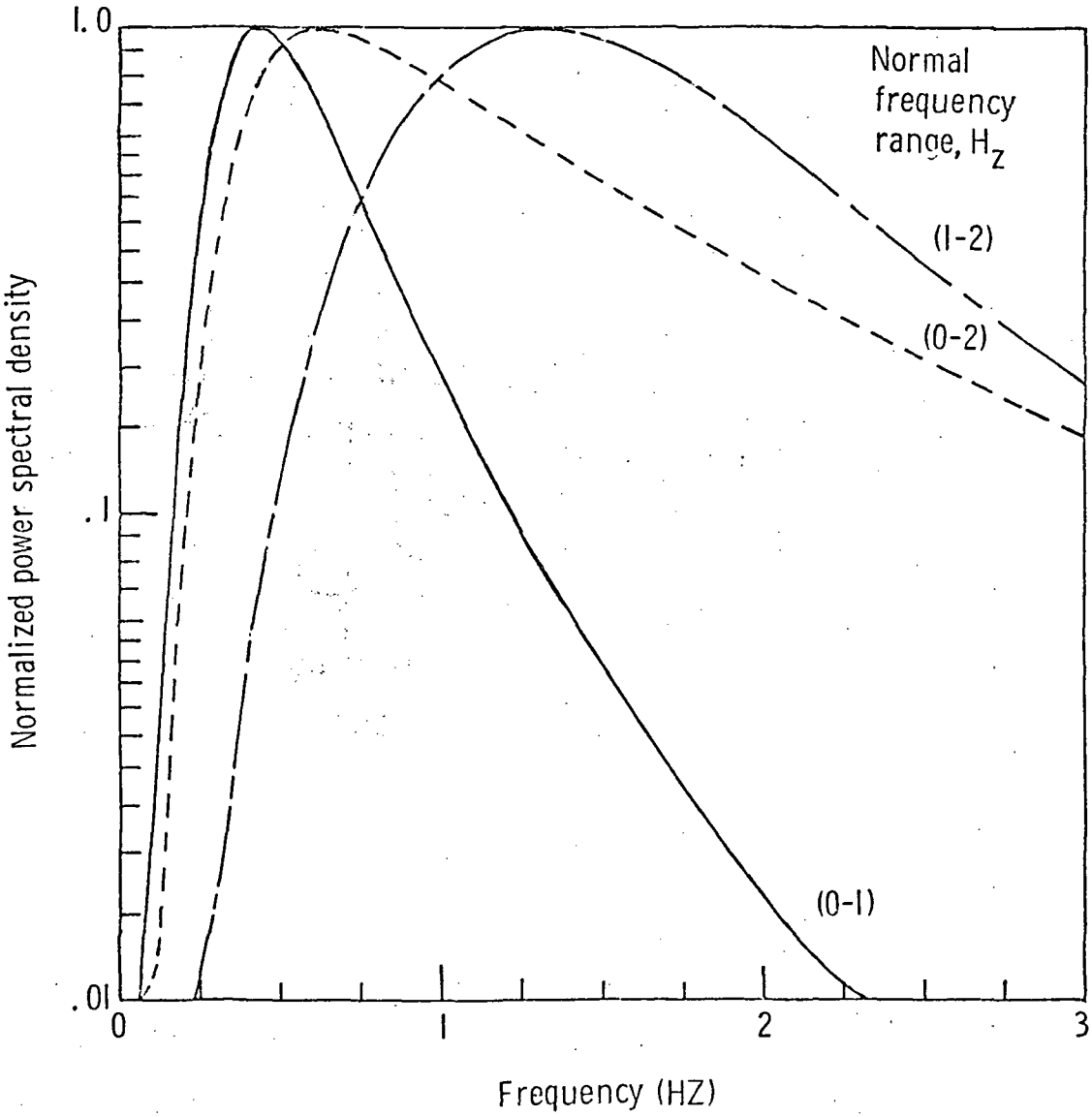

(a) Typical spectra.

Figure 9 - Nominal power spectra of motion components.

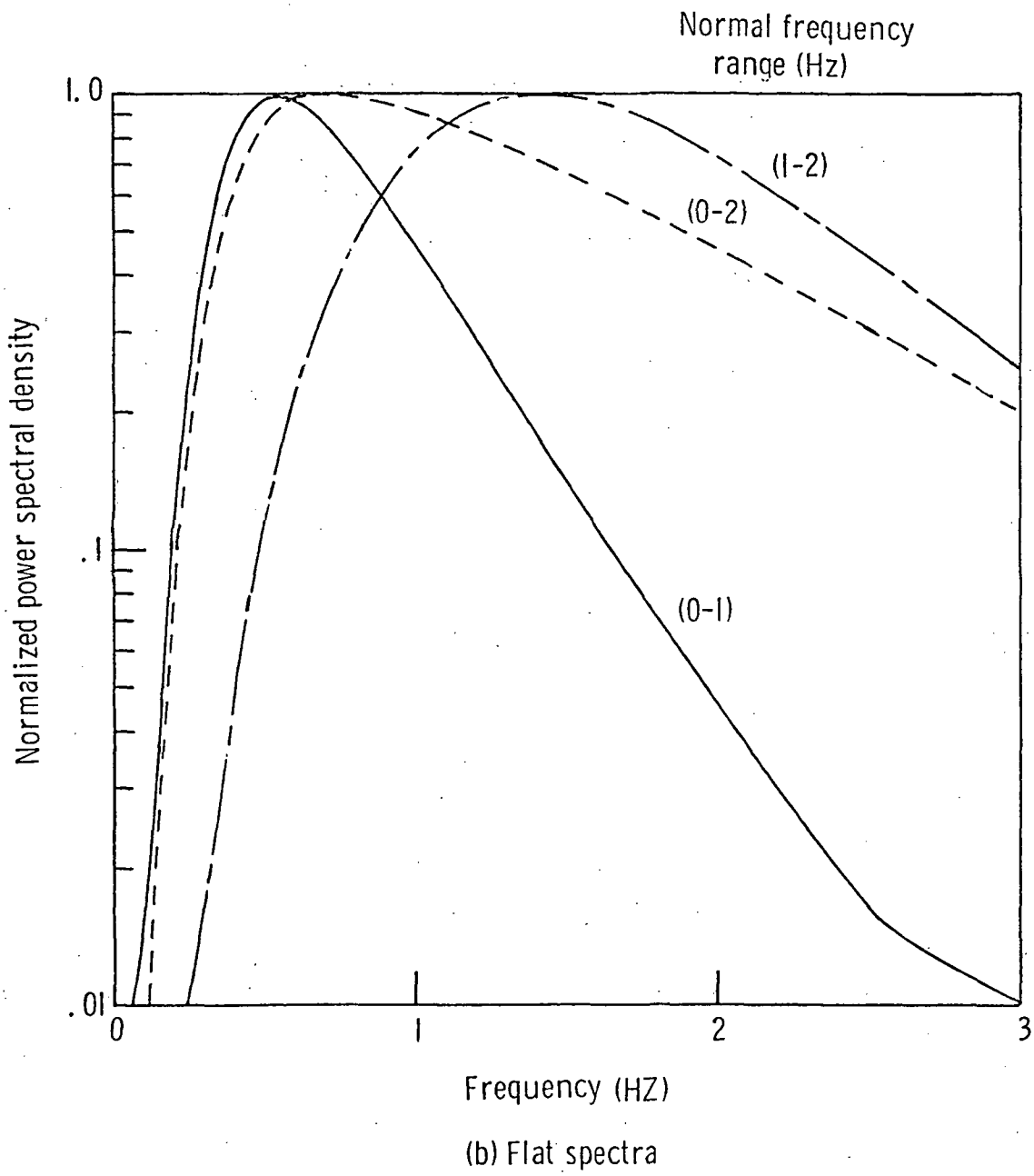

(b) Flat spectra

Figure 9 - Concluded.

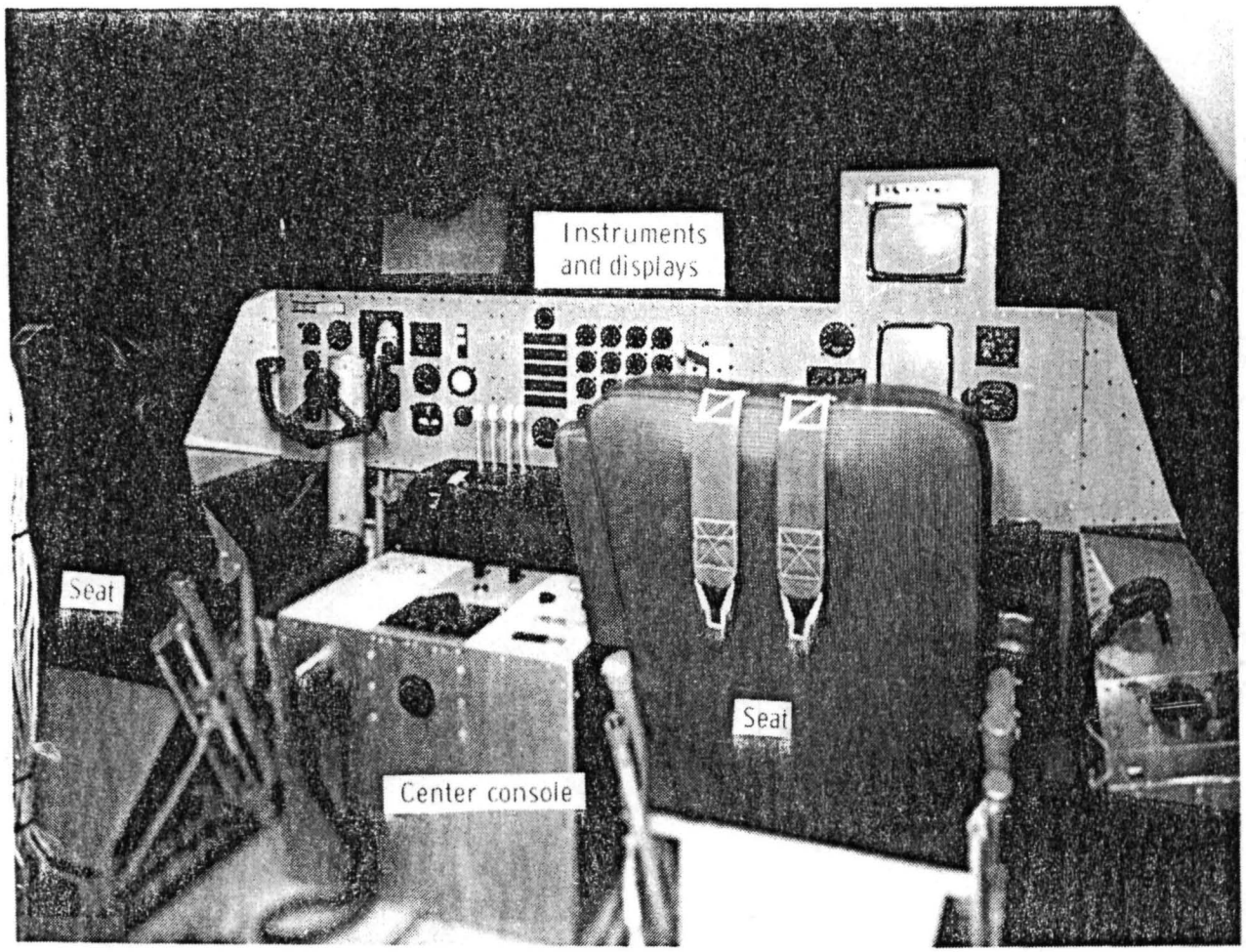

Figure 10- Interior of the Langley six-degree-of-freedom vision motion simulator.

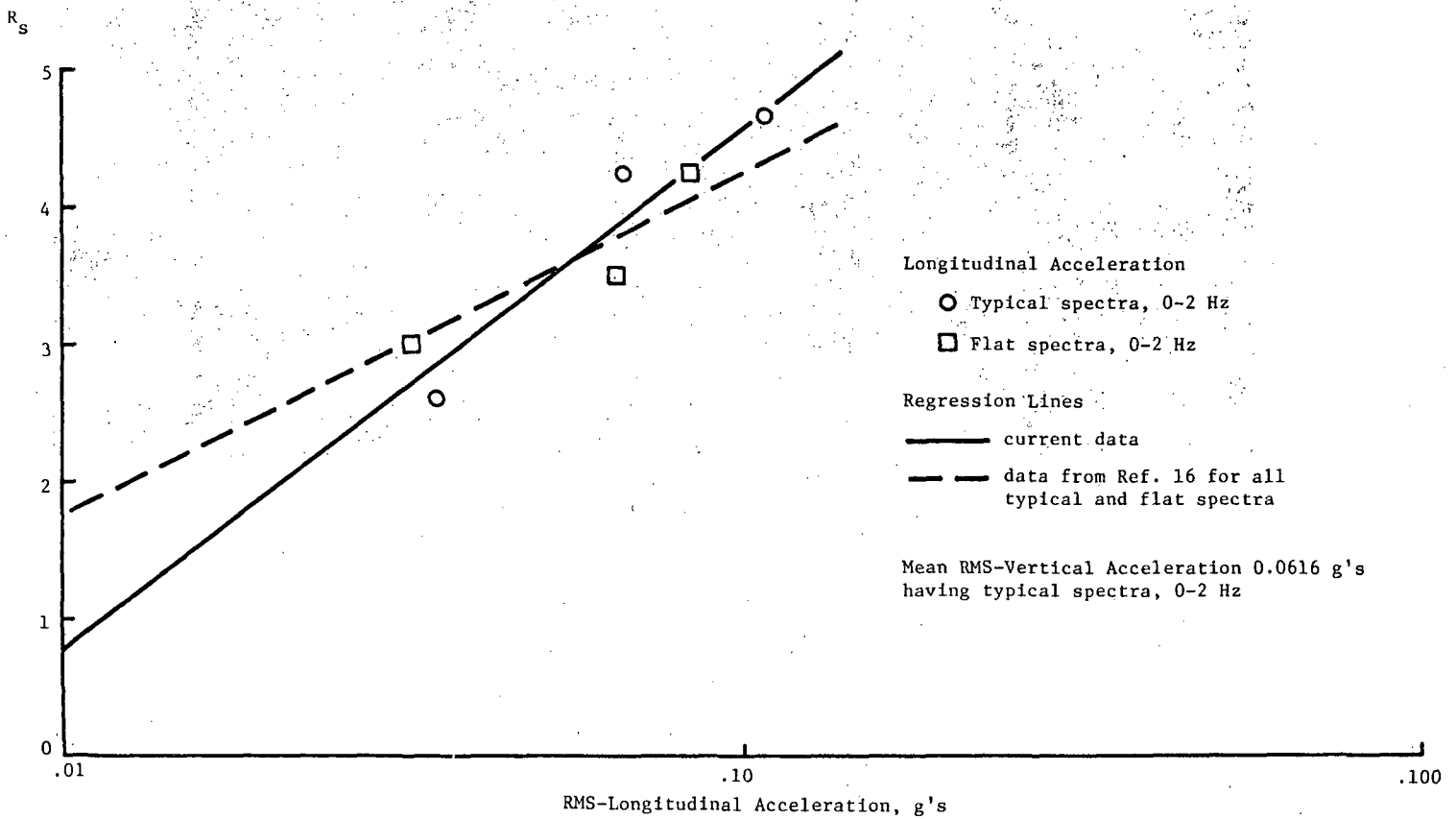

Figure 11. Effect of an approximately constant RMS-vertical acceleration added to a variable RMS-longitudinal acceleration on human comfort response

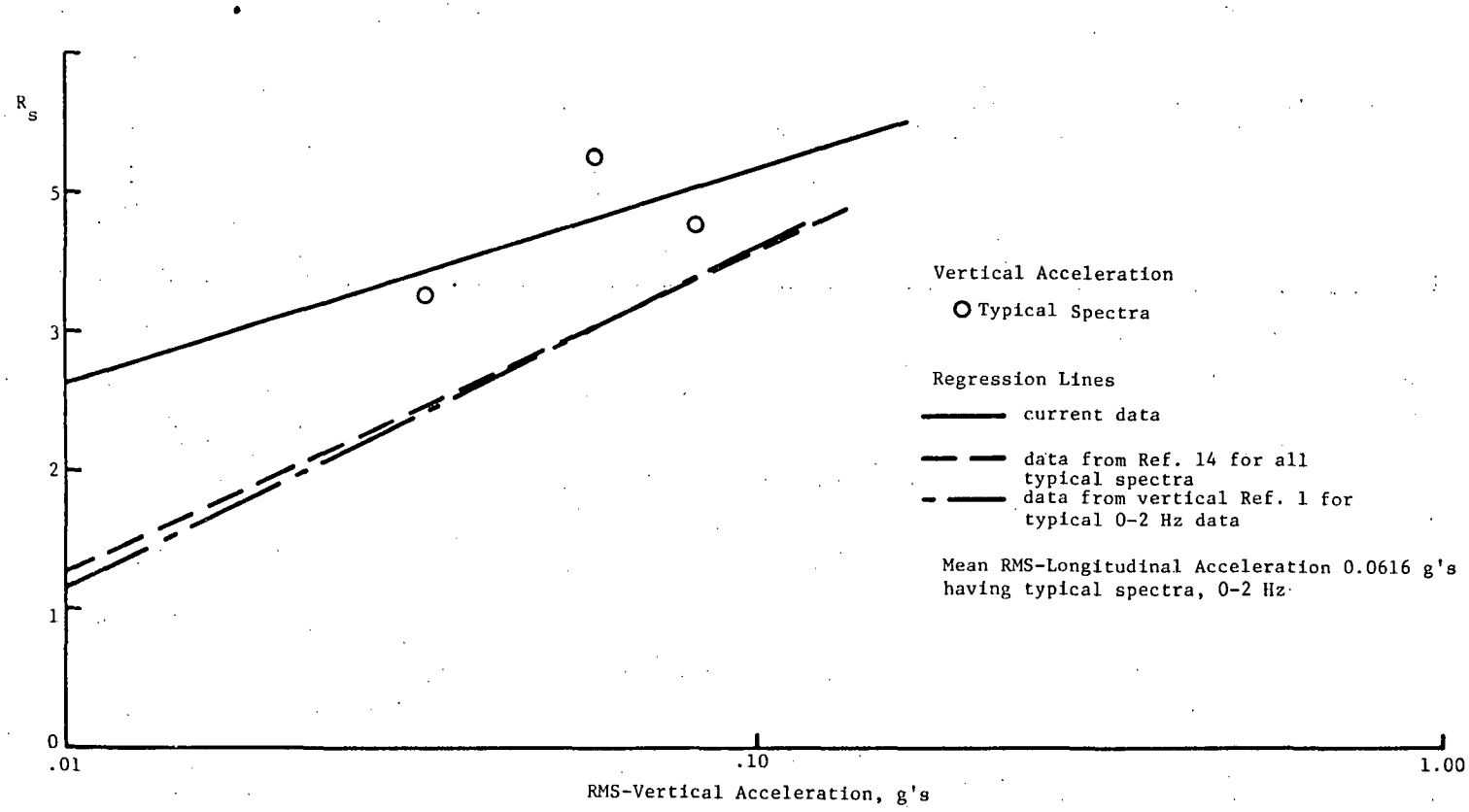

Figure 12. Effect of an approximately constant RMS-longitudinal acceleration added to a variable RMS-vertical acceleration on human comfort response

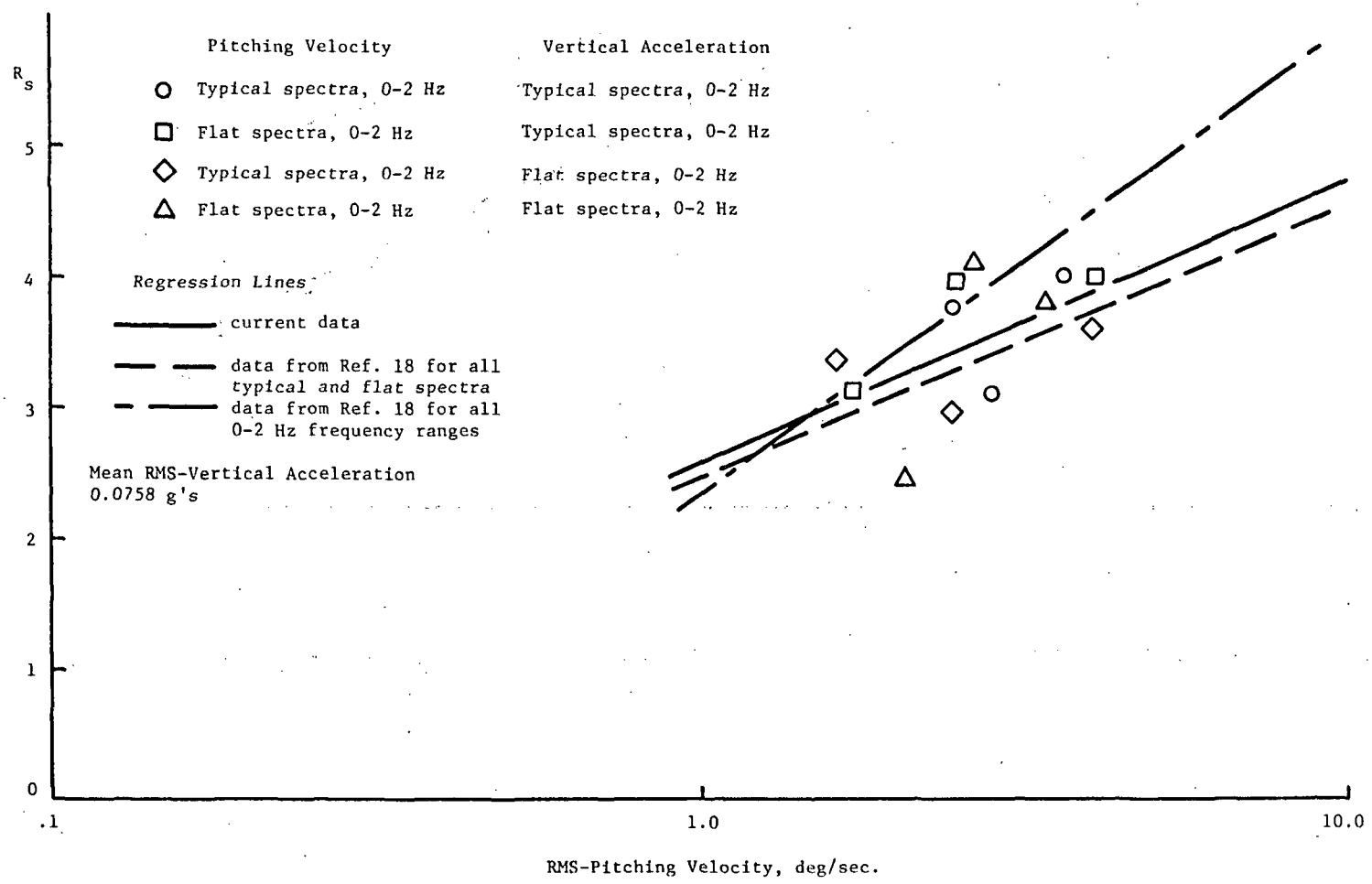

Figure 13. Effect of an approximately constant RMS-vertical acceleration added to a variable RMS-pitching velocity on human comfort response

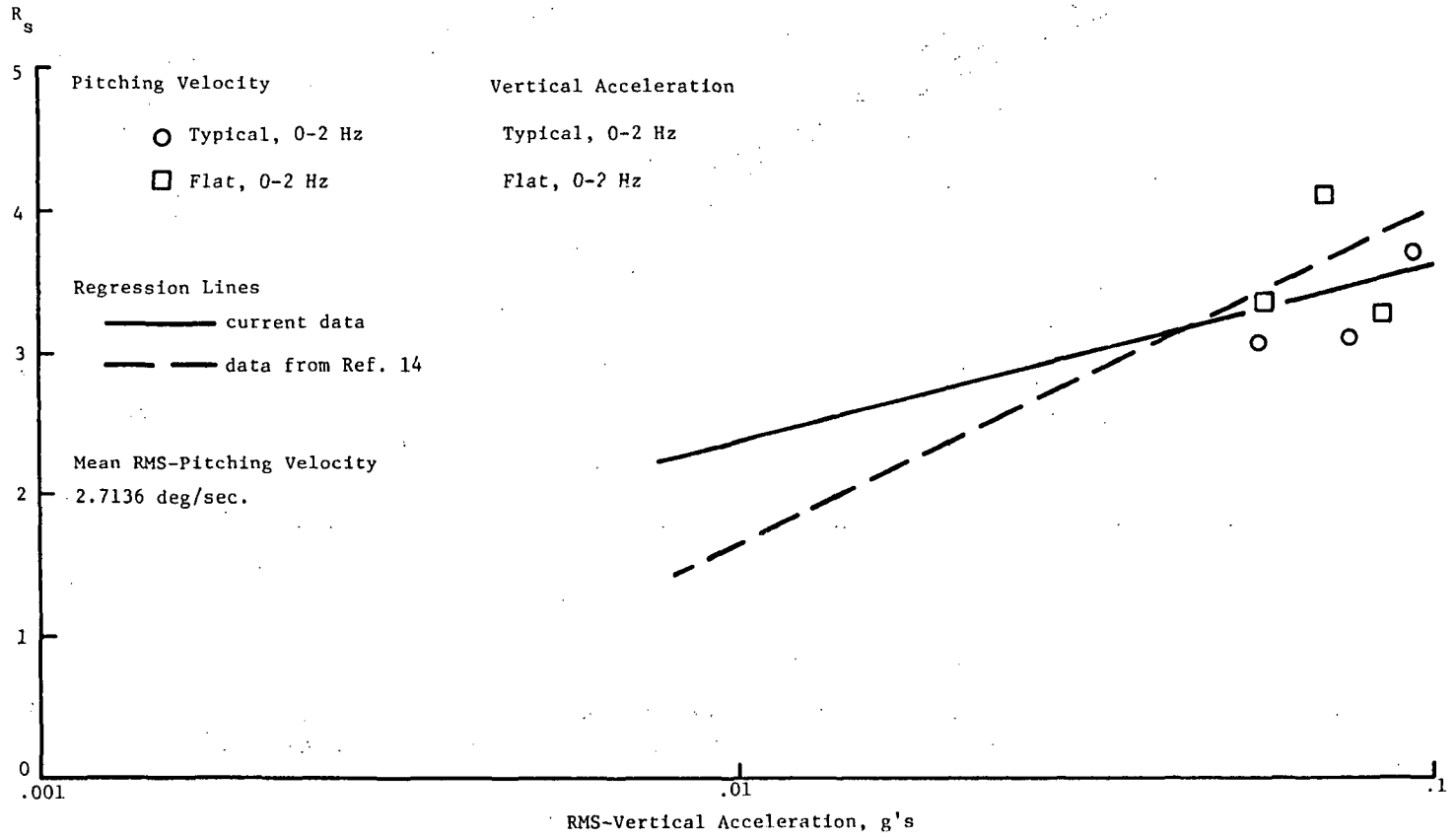

Figure 14. Effect of an approximately constant RMS-pitching velocity added to a variable RMS-vertical acceleration on human comfort response

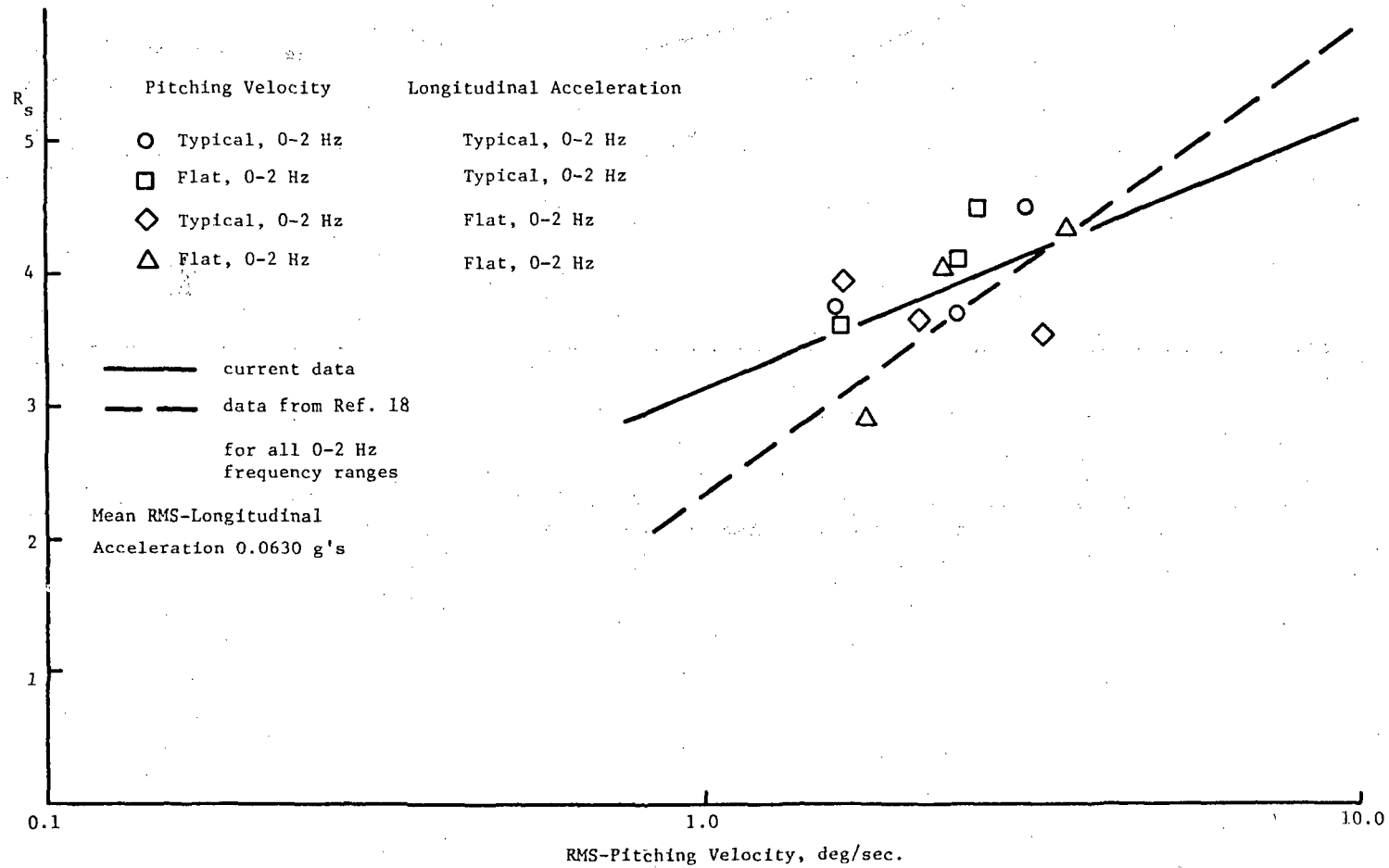

Figure 15. Effect of an approximately constant RMS-longitudinal acceleration added to a variable RMS-pitching velocity on human comfort response

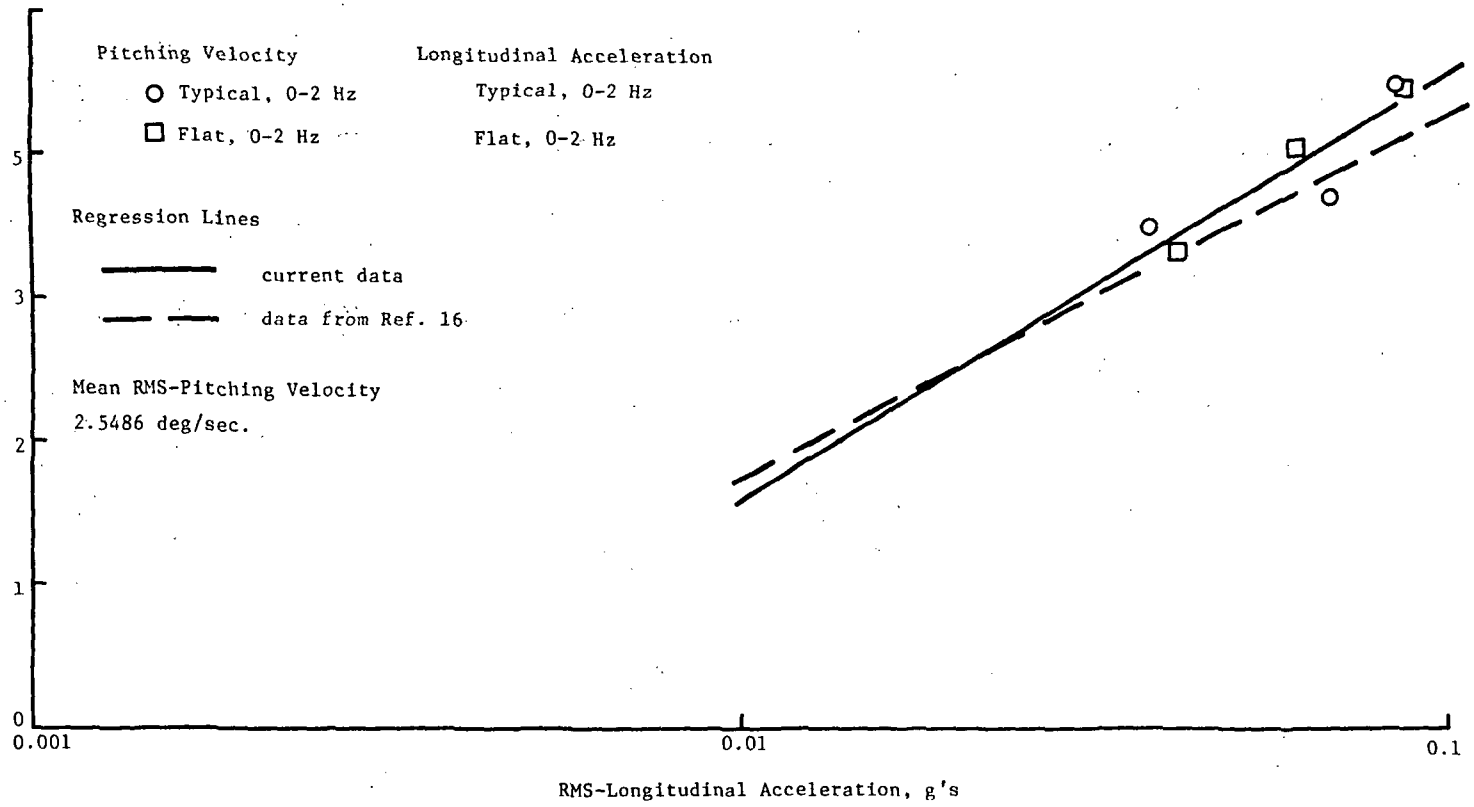

Figure 16. Effect of an approximately constant RMS-pitching velocity added to a variable RMS-longitudinal acceleration on human comfort response

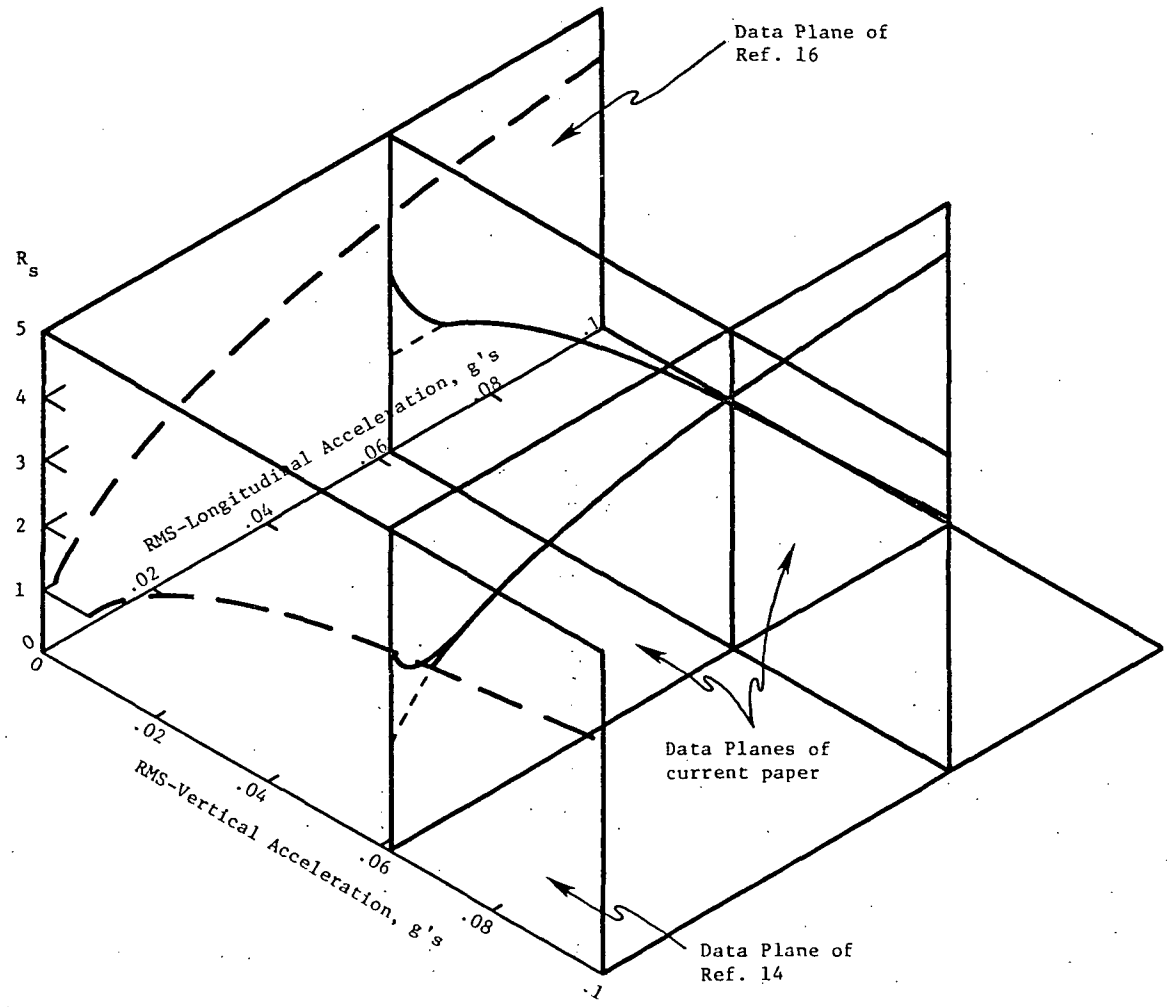

Figure 17. The effects of combined longitudinal and vertical RMS-accelerations on human comfort response

[The curves shown are transformations of the regression lines shown in Figures 11 and 12]

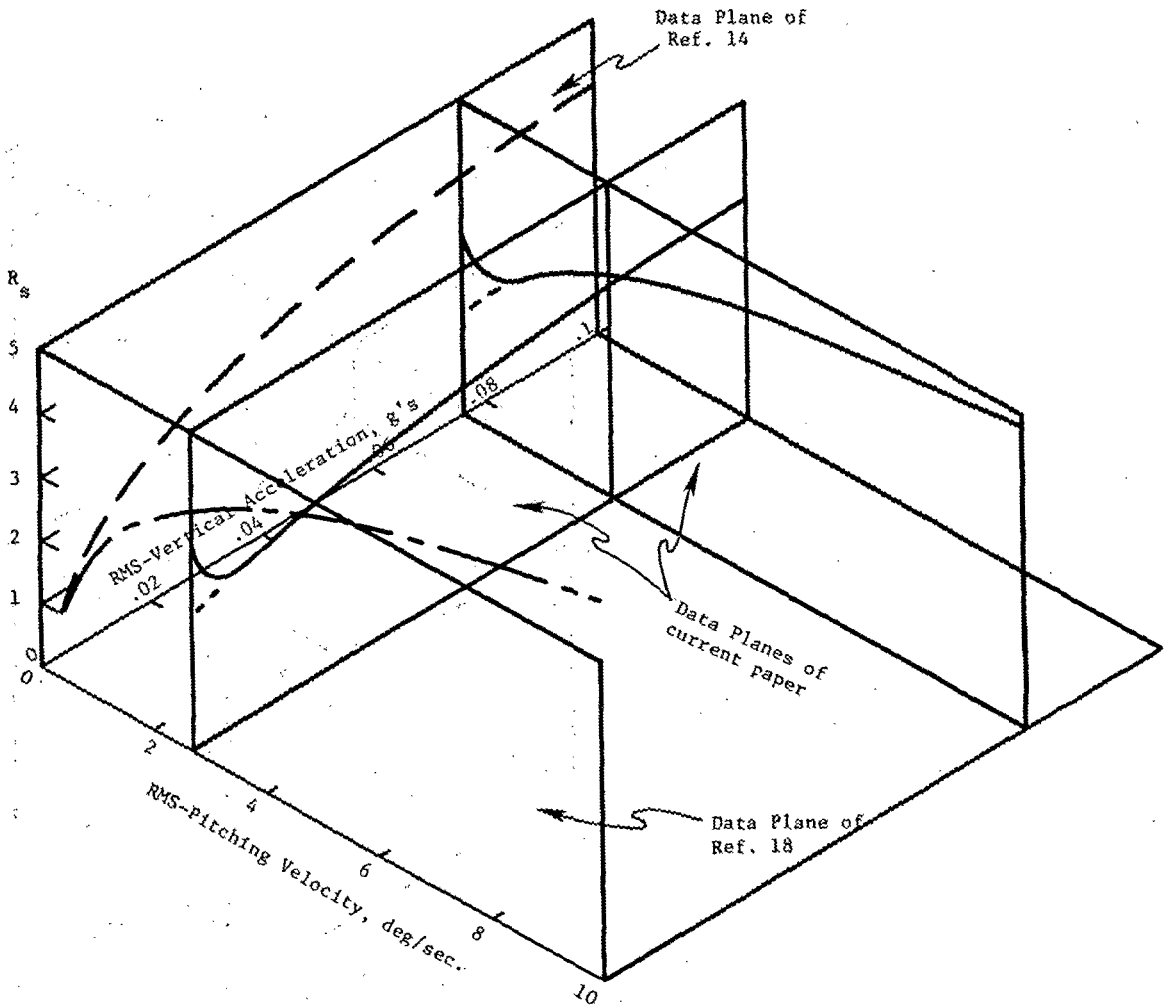

Figure 18. The effects of combined RMS-vertical acceleration and RMS-pitching velocity on human comfort response

[The curves shown are transformations of the regression lines shown in Figures 13 and 14]

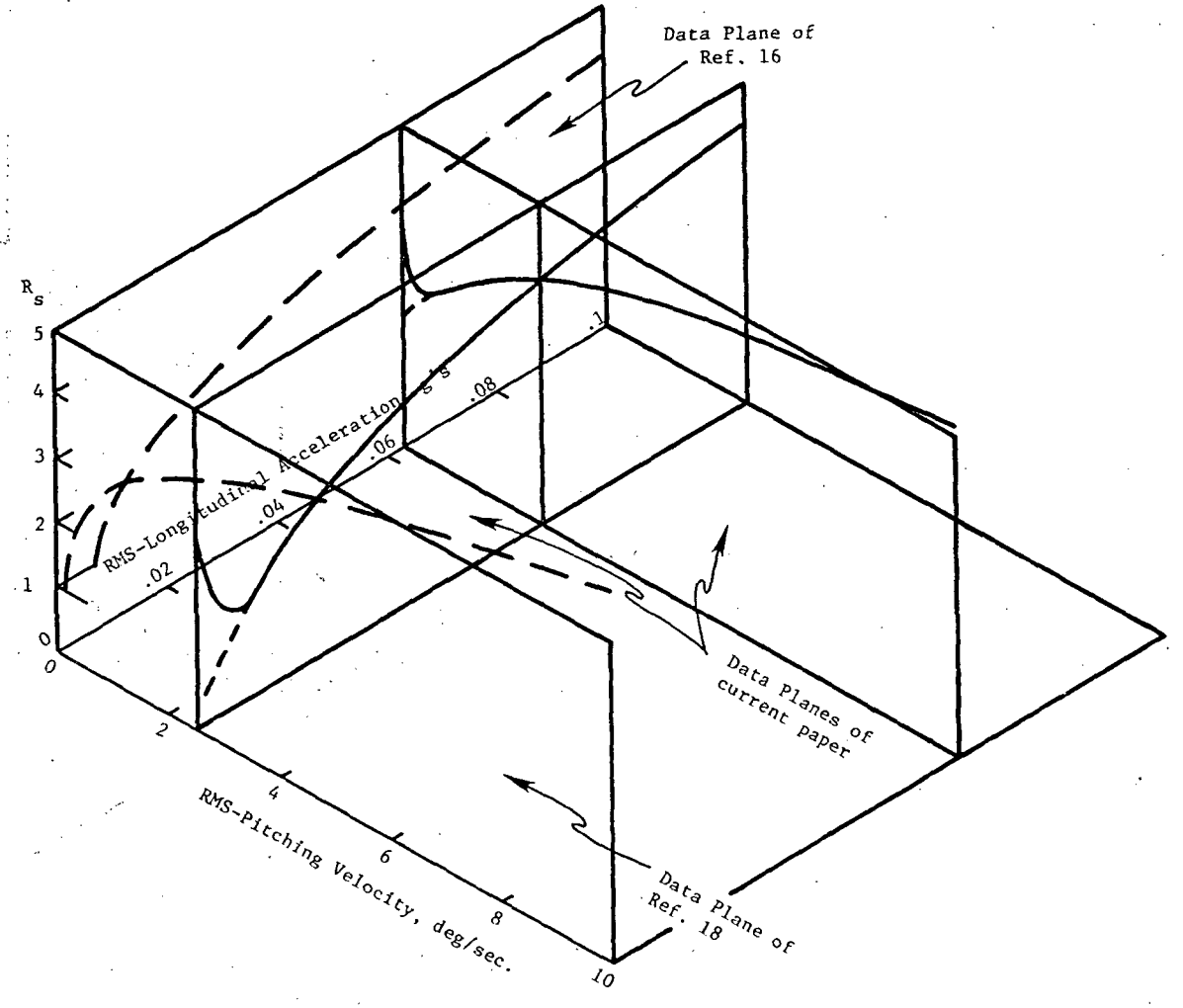

Figure 19. The effects of combined RMS-longitudinal acceleration and RMS-pitching velocity on human comfort response

[The curves shown are transformations of the regression lines shown in Figures 15 and 16]

NASA Contractor Report 159186

Distribution List
NAS1-14908-T8

Copy No.	
1	NASA Langley Research Center Hampton, VA 23665 Attention: Report and Manuscript Control Office Mail Stop 180A
2 - 21	NASA Langley Research Center Hampton, VA 23665 Attention: Thomas K. Dempsey, Mail Stop 463
22	NASA Ames Research Center Moffett Field, CA 94035 Attention: Library, Mail Stop 202-3
23	NASA Dryden Flight Research Center P.O. Box 273 Edwards, CA 93523 Attention: Library
24	NASA Goddard Space Flight Center Greenbelt, MD 20771 Attention: Library
25	NASA Lyndon B. Johnson Space Center 2101 Webster Seabrook Road Houston, TX 77058 Attention: JM6/Library
26	NASA Marshall Space Flight Center Marshall Space Flight Center, AL 35812 Attention: Library, AS61L
27	Jet Propulsion Laboratory 4800 Oak Grove Drive Pasadena, CA 91103 Attention: Library, Mail Code 111-113
28	NASA Lewis Research Center 21000 Brookpark Road Cleveland, OH 44135 Attention: Library, Mail Stop 60-3

DISTRIBUTION LIST (cont.)

Copy No.	
29	NASA John F. Kennedy Space Center Kennedy Space Center, FL 32899 Attention: Library, NWSI-D
30	National Aeronautics and Space Administration Washington, D. C. 20546 Attention: RTE-6
31 - 60 plus original	NASA Scientific and Technical Information Facility 6571 Elkridge Landing Road Linthicum Heights, MD 21090
61 - 62	R. W. Stone, Jr.
63	L. A. Hoel
64	I. A. Fischer Office of Sponsored Programs
65 - 66	E. H. Pancake Science/Technology Information Center Clark Hall
67	RLES Files

0045:jt